UNIVERSIDAD DE LAS PALMAS DE GRAN CANARIA

ESCUELA DE DOCTORADO

PROGRAMA DE DOCTORADO DE INVESTIGACIÓN EN BIOMEDICINA

TESIS DOCTORAL

ESTUDIO DE LAS COJERAS Y SU EVALUACIÓN POR TÉCNICAS BIOMECANICAS Y ESCALAS SUBJETIVAS.

Doctorando

Pedro Figueirinhas Paiva

Directores

José Manuel Vilar Guereño, David Oliverio Rodríguez Lozano

Las Palmas de Gran canaria, 2024

D. JOSE ALBERTO MONTOYA ALONSO, COORDINADOR DEL PROGRAMA DE DOCTORADO DE INVESTIGACIÓN EN BIOMEDICINA DE LA UNIVERSIDAD DE LAS PALMAS DE GRAN CANARIA

INFORMA,

De que la Comisión Académica del Programa de Doctorado, en su sesión de fecha..... tomó el acuerdo de dar el consentimiento para su tramitación, a la tesis doctoral titulada `` **ESTUDIO DE LAS COJERAS Y SU TRATAMIENTO POR TÉCNICAS BIOMECANICAS Y ESCALAS SUBJETIVAS.** ´´, presentada por el doctorando D. Pedro Figueirinhas Paiva y dirigida por los Doctores José Manuel Vilar Guereño y David Oliverio Rodriguez Lozano.

Y para que así conste, y a efectos de lo previsto en el Artº 11 del Reglamento de Estudios de Doctorado (BOULPGC 04/03/2019) de la Universidad de Las Palmas de Gran Canaria, firmo la presente en Las Palmas de Gran Canaria, a.....de.....de dos mil veinticuatro.

ULPGC · UNIVERSIDAD DE LAS PALMAS DE GRAN CANARIA

D. José Manuel Vilar Guereño, Doctor en veterinaria y profesor catedrático de Universidad del Departamento de Patología Animal de la Facultad de Veterinaria de la Universidad de Las Palmas de Gran Canaria

INFORMA:

Que **D. Pedro Figueirinhas Paiva**, Graduado en Veterinaria, ha realizado, bajo mi dirección y asesoramiento, el presente trabajo de tesis doctoral titulado: `` **ESTUDIO DE LAS COJERAS Y SU TRATAMIENTO POR TÉCNICAS BIOMECANICAS Y ESCALAS SUBJETIVAS**´´, que considero reúne las condiciones y calidad científica necesarias, para su presentación y defensa, para optar al título de Doctor por la Universidad de Las Palmas de Gran Canaria.

Lo que firmo, a los efectos oportunos, en Arucas (Las Palmas) a veinticinco de noviembre de dos mil veinticuatro.

VILAR GUEREÑO JOSE MANUEL - 42840080G

Firmado digitalmente por VILAR GUEREÑO JOSE MANUEL - 42840080G
Fecha: 2024.11.26 20:47:21 Z

ULPGC • UNIVERSIDAD DE LAS PALMAS DE GRAN CANARIA

D. David Oliverio Rodriguez Lozano, Doctor en veterinaria y Profesor Contratado Doctor de Universidad del Departamento de Patología Animal de la Facultad de Veterinaria de la Universidad de Las Palmas de Gran Canaria.

INFORMA:

Que **D. Pedro Figueirinhas Paiva**, Graduado en Veterinaria, ha realizado, bajo mi dirección y asesoramiento, el presente trabajo de tesis doctoral titulado: `` **ESTUDIO DE LAS COJERAS Y SU TRATAMIENTO POR TÉCNICAS BIOMECANICAS Y ESCALAS SUBJETIVAS**´´, que considero reúne las condiciones y calidad científica necesarias, para su presentación y defensa, para optar al título de Doctor por la Universidad de Las Palmas de Gran Canaria.

Lo que firmo, a los efectos oportunos, en Arucas (Las Palmas) a veinticinco de noviembre de dos mil veinticuatro.

RODRIGUEZ LOZANO DAVID OLIVER - 44706364E

Firmado digitalmente por RODRIGUEZ LOZANO DAVID OLIVER - 44706364E
Fecha: 2024.11.26 15:27:52 Z

Ao meu pai e ao meu irmão.
Os três, sempre juntos.

AGRADECIMIENTOS

Gracias a mi padre, mi mayor referente y la persona más importante de mi vida, por darme el privilegio de crecer admirando a alguien cuya fortaleza y honestidad son tan extraordinarias que, aún hoy, continúan sorprendiéndome e inspirándome profundamente.

Gracias a mis directores de tesis. A José Vilar, por su paciencia infinita, sus consejos y también sus reproches, siempre necesarios, así como por no rendirse incluso en los momentos más complicados del desarrollo de la tesis. Y a Oliver Rodríguez, mi otro director, compañero y amigo, por su inagotable buen humor y positivismo. ¿Quién habría dicho que terminaríamos haciendo una tesis juntos, eh?

Gracias a mi hermano mayor, por estar siempre a mi lado y por haberme educado y abierto las puertas del arte y la música desde que era muy pequeño, transmitiéndome su sensibilidad e inagotable imaginación. La portada de esta tesis es obra suya, como no podría ser de otra manera.

Gracias a todos mis compañeros del Hospital Clínico Veterinario por hacerme sentir parte de esta gran familia y permitirme disfrutar plenamente de esta profesión que tanto me apasiona. Un agradecimiento especial a Tere, por su lucha incansable y el ejemplo inspirador que nos brinda, y a Marcos, por su ayuda desinteresada y que incluso a la distancia, sigue siendo mi compañero.

Gracias a esta isla y a todos mis amigos, por llenarme de vida y arroparme siempre. Y gracias en especial a Anabel, por escucharme, por apoyarme en este camino y tener siempre ese abrazo, incluso en los momentos más difíciles.

INDICE

1. INTRODUCCIÓN 1

2. CAUSAS DE COJERAS 4

2.1. Lesiones Musculares, Tendinosas o de Ligamentos: 4

2.2. Lesiones Óseas: 4

2.3. Infecciones: 5

2.4. Problemas Neurológicos: 5

2.5. Objetos Extraños o Heridas: 6

2.6. Problemas Vasculares: 6

2.7. Enfermedades Sistémicas: 6

2.8. Problemas Articulares: 7

2.9. Neoplasias: 9

3. MÉTODOS DE DIAGNÓSTICO DE PATOLOGÍAS QUE CURSAN CON COJERA 10

3.1. Radiodiagnóstico 10

3.1.1. Radiografía convencional: 10

3.1.2. Tomografía Computarizada (TC): 11

3.1.3. Fluoroscopia: 11

3.1.4. Resonancia Magnética (RM): 12

3.2 Ultrasonidos: 12

4. MÉTODOS DE EVALUACIÓN DE COJERAS 13

4.1. Métodos Subjetivos: 13

4.1.1. Escala Visual Analógica de Cojera (CVAS): 13

4.1.2. Escala de Cojera de 5 Puntos: 13

4.1.3. Escala de Cojera de la Universidad de Pennsylvania (PennHIP): 13

4.1.4. Escala de Cojera de la Universidad de Glasgow (GUVARS): 14

4.1.5. Escala Bristol Osteoarthritis in Dogs (BrOAD): 14
4.1.6. Texas A&M Client:..... 14
4.1.7. Canine Brief Pain Inventory (CBPI):..... 14
4.1.8. Helsinki Chronic Pain Index (HCPI)..... 15
4.1.9. Escala Funcional Bioarth (EFB): 15
ARTÍCULO #1 17
4.2. Métodos Objetivos:..... 28
4.2.1. Análisis cinéticos:..... 28
4.2.1.1 Plataformas de fuerza:..... 29
4.2.1.2. Plataforma de presión:..... 31
ARTÍCULO #2 36
4.2.2. Análisis cinemáticos:..... 46
4.2.2.1. Electrogoniometria:..... 46
4.2.2.2. Cinematografía de alta velocidad: 46
4.2.2.3. Sensores Inerciales o unidades de medición inercial (IMU): 47
ARTICULO #3 51
5. CONCLUSIONES..... 66
6. RESUMEN 67
7. SUMMARY:..... 69
8. BIBLIOGRAFIA 71

1. INTRODUCCIÓN

La cojera, en términos científicos, se define como una disfunción en la marcha de un animal, caracterizada por una alteración en la capacidad de apoyo o sostén de uno o más miembros durante el movimiento.

Esta alteración puede manifestarse como una asimetría en la distribución del peso corporal o un patrón de locomoción irregular, y puede estar asociada con dolor, debilidad muscular, trastornos articulares, lesiones neurológicas u otras patologías subyacentes.

La cojera es un síntoma clínico importante que indica la presencia de una afección subyacente y es fundamental en el diagnóstico y tratamiento de trastornos musculoesqueléticos en animales (Mcgavin y cols., 2012).

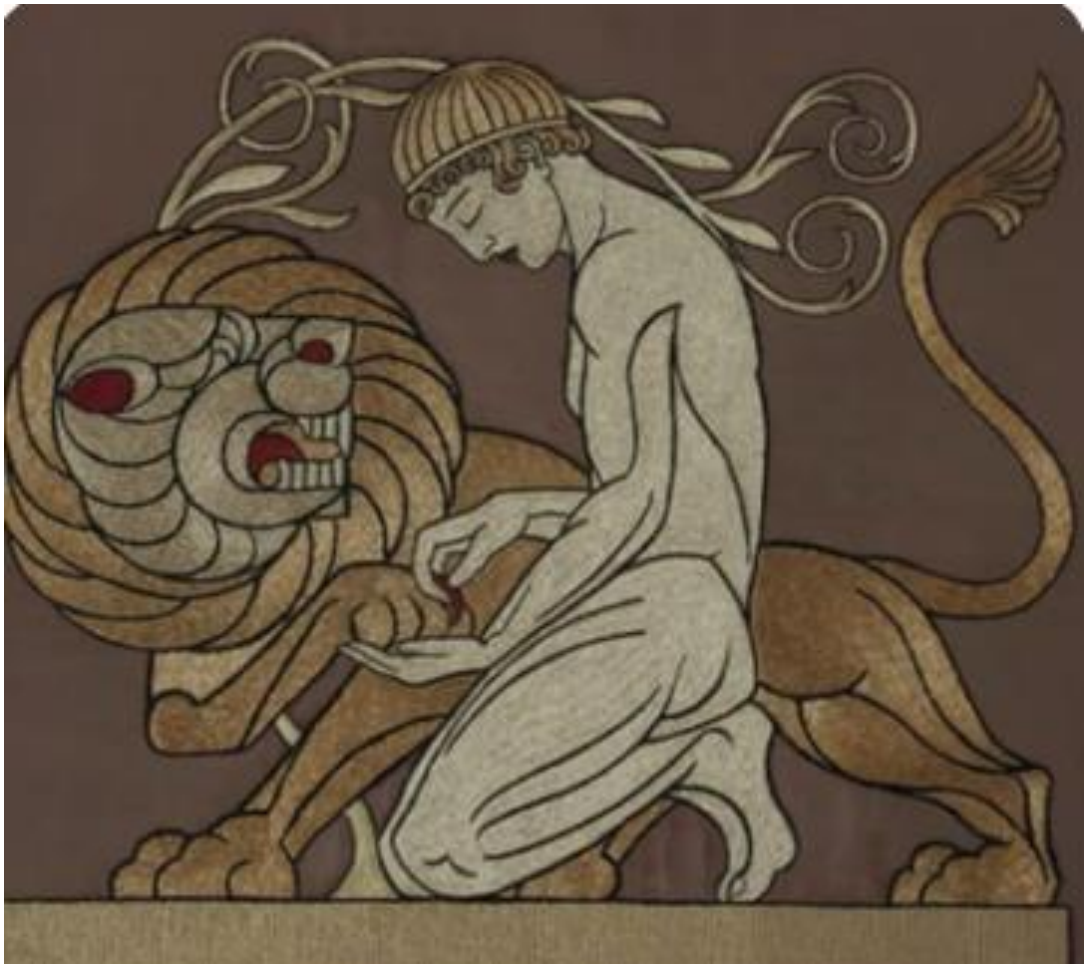

Figura 1. Portada del libro A Concise History of Veterinary Medicine (Jones y cols., 2022)

La historia de la ortopedia en medicina veterinaria es tan antigua como la propia práctica de la medicina veterinaria. Desde tiempos antiguos, se han registrado intentos de tratar lesiones y enfermedades musculoesqueléticas en animales.

Sin embargo, el desarrollo de la ortopedia veterinaria como una especialidad reconocida ha seguido un camino paralelo al de la ortopedia humana, aunque con algunas diferencias significativas.

En las civilizaciones antiguas, como la egipcia, griega y romana, existen registros de intentos de tratamiento de fracturas y lesiones en animales, particularmente en caballos y otros animales de trabajo. Estos tratamientos a menudo se basaban en la observación empírica y en métodos rudimentarios.

Figura 2. Herrador alemán o “médico de caballos” del siglo XVIII. Fuente: Revolutionary War Journal 2020

Durante la época medieval y el Renacimiento, la atención a los problemas ortopédicos en animales continuó, pero no fue hasta los tiempos modernos que la ortopedia veterinaria comenzó a desarrollarse como una disciplina más formal. En el siglo XIX, con el avance de la medicina veterinaria en general, la ortopedia veterinaria comenzó a recibir más atención y se realizaron avances en técnicas quirúrgicas y tratamientos para animales con problemas musculoesqueléticos (Cid 2000).

En el curso del siglo XX, la ortopedia veterinaria ha experimentado un notable progreso, especialmente con la incorporación de técnicas diagnósticas más sofisticadas, tales como el radiodiagnóstico y los métodos objetivos de análisis biomecánico, junto con procedimientos quirúrgicos más avanzados como la fijación interna y externa de fracturas, la artroscopia y la cirugía reconstructiva. Conforme la medicina veterinaria ha evolucionado hacia una disciplina más profesionalizada y especializada, la ortopedia veterinaria ha adquirido el estatus de una especialidad reconocida, con profesionales veterinarios dedicados exclusivamente al diagnóstico y tratamiento de trastornos musculoesqueléticos en animales.

En la actualidad, la ortopedia veterinaria constituye un componente esencial de la práctica veterinaria, con especialistas capacitados para abordar una amplia gama de condiciones ortopédicas en animales domésticos y de trabajo. Esto incluye el análisis biomecánico, la cirugía ortopédica y traumatológica, así como la rehabilitación y fisioterapia.

Los avances en tecnología médica, como la plataforma de fuerza y de presión, la tomografía computarizada y la resonancia magnética, han ampliado las opciones de diagnóstico y tratamiento disponibles, facilitando un cuidado más avanzado y personalizado para los pacientes animales (Jones y cols., 2022). En el marco de esta tesis, se abordará el tema de la cojera en cánidos desde una óptica contemporánea y prospectiva, con un enfoque en su diagnóstico y las técnicas de evaluación más emergentes.

2. CAUSAS DE COJERAS

Las causas de cojera en animales son variadas y muchas veces multifactoriales. Las más comunes son:

2.1. Lesiones Musculares, Tendinosas o de Ligamentos:

Distensiones, desgarros o lesiones en los músculos, tendones o ligamentos, las cuales pueden ser el resultado de ejercicio excesivo, traumas o movimientos bruscos. (Hittmair y cols., 2012; Wijdicks y cols., 2010)

2.2. Lesiones Óseas:

Las fracturas, luxaciones o enfermedades óseas. son lesiones normalmente producidas por traumatismos, caídas, problemas de desarrollo o congénitos. (Tomlin y cols., 2001; Perry y cols., 2021)

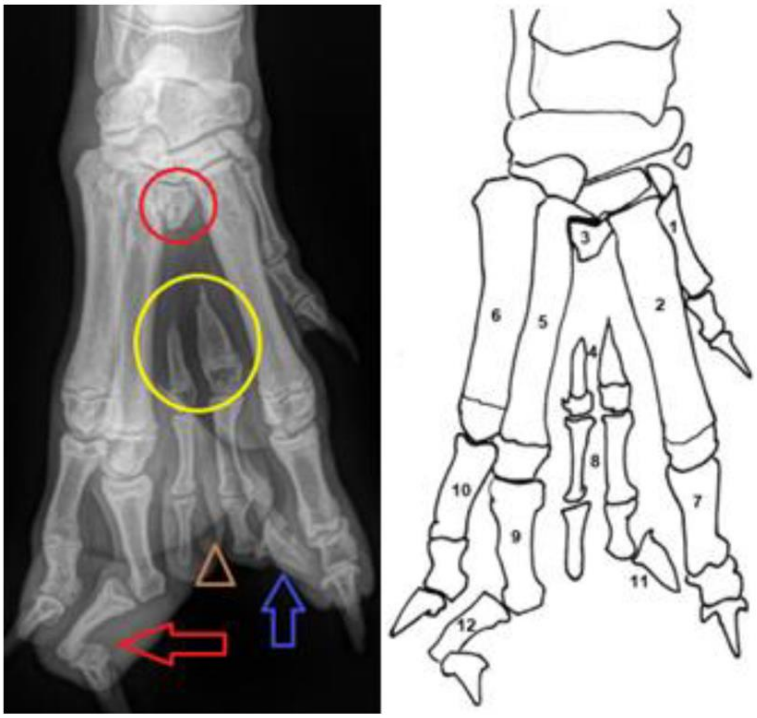

Figura 3. Radiografías preoperatorias (izquierda) y dibujo esquemático (derecha) de la pata anormal. (1) primer hueso metacarpiano; (2) segundo hueso metacarpiano; (3) parte proximal rudimentaria del tercer

hueso metacarpiano (el círculo rojo); (4) hipoplasia del tercer hueso metacarpiano (círculo amarillo); (5) cuarto hueso metacarpiano; (6) quinto hueso metacarpiano; (7) falange proximal del segundo dedo; (8) confirmación doble de la falange proximal y medial del tercer dedo (marcado con el triángulo marrón); (9) falange proximal del cuarto dedo; (10) falange proximal del quinto dedo; (11) nota que solo se desarrolló una única uña en el tercer dedo (flecha azul); (12) falange medial del cuarto dedo con deformidad severa en valgo y falange distal del cuarto dedo con deformidad en varo (flecha roja). Fuente: Animals mpdi https://doi.org/10.3390/ani14111647 (Wehrenpfennig y cols., 2024)

2.3. Infecciones:

Las infecciones en las extremidades ya sean de origen bacteriano, viral o fúngico, pueden causar inflamación y dolor, lo que usualmente se manifiesta como una cojera. (Ruoff y cols., 2017; Erne y cols., 2007)

2.4. Problemas Neurológicos:

Trastornos neurológicos que afectan los nervios responsables del control del movimiento, esto podría incluir patologías como la hernia discal (Kerwin y cols., 2020; McDonnell y cols., 2001).

Figura 4. Perro con ataxia del miembro pelviano. Fuente: Veterinary Medical Center at the University of Minnesota College of Veterinary Medicine

2.5. Objetos Extraños o Heridas:

La presencia de cuerpos extraños, como espinas, vidrios o astillas, además de heridas en las almohadillas o las uñas pueden ocasionar cojeras (Kunkel y cols., 2008).

2.6. Problemas Vasculares:

Trastornos vasculares que afectan el flujo sanguíneo hacia las extremidades (Boynosky y cols.,2014).

2.7. Enfermedades Sistémicas:

Algunas enfermedades sistémicas, como la leptospirosis, leishmaniosis, erliquiosis, pueden afectar las extremidades y causar cojera. (Wallborn F y cols., 2016; Vincent-Johnson 2003). Además de enfermedades endocrinas que cursan con obesidad o la obesidad por sí sola (Zomer y cols., 2024)

Figura 5. Radiografías de un perro con Leishmaniosis, caudocraneales (A, B) y mediolaterales (C, D) del miembro posterior derecho (A, C) y del izquierdo (B, D), incluyendo la articulación de la rodilla y el tarso. Se observa una reacción perióstea irregular y continua en la metáfisis proximal (1) y distal (2) de la tibia, más evidente en el lado derecho, así como en los huesos del tarso, principalmente en el calcáneo (3). También se puede observar un derrame articular y una hinchazón periarticular en la rodilla y el tarso (3). Fuente: Animals https://doi.org/10.3390/zoonoticdis2030010 (De Feo y cols., 2022)

2.8. Problemas Articulares:

Enfermedades articulares como la **osteoartritis (OA), la displasia de cadera o la displasia de codo** pueden causar cojera en animales. Estas condiciones a menudo afectan a perros mayores o razas predispuestas genéticamente (Rychel 2010; LaPrade y cols., 2021).

Dado que las etiologías de las cojeras en cánidos son variadas y frecuentemente multifactoriales, es común que se asocien con el desarrollo concomitante de **osteoartritis** en la mayoría de los casos (Malek y cols., 2012). La osteoartritis canina, también denominada artrosis, representa una enfermedad degenerativa de las articulaciones caracterizada por el deterioro progresivo del cartílago articular (Rychel, 2010).

Este deterioro es acompañado de cambios en las estructuras subyacentes como la formación de osteofitos, esclerosis subcondral, colapso articular, quistes subcondrales, y la inflamación de la membrana sinovial. (Ramirez-flores y cols., 2017; Bland 2015).

La prevalencia de la osteoartritis en la medicina veterinaria ha aumentado considerablemente, convirtiéndose en una causa común de consulta veterinaria (Malek y cols., 2012). Las articulaciones más comúnmente afectadas por la osteoartritis en medicina veterinaria incluyen el codo, la cadera y la rodilla (Malek y cols., 2012).

La principal etiología de la osteoartritis en la articulación de la rodilla es la ruptura del ligamento cruzado, que además constituye la causa predominante de cojera en el miembro pelviano (Duval y cols., 1999). También puede aparecer en animales con luxación de rótula (Kalff y cols., 2014).

La principal causa de OA en codo y cadera es la displasia. (Lau 2018, Anderson 2020).

La **displasia de codo** es un síndrome que engloba un conjunto de patologías que afectan la articulación del codo, alterando su congruencia y función biomecánica. Las patologías más reconocidas asociadas con la displasia de

codo en caninos incluyen la fragmentación del proceso coronoides, la osteocondritis disecante y la no unión el proceso ancóneo. (Tobias y Johnston 2011)

La **displasia de cadera** en caninos se define como una patología ortopédica caracterizada por una evolución anormal de la articulación coxofemoral, manifestada por una discrepancia anatómica entre la cabeza del fémur y el acetábulo pélvico. Esta incongruencia articular puede provocar sintomatología dolorosa, cojera y limitación de la movilidad, y en casos severos, puede desencadenar en degeneración articular y discapacidad funcional (Smith y cols., 2015; Rodriguez y cols., 2003).

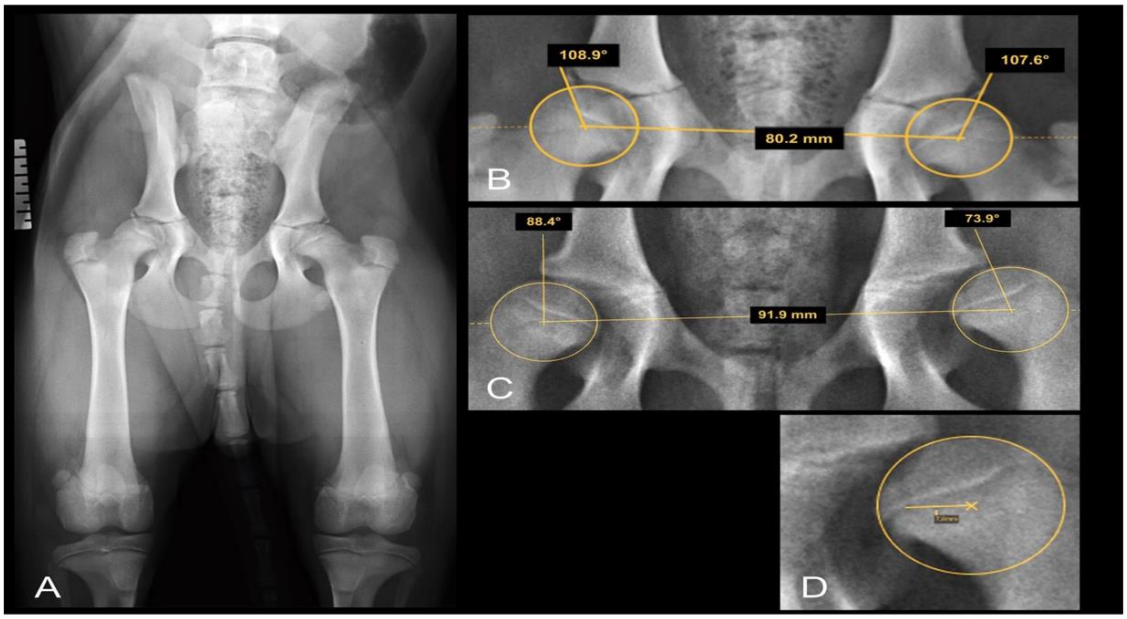

Figura 6. Radiografía ventrodorsal extendida de un Rottweiler de cuatro meses de edad con lo que se asumía eran articulaciones de cadera normales. Se observan las vértebras lumbosacras transicionales (tipo III). La derecha siempre está a la izquierda de las imágenes. (B) Ampliación de (A), enfocándose en las articulaciones de la cadera: demostración de la medición del ángulo de Norberg. (C) Sección de una radiografía VD en otro cachorro de Rottweiler de cuatro meses con evidente laxitud en ambas articulaciones de la cadera, más severa en el lado izquierdo. El centro de la cabeza femoral está posicionado sobre el borde acetabular dorsal en (B) y definitivamente lateral al borde acetabular dorsal en (C) bilateralmente. (D) Ampliación de (C), demostrando la distancia real del centro de la cabeza femoral al DAR. Fuente: Animals https://doi.org/10.3390/ani12101269 (Vidoni y cols., 2022)

2.9. Neoplasias:

Las neoplasias óseas son otra posible causa de cojera en la especie canina (Klein 2020). Estos tumores pueden afectar a cualquier tipo de hueso. Las más comunes incluyen: osteosarcomas, condrosarcomas, osteomas y fibrosarcomas (Liptak y cols., 2021, Patterson y cols., 2023). Debido a la agresividad de estas patologías en la mayoría de los casos la opción terapéutica pasa por la amputación de la extremidad afectada (Morris y cols., 2022).

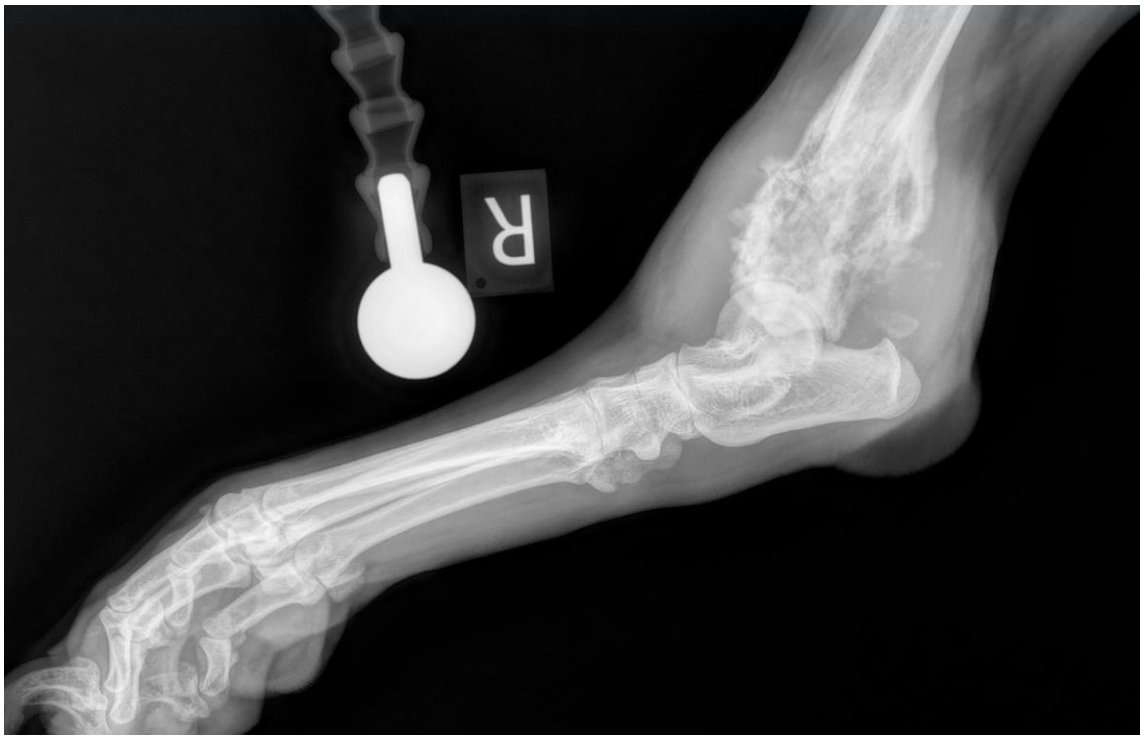

Figura 7. Radiografía de una tibia canina con osteosarcoma a nivel distal. Fuente: Fitz-Patrick Referrals

3. MÉTODOS DE DIAGNÓSTICO DE PATOLOGÍAS QUE CURSAN CON COJERA

3.1. Radiodiagnóstico

El radiodiagnóstico es una disciplina de la medicina veterinaria que se especializa en el uso de técnicas de diagnóstico por imagen médica para diagnosticar enfermedades y patologías médicas en los animales. Estas técnicas se basan en el uso de radiaciones ionizantes, como los rayos X, para producir imágenes de las estructuras internas del cuerpo.

El objetivo principal del radiodiagnóstico es obtener información visual sobre la anatomía y la funcionalidad de órganos y tejidos, lo que ayuda a los veterinarios a realizar diagnósticos más precisos. (Thrall 2018; Madsen y cols., 1995)

Algunas de las técnicas de radiodiagnóstico más comunes incluyen:

3.1.1. Radiografía convencional:

Emplea rayos x para generar imágenes bidimensionales de las estructuras internas, incluyendo huesos y órganos. (Klußmann y cols., 2024).

Figura 8. Fractura de Monteggia del miembro anterior de un perro. Hay una fractura oblicua corta en la diáfisis media del cúbito con desplazamiento craniolateral ensanchamiento del espacio articular humerorradial; y luxación lateral de la cabeza radial.
Fuente: Journal of the American Veterinary Medical Association https://doi.org/10.2460/javma.21.05.0254

3.1.2. Tomografía Computarizada (TC):

Fusiona múltiples imágenes obtenidas por rayos X desde distintos ángulos para reconstruir imágenes tridimensionales detalladas de los órganos internos (Klußmann y cols., 2024).

Figura 9. Fotografía de tomografía computarizada. Fuente: HCV-ULPGC

3.1.3. Fluoroscopia:

Proporciona imágenes en tiempo real mediante el uso de rayos X, permitiendo la visualización de la función en movimiento de los órganos (Berg y cols., 2023).

Figura 10. Fotografía de Fluoroscopia. Fuente: HCV-ULPGC

3.1.4. Resonancia Magnética (RM):

Emplea campos magnéticos y ondas de radiofrecuencia para obtener imágenes detalladas de tejidos blandos y estructuras internas, sin la exposición a radiación ionizante (Limpens 2024; Schachar y cols., 2024).

3.2 Ultrasonidos:

Utiliza ondas sonoras de alta frecuencia para generar imágenes en tiempo real de las estructuras internas del cuerpo (Otero y cols., 2024).

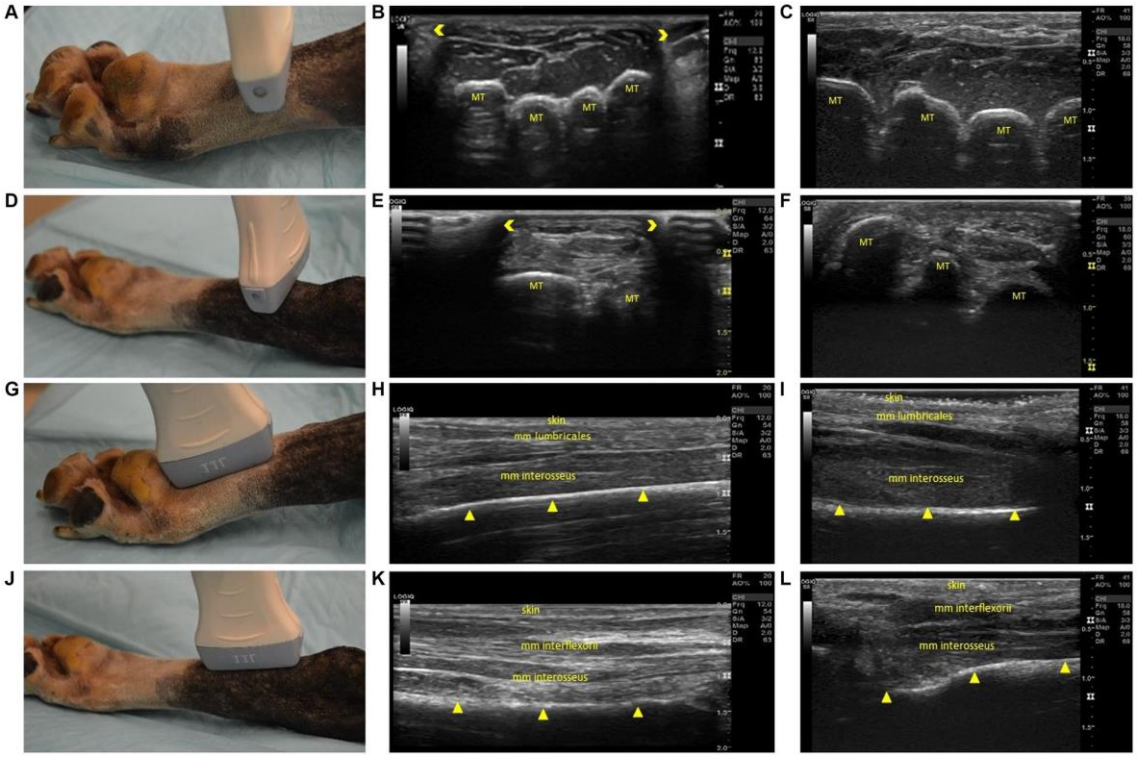

Figura 11. Diferentes cortes de una ecografía de la extremidad posterior de un perro a nivel de los metatarsianos. MT: metatarsiano; △, interfase ósea. Fuente: www.axoncomunicacion.net

4.MÉTODOS DE EVALUACIÓN DE COJERAS

4.1. Métodos Subjetivos:

Las escalas subjetivas en veterinaria son herramientas que permiten evaluar y cuantificar de manera subjetiva diversos aspectos del estado de un animal, como la intensidad de una cojera. Estas escalas se basan en la observación y evaluación de ciertos parámetros, y aunque no proporcionan mediciones objetivas, son útiles para guiar el tratamiento y la toma de decisiones (Finka y cols., 2019).

Algunas de las más comúnmente utilizadas incluyen:

4.1.1. Escala Visual Analógica de Cojera (CVAS):

Una herramienta que utiliza una línea horizontal donde los observadores o dueños marcan el nivel de cojera percibida por el perro, asignando valores en una escala continua de 0 a 10 (Brown y cols., 2007)

4.1.2. Escala de Cojera de 5 Puntos:

Este método clasifica la cojera en una escala ordinal de 0 a 4, donde 0 representa la ausencia de cojera y 4 indica la cojera más severa (Hudson y cols., 2010)

4.1.3. Escala de Cojera de la Universidad de Pennsylvania (PennHIP):

Utiliza una puntuación ordinal de 0 a 4 para evaluar la función de la extremidad, donde 0 indica una función normal y 4 representa una cojera grave con incapacidad para soportar peso (Smith y cols., 2001)

4.1.4. Escala de Cojera de la Universidad de Glasgow (GUVARS):

Es una escala ordinal que va de 0 a 6, donde 0 indica ausencia de cojera y 6 representa una cojera muy severa con completa incapacidad para soportar peso (Hielm-Björkman y cols., 2003).

4.1.5. Escala Bristol Osteoarthritis in Dogs (BrOAD):

Se usa para cuantificar la severidad de la osteoartritis en caninos. Diseñada para ofrecer una evaluación estandarizada, la BrOAD considera varios parámetros como la claudicación, la limitación de movilidad articular, la funcionalidad y la intensidad del dolor (Innes and Barr, 1998).

4.1.6. Texas A&M Client:

Es utilizada para medir la percepción subjetiva del propietario respecto a la calidad de vida de su mascota, particularmente en contextos de enfermedades crónicas o terminales en animales de compañía.

Esta escala solicita al propietario que califique diversos aspectos relacionados con el bienestar de su mascota, tales como el nivel de dolor, la actividad física, el apetito, la interacción social y otros comportamientos relevantes (Hudson y cols., 2004).

4.1.7. Canine Brief Pain Inventory (CBPI):

Es un inventario que solicita a los propietarios de los perros que califiquen la intensidad del dolor experimentado por su mascota en diferentes situaciones y momentos, así como el impacto que este dolor tiene en la calidad de vida del animal.

Además, se puede evaluar la respuesta del perro al tratamiento del dolor utilizando esta herramienta. La estructura del CBPI consta de dos secciones principales: una destinada a evaluar la intensidad del dolor y otra centrada en

determinar cómo el dolor afecta el comportamiento y la actividad cotidiana del perro (Cimino Brown y cols., 2007).

4.1.8. Helsinki Chronic Pain Index (HCPI)

El Índice de Comportamiento del Dolor en Caninos (HCPI) ha sido empleado de manera continua para la valoración del dolor crónico en perros afectados por osteoartritis en las articulaciones de la rodilla, codo y cadera (Hielm-Björkman y cols., 2003; Wernham y cols., 2011; Hielm-Björkman y cols., 2012; Hielm-Björkman y cols., 2014; Heikkilä y cols., 2014).

Estas herramientas de medición son de gran utilidad debido a que posibilitan una comunicación uniforme entre los profesionales veterinarios y los dueños de mascotas, simplifican la monitorización del avance del tratamiento y funcionan como indicadores clave para medir la eficacia de las intervenciones veterinarias.

Sin embargo, es importante tener en cuenta que todas estas escalas están sujetas a la percepción subjetiva del observador, lo cual puede impactar de forma significativa en la valoración definitiva (Horstam y cols., 2004)

4.1.9. Escala Funcional Bioarth (EFB):

Es un sistema de puntuación de cojera (de 0 a 3 y de 0 a 2 según el caso) que evalúa 12 parámetros, incluyendo limitación funcional, movilidad articular y atrofia muscular. Específicamente, estos parámetros incluyen cambios en la extremidad mientras está de pie, cambios en la postura al levantarse, cojera en reposo, cojera después de 10 minutos de caminata, resistencia para caminar, resistencia para correr, subir escaleras, limitaciones al realizar pequeños saltos (40–50 cm) y movilidad de la rodilla (Vilar y cols., 2016).

La Escala de Evaluación Bioarticular Radiológica (RBAS) constituye un complemento a la Evaluación Funcional de la Rodilla (EFB). Esta escala fue introducida por primera vez en el año 2006 (Sánchez-Carmona y col., 2006) y se emplea para cuantificar los hallazgos radiológicos asociados con la osteoartritis en la articulación de la rodilla, así como para clasificar el grado de severidad de

esta patología mediante un enfoque sencillo y objetivo. El procedimiento se fundamenta en un sistema de puntuación que varía en función de las alteraciones radiológicas observadas en los casos de osteoartritis de rodilla (Millis y col., 2004; Cuervo y col., 2014).

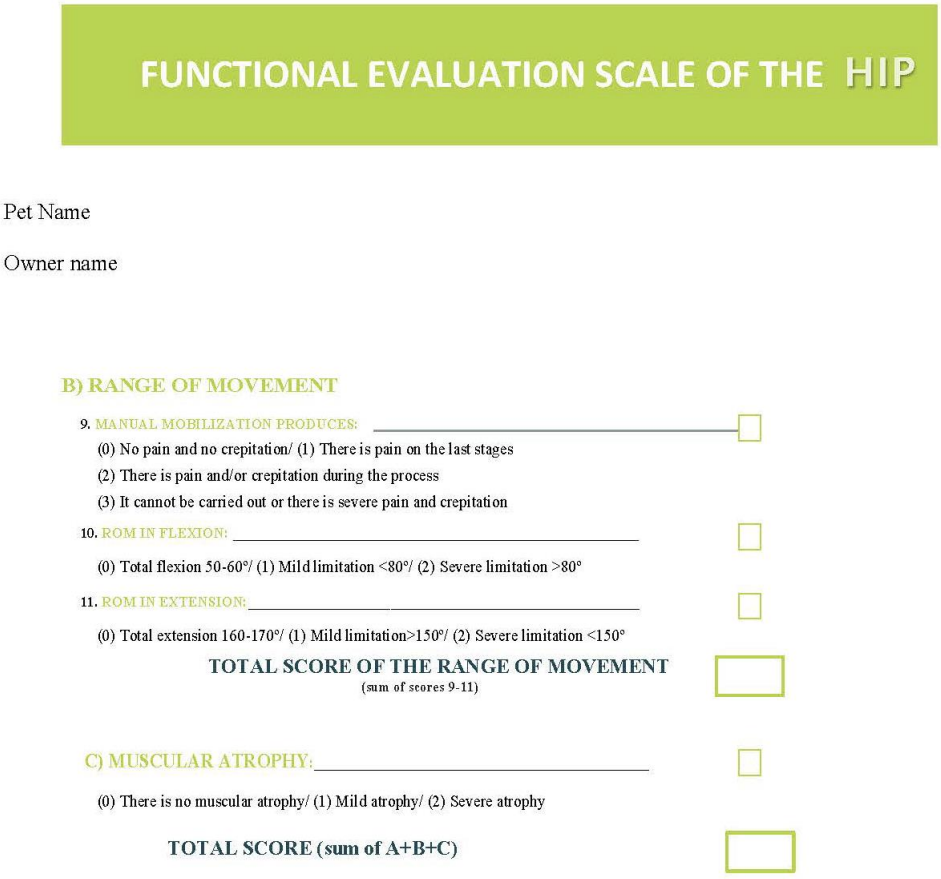

FUNCTIONAL EVALUATION SCALE OF THE HIP

Pet Name

Owner name

B) RANGE OF MOVEMENT

9. MANUAL MOBILIZATION PRODUCES: _____

(0) No pain and no crepitation/ (1) There is pain on the last stages

(2) There is pain and/or crepitation during the process

(3) It cannot be carried out or there is severe pain and crepitation

10. ROM IN FLEXION: _____

(0) Total flexion 50-60°/ (1) Mild limitation <80°/ (2) Severe limitation >80°

11. ROM IN EXTENSION: _____

(0) Total extension 160-170°/ (1) Mild limitation>150°/ (2) Severe limitation <150°

TOTAL SCORE OF THE RANGE OF MOVEMENT
(sum of scores 9-11)

C) MUSCULAR ATROPHY: _____

(0) There is no muscular atrophy/ (1) Mild atrophy/ (2) Severe atrophy

TOTAL SCORE (sum of A+B+C)

Figura 12. Escala Bioarth® para la evaluación de la articulación coxofemoral

Con el objetivo de comprobar la utilidad de dichos métodos subjetivos, se ha utilizado la escala Bioarth® para comparar el éxito de dos técnicas quirúrgicas utilizadas en la resolución de rotura de ligamento cruzado.

ARTÍCULO #1

Pedro Figueirinhas; José Manuel Gonzalo-Orden; Oliver Rodriguez; Marta Regueiro-Purriños; Ivan Prada; José Manuel Vilar; José Rodríguez-Altónaga.

Multiparametric Comparison of Two TTA-Based Surgical Techniques in Dogs with Cranial Cruciate Ligament Tears. *Animals* **2023***, 13*, 3453 .

JCR Impact factor: 2.7

Cuartil: Q1

Grupo: Veterinary sciences

Posición: 16/167

animals

MDPI

Article

Multiparametric Comparison of Two TTA-Based Surgical Techniques in Dogs with Cranial Cruciate Ligament Tears

Pedro Figueirinhas [1], José Manuel Gonzalo-Orden [2], Oliver Rodriguez [1,*], Marta Regueiro-Purriños [2], Ivan Prada [2], José Manuel Vilar [1] and José Rodríguez-Altónaga [2]

[1] Departamento de Patología Animal, Universidad de Las Palmas de Gran Canaria, Trasmontaña S/N, 35416 Arucas, Spain; pedro.figueirinhas@fpct.ulpgc.es (P.F.); jose.vilar@ulpgc.es (J.M.V.)
[2] Departamento de Medicina y Cirugia Veterinaria, Campus de Vegazana, Universidad de León, 24071 León, Spain; jmgono@unileon.es (J.M.G.-O.); mregf@unileon.es (M.R.-P.); jarodma@unileon.es (J.R.-A.)
* Correspondence: oliver.rodriguez@ulpgc.es

Simple Summary: The rupture of the cranial cruciate ligament is one of the most common causes of hindlimb lameness in dogs. In this study, we compared two different tibial tuberosity advancement (TTA)-based surgical techniques to treat this condition. No significant differences were found when both procedures were analyzed using different assessment parameters.

Abstract: Tearing of the cranial cruciate ligament causes hindlimb lameness in dogs. Different surgical procedures have been proposed to treat this condition. In this study, two different TTA-based techniques and implants were compared. A total of 30 dogs were separated into two groups according to the technique and implant used (Porous TTA® or Model Xgen®). The aim of the study was to assess whether one of these techniques has better functional recovery of the joint, better bone consolidation after the osteotomy procedure and fewer osteoarthritic changes. We compared both groups up to 3 months after surgery. No significant differences were found in any of the assessed parameters. Thus, both procedures were found to be equally effective and safe.

Keywords: canine; lameness; cranial cruciate ligament tear surgery; tibial tuberosity advancement; implant; orthopedic; osteoarthritis

check for updates

Citation: Figueirinhas, P.; Gonzalo-Orden, J.M.; Rodriguez, O.; Regueiro-Purriños, M.; Prada, I.; Vilar, J.M.; Rodríguez-Altónaga, J. Multiparametric Comparison of Two TTA-Based Surgical Techniques in Dogs with Cranial Cruciate Ligament Tears. *Animals* **2023**, *13*, 3453. https://doi.org/10.3390/ani13223453

Academic Editors: Filippo Maria Martini, Brunella Restucci and Gerardo Fatone

Received: 6 October 2023
Revised: 1 November 2023
Accepted: 7 November 2023
Published: 9 November 2023

1. Introduction

One of the main reasons dog owners visit a veterinary clinic is for lameness [1]. More specifically, the main etiology for hindlimb lameness are often conditions involving the stifle joint [2]. The cranial cruciate ligament (CCL) is the main structure that stabilizes the stifle, avoiding the cranial movement of the tibia and limiting the internal rotation and the hyperextension of the stifle [3]. Injury of the CCL alters these limitations and causes an abnormal movement between the stifle articular surfaces [4].

Repeated damage of the cartilage caused by interactions between the altered surfaces causes a progressive osteoarthritis (OA). Therefore, the goal of a CCL reconstruction is to restore the normal stifle dynamics in order to avoid the progression of OA [5,6].

Since the beginning of the 20th century there have been different approaches and discussions about the etiology, diagnosis, and treatments for a cranial cruciate ligament tear (CCLT) in the canine species [7]. The exact etiopathogenesis of the CCLT is unknown. Most of the diagnosed and treated cases are not preceded by trauma; instead, they are caused by a degenerative process that affects the collagen characteristics of the CCL, which can affect dogs of any gender or age [1].

The diagnosis of a CCLT can be achieved based on physical examination, imaging tests (X-ray, CT scan, MRI scan, ultrasounds) and arthroscopy [6]. CCLT treatment options can be medical, surgical or both. Regarding surgical techniques, different procedures have been proposed that aim to neutralize the cranial movement of the tibia by changing the tibia's

geometry. The axial force is redirected parallel to the patellar tendon and the tibio-femoral shear force is nullified, replacing the CCL function [8].

Tibial tuberosity advancement (TTA) techniques are based on an osteotomy that allows the advancement of the tibial tuberosity cranially. Then, it is stabilized using a special implant. This procedure was described in 2004 [9].

Since 2004, many authors have described other technical variations using different kinds of implants to obtain the cranial advancement of tibial tuberosity [10–12]. Among them, the Porous TTA® by the Instituto Tecnológico de Canarias (Gran Canaria, Spain) and the Model Xgen® by Securos Surgical with Xgen TTA (Securos Surgical, Fiskdale, MA, USA) techniques incorporate an osteotomy of the non-weight bearing portion of the tibia, where the implant is placed. The patellar ligament is aligned perpendicular to the common tangent of the femorotibial join, eliminating cranial tibial thrust. This new alignment eliminates the need for the CCL and results in a stable joint [9].

Porous TTA® uses a porous wedge made of titanium that refills the defect made by the osteotomy. This wedge allows a fast and good vascularization that promotes abundant bone tissue formation. The fast penetration of bone into the implant enables the early stabilization of the stifle [13,14].

Model XGEN by Securos® (Tibial Tuberosity Advancement System) is based on the original modified TTA technique by the Montavon and Kyon company in 2004 that was based on previous studies by Maquet [7]. This was the first system to use a forkless plate and cuttable cages. The cages are designed to establish early osteointegration (OI) and high resistance, reducing implant failure [10].

Several methods have been used to evaluate the hind function and OA progression after CCL treatment. In assessing stifle-related lameness, the Radiologic Bioarth Assessment Scale (RBAS) was first described in 2006 [15], and it is used to quantify the radiologic signs of OA in the joint of the stifle and classify the OA stage using a simple and objective method [15,16]. The method is based on a punctuation system that changes according to the radiologic changes observed on the OA of the stifle. To complement this, the Bioarth Functional Scale (FBAS) is a lameness scoring system (from 0 to 3 and 0 to 2 according to the case) that assesses 12 parameters, including functional limitation, joint mobility and muscular atrophy. Specifically, these parameters include changes in the limb while standing, changes in posture while getting up, lameness in rest, lameness after 10 min of walking, resistance to walk, resistance to run, climbing stairs, limitations doing small jumps (40–50 cm) and stifle mobility [17].

The aim of this study is to assess if one of these CCL techniques (the TTA Securos® implant or the TTA Porous® implant) has a better functional recuperation of the stifle, better bone healing after the osteotomy procedure and fewer osteoarthritic changes. Complications have also been reported; therefore, we also want to assess the safety of these techniques.

2. Materials and Methods

2.1. Dog Selection and Groups

All the dog owners of this study were clients of the Veterinary Teaching Hospital of the University of Leon (Leon, Spain).

A total of 30 dogs with unilateral CCLTs were used. Body weight and age ranged between 5 and 65 kg and between 12 and 210 months, respectively. The animals were randomly distributed into two groups by gender, breed and affected side (supplementary file, Tables S1–S3).

Group 1—TTA with the implant Securos® (model XGEN).

Group 2—TTA with the implant Porous®.

The inclusion criteria comprised the absence of any concurrent systemic or orthopedic diseases, and these criteria were assessed through hematologic, blood, and urine biochemical profiles. Furthermore, the subjects in the study could not have received any form of treatment for a minimum of one month.

A comprehensive clinical evaluation encompassing physical, neurologic and orthopedic examinations and assessment of vital signs was conducted to ensure that the sole cause of lameness in the subjects was specific joint osteoarthritis.

The physical examination was based on a complete evaluation of the affected limb, including pain and inflammation, and observing the dog standing and walking at different speeds (supplementary file, Table S4). The functional examination of the limb was performed using a procedure based on the FBAS (supplementary file, Tables S5–S16).

For hind limb examination, sedation with dexmedetomidine (3–5 µg/kg IM) and butorphanol (0.1 µg/kg IM) was used in order to perform the drawer test and the Finochietto test, also known as the jump test (an orthopedic test to assess meniscus tears in the stifle) [18].

2.2. Surgical Procedures

In Group 1, the Model XGEN by Securos® implant was used; the Porous® TTA implant was used in Group 2.

The surgeries were performed by two experienced surgeons. As we had two groups of fifteen animals, one surgeon performed seven surgeries using Porous TTA and eight using Model XGEN, whereas the other surgeon did eight surgeries using Porous TTA and seven using Model XGEN.

Both techniques have been previously described, but briefly:

Group 1: TTA with the Securos implant.

The patient was positioned in lateral recumbence so that the affected limb is lying flat on the table. The medial aspect of the proximal tibia is approached. A cranio-medial parapatellar incision is made from the patella to the medial saphenous vein.

The fascia is sharply incised and elevated until the tuberosity is medially and laterally visible. The patellar ligament is isolated by making an incision caudally and a small Gelpi retractor is used to protect it from the saw blade when performing the osteotomy.

The osteotomy line begins at the distal aspect of the tibial tuberosity and ends at the caudal arm of the Gelpi. The osteotomy must be curved gently in the distal tuberosity to minimize stress and avoid postoperative tibial fractures. Once the osteotomy is performed, the pre-contoured plate is placed with its cranial aspect parallel to the tuberosity and the screws are placed behind the cranial cortex. The distal screw should be positioned just above the osteotomy. Once the osteotomy cut is complete, the osteotomized tuberosity is spread apart to facilitate the TTA cage placement. Cancellous bone grafts can be collected from the tibial shaft and be placed later in the completed TTA cage. The width of the TTA cage was determined based on preoperative radiographs.

Finally, a 2.0 mm drill bit is used to fix the distal plate to the tibial shaft. The previously collected cancellous bone is now placed in the osteotomy gap (Figure 1a,b) [9].

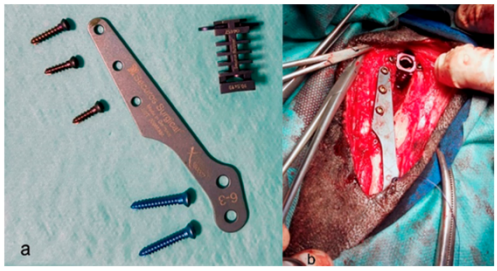

Figure 1. (**a**) View of the Securos implant. (**b**) View of the placed implant during the surgical procedure.

Group 2: TTA with the Porous® implant.

Before starting the surgery, the advancement of the tibial tuberosity should be measured.

The patient is positioned in lateral recumbence with the damaged stifle directly on the table. A medio-proximal approach to the tibia is performed. The incision starts over the patella and runs 1 cm distally to the end of the tibial tuberosity, and the proximal tibia is exposed. After drilling a distraction hole, an osteotomy is performed using a cutting guide. Then, the tibial tuberosity is slowly advanced distracting 1 mm per minute to avoid breakage. After this, the appropriate porous titanium wedge is placed to avoid cranial thrust. The wedge should be placed a few millimeters distally to the proximal aspect of the tuberosity. Finally, the plate is placed, fixing the tuberosity to the tibial diaphysis (Figure 2a,b) [19].

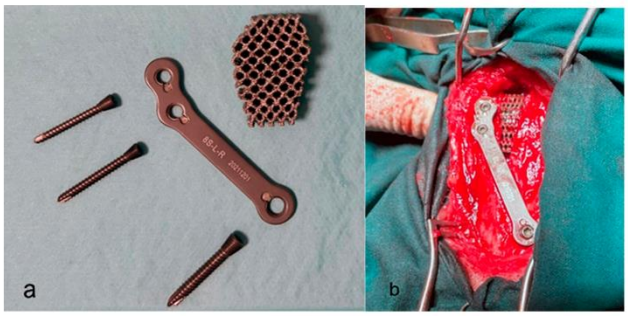

Figure 2. (**a**) View of the Porous implant. (**b**) View of the placed implant during the surgical procedure.

2.3. Postoperative Assessment

For OA assessment, radiographs were taken for all dogs on the day of surgery and one month and three months after surgery, with mediolateral and caudocranial projections. In the mediolateral projection, we assessed and scored the lips of the trochlea, proximal and distal poles of the patella, femoral condyles, tibial tuberosity, sesamoids bones of the gastrocnemius muscle and tibial plateau or proximal articular surface of the tibia. In the craniocaudal projection, we evaluated and scored the tibial plateau or articular surface proximal tibia, lateral epicondyle, medial epicondyle, intercondylar fossa of femur, head of the fibula and edge of the medial condyle of the tibia. The scoring values ranged from 0 to 3 points depending on the radiological signs of OA (0 points for no radiological signs of osteoarthritis, 1 point for mild osteoarthritis, 2 points for moderate osteoarthritis and 3 points for severe osteoarthritis). To determine the degree of total OA, the sum of the assigned score was be added to each of the anatomical indicated areas. This radiological assessment was performed by two veterinarians in each clinical case and each assessment score was averaged. Both veterinarians were experienced orthopedic surgeons. The values obtained by the two veterinarians were added to the final results table, placing the stifle in one of the following four groups: 0–2 points for stifles without radiological signs of osteoarthritis, 3–8 points for stifles with mild osteoarthritis, 9–18 points for stifles with moderate osteoarthritis and $\geq$18 points for stifles with severe osteoarthritis (supplementary file, Table S17).

Osteointegration (OI) was evaluated according to an increase in the width and the extent of radiolucent lines between the bone and implant over time in the patient. These could be a sign of a lack of OI. The formation of radiopaque lines at the points of osteotomy indicates proper OI [20]. In our study, the presence of radiopaque lines at the points of the osteotomy was considered as good OI (supplementary file, Table S18).

2.4. Experimental Design

The dogs were randomly assigned to each of the experimental groups. The groups were initially tested for comparability (supplementary file, Tables S1–S4); there were no

significant differences between the groups in any relevant variables before the treatments were applied. The variables used to assess the effect of each surgery were measured on an ordinal scale, with values ranging from 0 (good condition) to 3 (worst condition) and were summarized as median and quartiles. A comparison of the distributions of these variables between the two treatments was performed using the Wilcoxon–Mann–Whitney test for independent samples. To compare each treatment's effects before and after surgery, the Wilcoxon test for paired samples was used. The proportions (of gender, side of disease, pain, etc.) between groups were tested using the chi-squared test. McNemar's test was used to compare the proportion of dogs with good OI at one and three months after surgery.

We also calculated the length of time of each surgery for each dog (supplementary file, Table S21).

In all cases, a significance level of 0.05 was used.

3. Results

The comparison data of the characteristics and clinical findings of dogs in Groups 1 and 2 prior to the surgery is summarized in Table 1. Considering the *p*-values, there were no significant differences between the groups in any of the variables considered.

Table 1. Comparison of gender, side of the disease, and physical examination of dogs with CCLTs treated with two different TTA-based techniques.

Variable	Group 1 (n = 15)	Group 2 (n = 15)	p Value
Female	8 (53.3%)	7 (46.7%)	1.0000
Spayed	3 (20.0%)	5 (33.3%)	0.6800
Right stifle	6 (40.0%)	8 (53.3%)	0.7140
Pain	12 (80.0%)	11 (73.3%)	1.0000
Inflammation	13 (86.7%)	14 (93.3%)	1.0000
Joint leak	13 (86.7%)	12 (80.0%)	1.0000
Finochietto	5 (35.7%)	6 (37.5%)	1.0000
Drawer test			0.8560
Absent	3 (20.0%)	2 (13.3%)	
Present	8 (53.3%)	8 (53.3%)	
Clear	4 (26.7%)	5 (33.3%)	

The Bioarth Functional Scale scores prior to surgery are shown in Table 2. No significant differences were found between the groups in any of the variables considered.

Table 2. Mean and standard deviations of different variables using the Bioarth scale at baseline in each group.

Variable	Group 1	Group 2	p-Value
Changes in the affected limb while standing	1.60 ± 0.74	1.73 ± 0.70	0.5700
Changes in posture while getting up	1.00 ± 0.65	1.20 ± 0.68	0.4157
Lameness	2.13 ± 0.99	2.07 ± 0.96	0.8538
Lameness after 10 min of walk	1.67 ± 0.90	1.53 ± 0.99	0.7103
Resistance to walk	0.87 ± 0.92	0.80 ± 0.94	0.8065
Resistance to run and play	2.00 ± 0.53	1.60 ± 0.91	0.1363
Resistance to climb stairs	1.20 ± 0.94	1.40 ± 1.06	0.6115
Limitation to take small jumps	1.07 ± 0.70	1.07 ± 0.80	1.0000
Manual articular mobility of the stifle	1.33 ± 0.72	1.40 ± 0.74	0.7797

Table 2. *Cont.*

Variable	Group 1	Group 2	*p*-Value
Limitation of the articular flexion movement	0.87 ± 0.52	0.80 ± 0.56	0.7370
Limitation of the articular extension movement	0.87 ± 0.52	0.80 ± 0.56	0.7370
Muscular atrophy	0.60 ± 0.63	0.53 ± 0.52	0.8690

The results three months after the surgical procedure were also compared in Table 3. Considering the *p*-values, there were no significant differences between both TTA techniques for any of the variables considered.

Table 3. Mean and standard deviations of different variables using the Bioarth scale three months after surgery in each group.

Variable	Group 1	Group 2	*p*-Value
Changes in the affected limb while standing	0.33 ± 0.49	0.20 ± 0.41	0.4326
Changes in posture while getting up	0.47 ± 0.52	0.53 ± 0.64	0.8871
Lameness	0.73 ± 1.03	0.80 ± 1.01	0.7840
Lameness after 10 min of walk	0.33 ± 0.82	0.33 ± 0.49	0.5182
Resistance to walk	0.40 ± 0.91	0.13 ± 0.52	0.3087
Resistance to run and play	0.33 ± 0.62	0.33 ± 0.49	0.8153
Resistance to climb stairs	0.27 ± 0.46	0.13 ± 0.35	0.3856
Limitation to take small jumps	0.00 ± 0.00	0.13 ± 0.35	0.1641
Manual articular mobility of the stifle	0.27 ± 0.59	0.13 ± 0.52	0.3431
Limitation of the articular flexion movement	0.13 ± 0.35	0.13 ± 0.35	1.0000
Limitation of the articular extension movement	0.07 ± 0.26	0.07 ± 0.26	1.0000
Muscular atrophy	0.33 ± 0.62	0.13 ± 0.35	0.3554

Raw Bioarth scale data can be found in the Supplementary Material (supplementary file, Tables S5–S16).

Radiologically, there were almost no changes in OA during the three months after surgery. There were only two dogs (#1 and #22) that slightly increased their score (supplementary file, Table S17). Regarding the OI of the implant in the first and third months after surgery (supplementary file, Table S18), there were no significant differences between the two techniques.

Regarding post-surgical complications, only one minor complication was present in one dog from Group 1 (superficial wound) and there was one major complication in each group (implant failure and avulsion of tibial crest, respectively) (supplementary file, Tables S19 and S20).

Both procedures took a similar length of time to be performed (43.26 vs. 43.60 min) (supplementary file, Table S21).

4. Discussion

Surgical joint stabilization to avoid OA progression in the CCLT and the restoration of limb function is still challenging for clinicians and researchers. Until now, none of the surgical procedures have been shown to completely fulfill these aspects [21]. In the present study, we compared the effectiveness of two different TTA-based surgical techniques to treat CCLTs.

Vezzoni et al. showed that 71% of CCL injuries are degenerative and 29% are caused by trauma; in both cases, the tear was complete [22]. In our study, we observed that 13% of CCL injuries were caused by trauma and 87% were degenerative.

The percentage of dogs with a CCLT in our study match with the values from Johnson et al. (1.55%), Whitehair et al. (1.82%) and Witsberger et al. (2.55%) [23–25]. We found 45 cases of CCLT in a total of 2400 dogs, a percentage of 1.87%, which is similar to the above studies.

The efficacy of TTA has been widely proven since 2004 when the technique was first described [9]. Many years later, TTA is considered a successful surgery to treat CCLT [10].

There are many different parameters we may use to compare the effectiveness of surgical techniques to treat CCLTs. One study used a pressure platform analysis, which is an objective parameter, performed prior to surgery and at four different postoperative time points to obtain a short-term comparison of tibial tuberosity advancement and tibial plateau levelling osteotomy (TPLO) [26]. Livet et al. used radiographic examination, lameness score evaluation and gait analysis to compare outcomes associated with TPLO and TTA [27]. These parameters are subjective but in very relevant. Another study critically reviewed the available literature focused on the preoperative planning, surgical procedure, follow-up and complications of CCLTs using different tibial tuberosity advancement techniques [28]. This study concluded that nearly 90% of the stifles examined in short-, mid- and long-term follow-ups showed full and acceptable functionality. It did not find any significant differences between TTA techniques. In our opinion, in order to compare very similar techniques, the validation of any results should be obtained from homogeneous groups. For this reason, we compared multiple characteristics of the dogs from both groups (gender, lameness in the affected limb, proportion of dogs with pain, etc.), finding no significant differences between the groups.

Regarding the techniques compared in our study, one study demonstrated the effectiveness of the Porous TTA in 61 dogs, which had a minor complication rate of 47.69% after 3 weeks, 10.77% after 6 weeks and 4% after 12 weeks of surgical intervention [13].

The Securos TTA is similar to the modified Maquet TTA; however, in this case, the tibial tuberosity is completely cut, leaving the Maquet hole apart. It has been concluded that the modified Maquet TTA obtains similar outcomes and complication rates when compared with traditional TTA [10]. In our case, the comparison of initial values between groups for all the physical variables of the animals showed no significant differences between groups, as all the p-values were greater than 0.05.

Regarding the evolution of OA, one study compared the OA changes in 33 stifles from 24 dogs treated with TTA and TPLO [29]. They concluded that the OA had progressed a little bit more in TTAs than in TPLOs but that the difference was not significant. In our study, only two dogs from the first group showed a minimal progression of OA, allowing us to conclude that there were also no significant differences between the TTA techniques.

Concerning the OI of the implants, we also obtained very good results for both groups after 1 month (86.7%) and after 3 months (93.3%). This fact is in concordance with a previous study, proving that porous TTA implants show excellent OI and osteoconduction properties [30].

In our study, we also compared the presence of complications when using both techniques. A previous study by Matchwick et al. reported a complications rate of 15.2% in TTAs performed by six different non-specialized surgeons, where 7.5% were major and 7.7% were minor complications [31]. Costa et al. obtained a complications rate of 13.4%, where 1% had implant failure, 1.2% had patella luxation and 0.9% had tibial tuberosity fractures [32]. They also concluded that complications are uncommon when performing TTAs. In our case, we believe that both major complications were due to the same problem: on the first surgeries using the Porous implant procedure, the osteotomy was made too close to the external cortical of the tibia. We realized this caused the avulsion of the tibia. After correcting this issue, the problem stopped occurring for the subsequent surgeries.

Finally, we compared surgery times in both groups, and we can confirm that there are no significant differences between them.

Although we tried to provide a sound study design, our study has some limitations. The first limitation is that the study only assesses a three-month evolution and problems affecting implant stability and/or OA progression may arise over a longer period of time. Second, the assessment of the functional status prior to and after surgery should have improved with the objective methods based on kinetic and kinematic parameters, as shown by other authors [32]. However, this was not possible because these methods are limited to animals of a certain size and our group was very heterogeneous and included patients of small sizes. Lastly, a larger number of patients in our study would have had given greater statistical significance. However, it was challenging to schedule the necessary reviews and reevaluations to accommodate the patients' owners.

5. Conclusions

After comparing both groups 3 months post-surgery, we can conclude that the functional recuperation is similar for both procedures. This study also shows that the OI of the implants after 3 months is correct in both procedures. We also observed no progression of OA in both groups; therefore, we believe that there should be future radiologic and clinical control assessments to determine the long-term effects of these procedures. Minimal complications were noticed; therefore, we can confirm that both procedures are safe in a short-term follow-up.

Supplementary Materials: The following supporting information can be downloaded at: https://www.mdpi.com/article/10.3390/ani13223453/s1, The supplementary *doc file contains additional tables and raw data.

Author Contributions: Conceptualization, J.R.-A. and J.M.G.-O.; methodology O.R. and P.F.; investigation, P.F. and O.R.; resources, J.M.G.-O., I.P. and M.R.-P.; writing—original draft preparation P.F., O.R. and M.R.-P. writing—review and editing, J.M.V., J.R.-A. and I.P. All authors have read and agreed to the published version of the manuscript.

Funding: This research received no external funding.

Institutional Review Board Statement: Ethical review and approval were waived for this study because all the animals had owners who were informed of the study and gave written consent to participate and the animals received standard surgical procedures according to their disease.

Informed Consent Statement: Informed consent was obtained from each dog owner involved in the study.

Data Availability Statement: Data are contained within the article and supplementary materials.

Acknowledgments: Thanks to the dog owners for their cooperation.

Conflicts of Interest: The authors declare no conflict of interest.

References

1. Knebel, J. Etiology, pathogenesis, diagnostics and therapy of cranial cruciate ligament rupture in dogs. *Tierärztliche Prax. Ausg. K Kleintiere/Heimtiere* **2014**, *42*, 36–47.
2. Giansetto, T.; Picavet, P.; Lefebvre, M.; Balligant, M. Determination of the stifle angle at standing position in dogs. *Vet. Sci.* **2022**, *9*, 644. [CrossRef] [PubMed]
3. Lapman, T.J.; Lund, E.M.; Lipowitz, A.J. Cranial cruciate disease: Current status of diagnosis, surgery, and risk for disease. *Vet. Comp. Orthop. Traumatol.* **2003**, *16*, 122–126.
4. Anderst, W.J.; Tashman, S. The association between velocity of the center of closest proximity on subchondral bones and osteoarthritis progression. *J. Orthop. Res.* **2009**, *27*, 71–77. [CrossRef] [PubMed]
5. Pozzi, A.; Litsky, A.S.; Field, J. Effect of medial meniscal release on tibial translation after tibial plateau leveling osteotomy. *Vet. Surg.* **2006**, *35*, 486–494. [CrossRef]
6. Pozzi, A.; Litsky, A.S.; Field, J.; Apelt, D.; Meadows, C.; Johnson, K.A. Pressure distributions on the medial tibial plateau after medial meniscal surgery and tibial plateau levelling osteotomy in dogs. *Vet. Comp. Orthop. Traumatol.* **2008**, *21*, 8–14. [CrossRef]

7. Lampart, M.; Knell, S.; Pozzi, A. A new approach to treatment selection in dogs with crucial ligament rupture: Patient—Specific treatment recommendations. *Schweiz. Arch. Tierheilkd.* **2020**, *162*, 345–364. [CrossRef]
8. Spinella, G.; Arcamone, G.; Valentini, S. Cranial Cruciate Ligament Rupture in Dogs: Review on Biomechanics, Etiopathogenetic Factors and Rehabilitation. *Vet. Sci.* **2021**, *8*, 186. [CrossRef]
9. Montavon, P.M. Tibial tuberosity advancement (TTA) for the treatment of cranial cruciate disease in dogs: Evidence, technique and initial clinical results. In Proceedings of the 12th ESVOT Congress, Munich, Germany, 10–12 September 2004; pp. 254–255.
10. Retallack, L.M.; Daye, R.M. A modified Maquet-tibial tuberosity advancement technique for treatment of canine cranial cruciate ligament disease: Short term outcome and complications. *Vet. Surg.* **2018**, *47*, 44–51. [CrossRef]
11. Zhalniarovich, Y.; Mieszkowska, M.; Przyborowska-Zhalniarovich, P.; Głodek, J.; Sobolewski, A.; Waluś, G.; Adamiak, Z. A novel tibial tuberosity advancement technique with cranial implant fixation (TTA CF): A pilot study in sheep. *Vet. Res.* **2018**, *14*, 231. [CrossRef]
12. Etchepareborde, S.; Brunel, L.; Bollen, G.; Balligand, M. Preliminary experience of a modified Maquet technique for repair of cranial cruciate ligament rupture in dogs. *Vet. Comp. Orthop. Traumatol.* **2011**, *24*, 223–227. [PubMed]
13. Bernardi-Villavicencio, C.; Jimenez-Socorro, A.N.; Rojo-Salvador, C.; Robles-Sanmartin, J.; Rodriguez-Quiros, J. Short-term outcomes and complications of 65 cases of porous TTA with flange: A prospective clinical study in dogs. *Vet. Res.* **2020**, *16*, 279. [CrossRef] [PubMed]
14. Crovace, A.M.; Staffieri, F.; Monopoli, D.; Artiles, A.; Fracassi, L.; Crovace, A.; Lacitignola, L. Role of Tibial Tuberosity Fracture/Fissure through the Maquet Hole in Stifle Osteoarthritis after Porous Tibial Tuberosity Advancement in Dogs at Mid-Term Follow-Up. *Vet. Sci.* **2019**, *7*, 1. [CrossRef] [PubMed]
15. Millis, D.L. *Canine Rehabilitation and Physical Therapy*, 2nd ed.; Saunders: Philadelphia, PA, USA, 2004; pp. 211–227.
16. Cuervo, B.; Rubio, M.; Sopena, J.; Dominguez, J.M.; Vilar, J.; Morales, M.; Cugat, A.; Carrillo, J.M. Hip osteoartritis in dogs: A randomized study using mesenquimal stem cells from adipose tissue and plasma rich in growth factors. *Int. J. Mol. Sci.* **2014**, *15*, 13437–13460. [CrossRef]
17. Vilar, J.M.; Cuervo, B.; Rubio, M.; Sopena, J.; Domínguez, J.M.; Santana, A.; Carrillo, J.M. Effect of intraarticular inoculation of mesenchymal stem cells in dogs with hip osteoarthritis by means of objective force platform gait analysis: Concordance with numeric subjective scoring scales. *Vet. Res.* **2016**, *12*, 223. [CrossRef]
18. Espejo-Baena, A.; Espejo-Reina, A.; Espejo-Reina, M.J.; Ruiz-Del Pino, J. The Finochietto sign as patognomonic of ramp lesión of the medial meniscus. *Arthrosc. Tech.* **2020**, *9*, e549–e552. [CrossRef]
19. Trisciuzzi, R.; Fracassi, L.; Afonso Martin, H.; Monopoli, D.; Amat, D.; Santo-Ruiz, L.; De Palma, E.; Crovace, A. 41 cases of treatment of craneal cruciat ligament ruptura with Porous TTA. Three years of follow up. *Vet. Sci.* **2019**, *6*, 18. [CrossRef]
20. Bjorn, M.; Augat, P.; Berninger, M.; Keppler, L.; Simon, G.; Von Rueden, C.; Birkenmaier, C.; Schipp, R.; Becker, J. Influence of different CCD angles on osseointegration and radiological changes after total hip arthroplasty of a triple wedge shape cementeless femoral stem: A prospective cohort study. *Int. Orthop.* **2023**, *47*, 1747–1755.
21. Muir, P. *Advances in the Cranial Crutial Ligament*, 1st ed.; Wiley Online Library: Hoboken, NJ, USA, 2017; pp. 217–242.
22. Vezzoni, A.; Demaria, M.; Corbari, A. Non-traumatic cranial cruciate ligament injuries. In Proceedings of the 1st World Veterinary Orthopedics Congress of the ESVOT/VOS, Munich, Germany, 5–8 September 2002.
23. Johnson, J.A.; Austin, C.; Breur, G.J. Incidence of canine appendicular musculoeskeletal disorders in 16 veterinary teaching hospitals from 1980–1989. *Vet. Comp. Orthop. Traumatol.* **1994**, *7*, 56–69. [CrossRef]
24. Whitehair, J.G.; Vasseur, P.B.; Willits, N.H. Epidemiology of cranial cruciate ligament rupture in dogs. *J. Am. Vet. Med. Assoc.* **1993**, *203*, 1016–1019.
25. Witsberger, T.H.; Villamil, J.A.; Schultz, L.G.; Hahn, A.W.; Cook, J.L. Prevalence of and risk factors for hip dysplasia and cranial cruciate ligament deficiency in dogs. *J. Am. Vet. Med. Assoc.* **2008**, *232*, 1818–1824. [CrossRef]
26. Ferreira, M.P.; Ferrigno, C.R.; de Souza, A.N.; Caquias, D.F.; de Figueiredo, A.V. Short-term comparison of tibial tuberosity advancement and tibial plateau levelling osteotomy in dogs with cranial cruciate ligament disease using kinetic analysis. *Vet. Comp. Orthop. Traumatol.* **2016**, *29*, 209–213. [PubMed]
27. Livet, V.; Baldinger, A.; Viguier, É.; Taroni, M.; Harel, M.; Carozzo, C.; Cachon, T. Comparison of Outcomes Associated with Tibial Plateau Levelling Osteotomy and a Modified Technique for Tibial Tuberosity Advancement for the Treatment of Cranial Cruciate Ligament Disease in Dogs: A Randomized Clinical Study. *Vet. Comp. Orthop. Traumatol.* **2019**, *32*, 314–323. [CrossRef] [PubMed]
28. Aragosa, F.; Caterino, C.; Della Valle, G.; Fatone, G. Tibial Tuberosity Advancement Techniques (TTAT): A Systematic Review. *Animals* **2022**, *12*, 2114. [CrossRef] [PubMed]
29. Moore, E.V.; Weeren, R.; Paek, M. Extended long-term radiographic and functional comparison of tibial plateau leveling osteotomy vs tibial tuberosity advancement for cranial cruciate ligament rupture in the dog. *Vet. Surg.* **2020**, *49*, 146–154. [CrossRef] [PubMed]
30. Matchwick, A.I.M.; Bridges, J.P.; Scrimgeour, A.B.; Worth, A.J. A retrospective evaluation of complications associated with forkless tibial tuberosity advancement performed in primary care practice. *Vet. Surg.* **2021**, *50*, 121–132. [CrossRef]

31. Costa, M.; Craig, D.; Cambridge, T.; Sebestyen, P.; Su, Y.; Fahie, M.A. Major complications of tibial tuberosity advancement in 1613 dogs. *Vet Surg.* **2017**, *46*, 494–500. [CrossRef]
32. Della Valle, G.; Caterino, C.; Aragosa, F.; Micieli, F.; Costanza, D.; Di Palma, C.; Piscitelli, A.; Fatone, G. Outcome after Modified Maquet Procedure in dogs with unilateral cranial cruciate ligament rupture: Evaluation of recovery limb function by use of force plate gait analysis. *PLoS ONE* **2021**, *16*, e0256011. [CrossRef]

4.2. Métodos Objetivos:

El análisis objetivo de la biomecánica para detectar cojeras en perros implica una variedad de métodos y herramientas que se utilizan para evaluar la marcha y el movimiento del animal de manera cuantitativa y objetiva (Gundersen K y cols., 2022).

Estos métodos de análisis se pueden dividir en cinéticos y cinemáticos.

4.2.1. Análisis cinéticos:

La cinética es una subdisciplina de la biomecánica que se especializa en el estudio del movimiento, enfocándose principalmente en las fuerzas que lo originan y modulan.

Entre estas fuerzas están:

- **Fuerzas de reacción del suelo (GRF, por sus siglas en inglés):** son de especial relevancia debido a su frecuente aplicación en estudios biomecánicos. La GRF es la fuerza que ejerce el suelo sobre un cuerpo que está en contacto con él, Esta fuerza es fundamental para entender la biomecánica del movimiento en animales, así como para evaluar la locomoción y la salud ortopédica de los mismos (McCarthy y cols., 2021).

- **Pico de Fuerza Vertical (PVF, por sus siglas en inglés)**: El PVF en biomecánica veterinaria consiste en la capacidad máxima de un animal para ejercer fuerza vertical, típicamente expresada en unidades de Newtons (N). Esta medida es fundamental para evaluar la aptitud de los animales en actividades como saltos, carreras y otras acciones que involucran fuerza vertical, siendo crucial tanto en su comportamiento natural como en actividades atléticas (MarcFarlane y cols., 2018; Clayton y cols., 2017; Wilson y cols., 2001; Back y cols., 2002).

- **Impulso Vertical (VI, por sus siglas en inglés)**: El VI en biomecánica veterinaria hace referencia al resultado del producto entre la magnitud de la fuerza y la duración del tiempo de apoyo (López 2019). Dicho índice resulta valioso para evaluar la eficiencia del movimiento en animales, así como su capacidad para generar fuerza en relación con la velocidad en diversas actividades físicas, como el galope en caballos, el salto en perros, entre otras (Van Weeren y cols., 2017; Lopes y cols., 2020).

- **Centro de Masas (COM, por sus siglas en inglés)**: Se describe como la representación en forma de vector que resulta de la suma de las trayectorias de todos los segmentos corporales implicados en la generación de fuerzas (Winter y cols., 1991).

- **Centro de Presiones (COP, por sus siglas en inglés)**: Se refiere a la proyección vertical del centro de gravedad sobre la base de apoyo, lo cual es fundamental para el análisis del equilibrio y la estabilidad (Baratto y cols., 2002).

4.2.1.1 Plataformas de fuerza:

Son dispositivos sensibles que registran las fuerzas ejercidas por las extremidades del perro durante la marcha, lo que facilita la evaluación de la distribución de la carga y la simetría de la marcha (Mölsä y cols., 2010).

Figura 13. Plataforma dinamométrica de fuerza con 4 sensores de la marca Pasco®

Las plataformas de fuerza se utilizan en una variedad de aplicaciones en medicina veterinaria, investigación biomecánica y rehabilitación animal, incluyendo:

Evaluación del paso: Las plataformas de fuerza permiten analizar la forma en que un animal distribuye su peso corporal durante el movimiento, lo que es fundamental para diagnosticar y monitorizar trastornos musculoesqueléticos, lesiones neurológicas o cambios en la biomecánica de la marcha (Lascelles y cols., 2006).

Análisis funcional (dinámico): Estos dispositivos proporcionan datos precisos sobre la fuerza y el tiempo de contacto de las extremidades con la superficie durante actividades como el salto, la carrera o el aterrizaje. Este aspecto es fundamental para entender la mecánica del movimiento y optimizar el rendimiento en animales atletas, permitiendo un enfoque más preciso en la mejora de la eficiencia y la prevención de lesiones. (Pereira y cols., 2019).

Rehabilitación animal: En el campo de la fisioterapia y rehabilitación veterinaria, las plataformas de fuerza se utilizan para evaluar la progresión del tratamiento, monitorear la recuperación de lesiones musculoesqueléticas y diseñar programas de ejercicio específicos para mejorar la fuerza y la función muscular (Roush y cols., 2010).

Investigación científica: Las plataformas de fuerza son herramientas valiosas en estudios de investigación para comprender la biomecánica de diversas especies animales, investigar la eficacia de tratamientos médicos o quirúrgicos y desarrollar nuevas técnicas de evaluación y rehabilitación (Schwarz y cols., 2012).

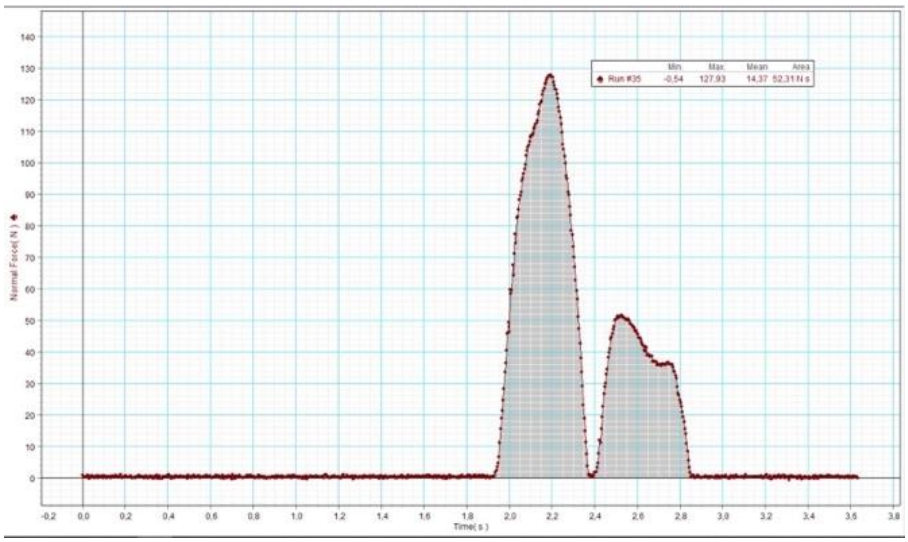

Figura 14. Gráfica resultante de una plataforma de fuerza. Fuente: Hospital Clínico Veterinario ULPGC

4.2.1.2. Plataforma de presión:

Es un sistema equipado con sensores de presión distribuidos en su superficie, diseñado para registrar la distribución de la carga y las fuerzas aplicadas por las extremidades del canino durante la marcha. Este dispositivo proporciona mediciones cuantitativas de la presión ejercida en diferentes áreas de contacto con la plataforma, permitiendo un análisis objetivo de la biomecánica de la marcha.

La información recopilada se utiliza para identificar desequilibrios en la carga de peso entre las extremidades, así como para detectar anomalías en el patrón de marcha que puedan indicar la presencia de cojeras u otras disfunciones locomotoras (Evan y cols 2005; Waltons y cols 2014; Vilar y cols 2013).

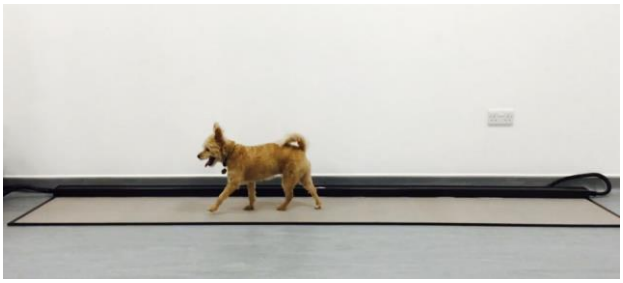

Figura 15. Las plataformas de presión de gran longitud (hasta 2 metros), permiten el registro de varios pasos consecutivos. Plataforma Tekscan. Fuente: https://twitter.com/vetbiomechanics/status/666602613715173376

Es un dispositivo extensamente utilizado en la investigación biomecánica, además de su aplicación en el entorno clínico, habiendo sido incorporado gradualmente en los últimos años al arsenal de herramientas para la obtención de parámetros derivados de las GRF.

Su característica principal radica en la presencia de múltiples sensores distribuidos a lo largo del área de estudio, lo que permite la recopilación de datos específicos de regiones particulares. De modo similar a las plataformas de fuerza, la velocidad de adquisición de datos puede ajustarse según las necesidades (Oosterlinck y cols., 2010a).

Estos dispositivos no representan un costo significativamente mayor en comparación con sus predecesores, pero presentan una ventaja considerable al ser capaces de cubrir áreas extensas (hasta 2 metros de longitud), lo que facilita el registro de datos de múltiples puntos de apoyo.

Otra aplicación relevante de estos análisis radica en la capacidad de obtener, además de los parámetros tradicionales como el PVF y el VI, mediciones adicionales de creciente importancia, tales como la distribución de la carga corporal y las presiones media y máxima ejercidas durante el apoyo. Cuando estos parámetros se analizan de manera integrada, configuran el estudio podobarométrico, una herramienta avanzada para la evaluación biomecánica del pie, que proporciona información detallada sobre la dinámica de la distribución de fuerzas y la eficiencia del soporte plantar (Oosterlinck y cols., 2011).

En definitiva, el análisis cinético está considerado el “gold standard” para la evaluación de la marcha. Si hay una patología que genera alteraciones más graves de la marcha, esta sería la amputación de un miembro de forma traumática o como tratamiento quirúrgico en casos de tumores que afectan a las extremidades. En este sentido parece interesante investigar en profundidad dichas alteraciones de la marcha con esta tecnología, y es que la amputación de miembros ya sea por lesión o como consecuencia de un procedimiento quirúrgico de salvamento, compromete el rendimiento locomotor de los cuadrúpedos y afecta el funcionamiento de todo el sistema musculoesquelético. Como consecuencia, los perros amputados desarrollan mecanismos compensatorios

en un intento de caminar sin perder el equilibrio (Black, 1970; Fuchs y cols., 2015; Galindo-Zamora y cols., 2016).

En términos generales, se ha informado una excelente recuperación funcional cuando se ha amputado un miembro torácico o pelviano en perros (Carberry y Harvey, 1987; Withrow y Hirsch, 1979; Kirpensteijn y cols., 1999); aunque, teóricamente, en la mayor parte de los casos, la postura y la capacidad locomotora de los perros amputados pueden modificarse (Ben-Amotz y cols., 2020; Raske y cols., 2015).

Sin embargo, la literatura científica que informa de manera objetiva sobre los cambios en la marcha del perro y las variaciones cinéticas debido a la redistribución de las fuerzas sigue siendo muy escasa (Goldner y cols., 2015). Específicamente, las variaciones cinéticas en perros amputados de miembros torácicos a menudo proporcionan la fuerza vertical máxima y el impulso vertical clásicos (Kirpensteijn y cols., 2000; Jarvis y cols., 2013).

Para comprender completamente la adaptación musculoesquelética a la marcha trípeda, sería interesante necesario complementar los datos clásicos de la GRF con nuevos parámetros adicionales.

Figura 16. Examen postural de un perro amputado, en una plataforma de presión. Fuente: Hospital Veterinario de la ULPGC

Parece lógico pensar que estas adaptaciones funcionales que alteran la dinámica normal de las unidades musculoesqueléticas (tendones, músculos, ligamentos y articulaciones) deberían tener algunas consecuencias clínicas. En términos relativos, el miembro restante debería soportar más peso después de una amputación de miembro torácico que la extremidad restante después de una amputación de miembro pelviano (Kirpensteijn y cols., 2000), lo que significa que los amputados de miembros torácicos son más propensos a sufrir lesiones causadas por sobrecarga.

Por esta razón, es necesario comprender las adaptaciones biomecánicas específicas en perros amputados (Fuchs y cols., 2014; Carberry y cols., 1987; Kirpensteijn y cols., 1999). En este sentido, se planteó la hipótesis de que la amputación cambiaría la magnitud no solo de las GRF verticales, sino también en el plano horizontal y sus impulsos correspondientes; en esta situación, también debería aumentar la carga sobre las extremidades restantes (especialmente la contralateral) y desplazar el centro de gravedad del perro lejos del sitio de amputación (Kirpensteijn y cols., 2000).

Aunque se basan en diferentes principios físicos, se asume que el COP es la proyección vertical del centro de gravedad sobre el plano de soporte (Blaszcyk y cols., 1994). Las modificaciones del COP se miden actualmente con plataformas de presión; estos dispositivos, gracias a sus múltiples sensores, están validados para estudiar el balance del COP en perros sanos y cojos, tanto en la fase de locomoción como en la posición estática. (Charalambous y cols., 2023; Virag y cols., 2022).

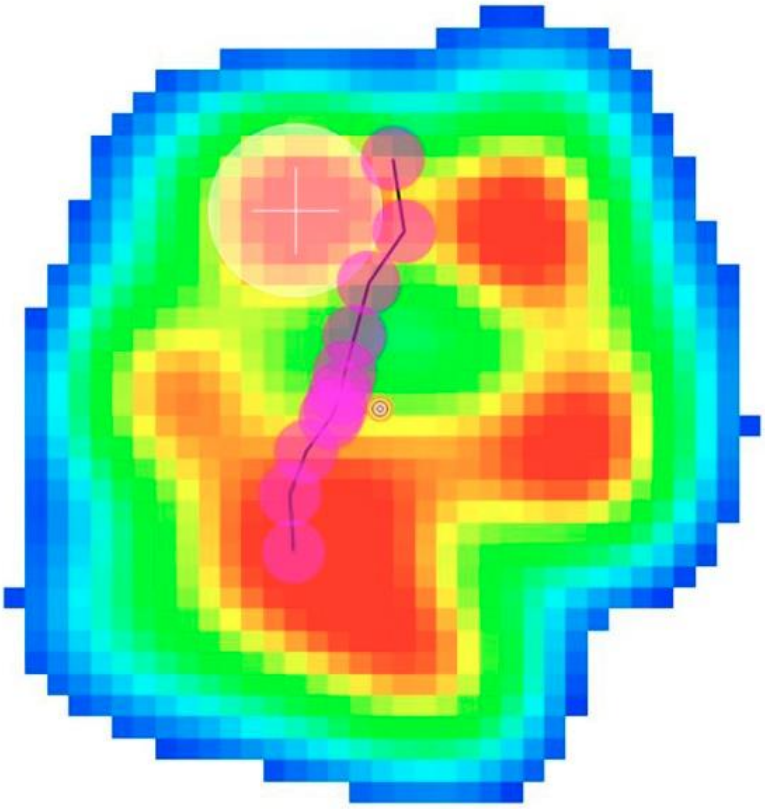

Figura 17. Presión de la pata registrada durante la fase de apoyo de un perro amputado. Los puntos rosa representan la ruta COP. La parte superior de la imagen es craneal, la inferior es caudal, la derecha es medial y la izquierda es lateral. El trayecto empieza más caudalmente a nivel de la almohadilla metacarpiana y discurre cranealmente; esto demuestra que cuando la extremidad hace contacto con el suelo, se coloca más cranealmente que unas extremidades anteriores sanas. Fuente: Figueirinhas y cols., 2024

Con el propósito de investigar en profundidad los cambios dinámicos (marcha) y estáticos (posturales) en la especie canina tras la amputación de un miembro torácico, se ha decidido llevar a cabo un estudio que permita la obtención de diversos parámetros biomecánicos, tales como el GRF, el VI, y el COP en estática, mediante la utilización simultánea de plataformas de fuerza y presión.

ARTÍCULO #2

Rodriguez, O.; Regueiro-Purriños, M.; Figueirinhas, P.; Gonzalo-Orden, J.M.; Prada, I.; Vilar, J.M.; Millán, L.; Rodríguez-Altónaga, J.

Dynamic and Postural Changes in Forelimb Amputee Dogs: A Pilot Study.

Animals **2024**, *14*, 1960. https://doi.org/10.3390/ani14131960

JCR Impact factor: 2.7

Cuartil: Q1

Grupo: Veterinary sciences

Posición: 16/167

animals

MDPI

Article

Dynamic and Postural Changes in Forelimb Amputee Dogs: A Pilot Study

Oliver Rodriguez [1], Marta Regueiro-Purriños [2], Pedro Figueirinhas [1], José Manuel Gonzalo-Orden [2], Iván Prada [2], José Manuel Vilar [1,*], Lorena Millán [2] and José Rodríguez-Altónaga [2]

[1] Departamento de Patología Animal, Universidad de Las Palmas de Gran Canaria, Trasmontaña S/N, 35416 Arucas, Spain; oliver.rodriguez@ulpgc.es (O.R.); pedro.figueirinhas@fpct.ulpgc.es (P.F.)
[2] Departamento de Medicina y Cirugía Veterinaria, Campus de Vegazana, Universidad de León, 24071 León, Spain; mregf@unileon.es (M.R.-P.); jmgono@unileon.es (J.M.G.-O.); vetivi@hotmail.com (I.P.); lmilv@unileon.es (L.M.); jarodma@unileon.es (J.R.-A.)
* Correspondence: jose.vilar@ulpgc.es

Simple Summary: It is assumed that dogs with an amputated limb experience difficulty with their tripedal gait in terms of energy and balance. This is especially true when the missing limb is a forelimb. The aim of our study is to objectively deepen the knowledge about biomechanical (postural and dynamic) modifications in forelimb amputee dogs by using force and pressure platforms. Based on our results, the amputee dogs in our study had increased vertical, braking and propulsion forces and their respective impulses on their remaining limb also increased, except for the propulsion impulse during walking. The amputee dogs also had increased peak pressure, mean pressure and area of the paw. Surprisingly, the amputee dogs were able to preserve the same level of balance when compared with the control, four-legged dogs of the same breed at stance. Although amputee dogs were able to preserve balance during stance and gait, there was a higher force (and pressure) demand on the remaining forelimb. This situation may potentially predispose these animals to injury caused by an overload of the anatomical structures involved in weight bearing.

Abstract: The amputation of a limb in quadrupeds can overload the remaining limbs, especially the contralateral one. The compensatory effort is especially high if it is a forelimb. It is, therefore, important to objectively know the changes in weight redistribution that occur in the animal while walking and standing still. With this objective, static (postural) and dynamic kinetic examinations were carried out on five French bulldogs with an amputated forelimb and five intact French bulldogs. For this examination, force and pressure platforms were used. The results were statistically compared using the student *t*-test. The parameters derived from the ground reaction forces were significantly higher in the amputee group. Surprisingly, postural examination showed that amputated dogs reached the same stability as healthy ones. Tripedal support in dogs does not objectively imply a loss of balance in quantitative terms; although the increase in force used by the remaining limb, as well as its altered cranial disposition during the support phase, may potentially predispose the animal to additional injuries in the future due to an overuse of different musculoskeletal units.

Keywords: limb amputation; force; pressure; dog

Citation: Rodriguez, O.; Regueiro-Purriños, M.; Figueirinhas, P.; Gonzalo-Orden, J.M.; Prada, I.; Vilar, J.M.; Millán, L.; Rodríguez-Altónaga, J. Dynamic and Postural Changes in Forelimb Amputee Dogs: A Pilot Study. *Animals* **2024**, *14*, 1960. https://doi.org/10.3390/ani14131960

Academic Editor: Cynthia M. Otto

Received: 20 May 2024
Revised: 29 June 2024
Accepted: 1 July 2024
Published: 2 July 2024

1. Introduction

Limb amputation due to an injury or as a consequence of a salvage surgical procedure compromises a quadruped's locomotor performance and affects the functioning of the whole musculoskeletal system. Therefore, amputee dogs develop compensatory mechanisms in order to walk without losing balance [1–3]. Nevertheless, and in general terms, when a dog's fore or hindlimb has been amputated, an excellent functional recovery has been reported [4–6], although the posture and mobility of amputee dogs are modified in most instances [7,8]

Nevertheless, there is little scientific literature objectively reporting on the changes in a dog's gait and kinetic variations due to the redistribution of force [9]. Specifically, kinetic variations in forelimb amputee dogs often provide a classic peak vertical force (PVF) and vertical impulse (VI) [10,11]; however, no references regarding postural exams in amputee dogs could be found by this research team. In order to fully understand the musculoskeletal adaptation of the tripedal gait, it is necessary to complement the abovementioned PVF and VI with new, additional parameters. It is also crucial that we understand how these functional adaptations alter the normal dynamics of musculoskeletal units (tendons, muscles, ligaments, joints. . .) to better understand possible clinical consequences.

For instance, the remaining forelimb carries more weight after a forelimb amputation than a remaining hindlimb would after a hindlimb amputation [10], which means that forelimb amputees are more prone to suffer injuries resulting from weight overload; specifically, after the amputation of a forelimb, at the level of the contralateral limb's triceps brachii and deltoid muscles, the load bearing increases, leading to fatigue and potential overuse injuries. In addition, the latissimus dorsi and erector spinae muscles of the trunk and spine have to work harder to stabilize and move the body, often resulting in back pain and muscle fatigue. But muscular and articular consequences are also suffered by the biceps femoris, quadriceps femoris and gluteus medios muscles of the hindlimb because of their increased strain to aid in locomotion and balance [2,12–15]. For this reason, it is necessary to understand the specific biomechanical adaptations in forelimb amputated dogs [4,6,12]. It was hypothesized that the amputation would change not only the magnitude of the vertical GRFs, but also the horizontal plane and their corresponding impulses. If this scenario were true, it would also increase the load on the remaining limbs, especially the contralateral limbs, and move the dog's center of gravity away from the site of amputation [10].

Using the basic principles of physics, the center of pressure (COP) is assumed to be the vertical projection of the center of gravity over the plane of support [16]. Modifications of the COP are currently measured with pressure platforms; these devices utilize multiple sensors to study the COP sway in sound and lame dogs, both at walk and at standing [17,18]. In this sense, our hypothesis is that forelimb amputee dogs alter a number of parameters at walk and even when standing still, and these changes could be objectively assessed.

The aim of this paper is to objectively detect and measure the dynamic (gait) and static (postural) changes in single forelimb amputee French bulldogs when compared with sound dogs of the same breed and conformation. With this aim, different parameters (vertical and horizontal forces and impulses, COP pathway, statokinesiogram, etc.) will be obtained by using force and pressure platforms.

2. Materials and Methods

2.1. Animals

A total of 10 adult, client-owned French bulldogs were enrolled in this retrospective, controlled study. A total of 5 dogs had a single forelimb amputation, and the other 5 dogs were sound and served as the control group. Both groups had 2 male and 3 female dogs.

2.1.1. Amputee Group

The 5 dogs comprising the amputee group had their forelimbs amputated for the following reasons: sarcoma (n = 3) and trauma (n = 2). These dogs were clinical cases from the Hospital Clinico Veterinario of the University of Las Palmas de Gran Canaria from February 2021 to June 2023 and were retrospectively included in this study. All animals received standard forelimb amputation including scapulectomy. Dogs unable to walk comfortably or that had any orthopedic and/or neurological abnormal findings in any of the remaining limbs on previous clinical examination performed 1 week before the force and pressure platform analyses were excluded from the study. These analyses were performed a minimum of 4 and a maximum of 7 months post amputation. Age and weight ranged from 5 to 8 years and 9.5 to 14 kg, respectively.

2.1.2. Control Group

All 5 dogs comprising the control group were healthy, sound animals which came to our hospital for their annual routine examination and vaccination. These animals did not have current or previous history of orthopedic and/or neurological disease. Age and weight ranged from 6 to 9 years and 10 to 12.5 kg, respectively.

All dogs belonging to both groups received a score of 5–6 on the Body Condition Score (BCS) scale from the Association for Pet Obesity Prevention (https://www.petobesityprevention.org/ accessed on 10 May 2024).

2.2. Force and Pressure Platform Analysis

The design of the study for the acquisition of force- and pressure-related parameters has been developed in agreement with previous studies [19,20].

2.2.1. Force Platform Analysis

The force platform (Pasco, Roseville, CA, USA) consisted of a dynamometric, 4-sensor force platform of 35 × 35 cm and a sample frequency of 250 Hz. The device was placed in a 10 m long corridor. The platform was inserted into a purpose-built hole in such a way that the device's surface was level with the ground and was covered with a rubber mat. Specific software (DataStudio® version 1.9.8r10, Pasco, Roseville, CA, USA) was used to obtain peak vertical (Fvmax), cranial or braking (Fcrmax) and caudal or propulsive (Fcamax) forces (N) from three valid trials (Figure 1). Walk velocity was measured with a motion sensor (Pasco, Roseville, CA, USA) positioned 1 m from the platform. A trial was considered valid when the dog's walking speed was within the range of 0.5–0.7 ± 0.2 m/s, no movement of the limbs, head and/or neck was observed and the handler did not have any physical contact with and/or did not restrain the animal during the recording (Video S1). Mean values were normalized to body weight (%BW). Vertical impulses (N*s) for the vertical, cranial and caudal directions were also obtained (VIv, VIcr and VIca, respectively) (Figure 1).

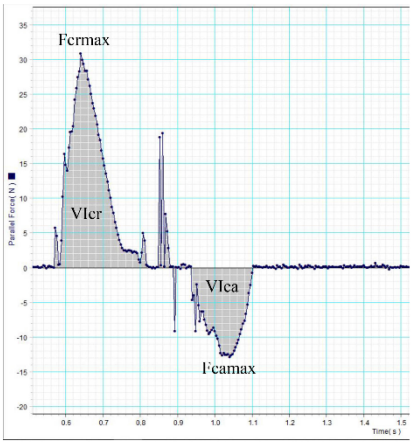

Figure 1. Force platform recording of an amputee dog. Horizontal forces and impulses are represented.

2.2.2. Pressure Platform Analysis

A pressure platform (EPS/R1, Loran Engineering, Bologna, Italy) with Biomech software version 1.6.1.14687 (Loran Engineering, Bologna, Italy) was used, consisting of 2096 pressure sensors (density 1 sensor/cm^2) evenly spread over a quadrangular frame. The acquisition frequency was 100 Hz, and the range of pressure measured was 30–400 Kpa. The platform was placed in another purpose-built cavity level with the floor and adjacent

to the force platform in order to ensure that the recordings from the animals were obtained in the same trial. To perform the postural exam (posturography), the dogs were placed with both forelimbs on the platform. The dog remained standing still for at least 10 s (Figure 2). To ensure that the dog stayed in place, the owner was directly placed in front of the dog to ensure that the head and neck were facing forward without turning to the side. A total of three trials were carried out for each animal. The obtained posturographic data included statokinesiogram (Stat, mm^2), peak and mean pressure (PP, MP, Kpa) and paw area (PA, cm^2). To study the COP pathway characteristics, dogs were leash led and walked in the same way as they were during the force platform analysis.

Figure 2. Postural exam of an amputee dog. Note that the leash around the neck is loose.

As general criteria during the force and platform analyses and in order to obtain the most representative data possible for the statistical analysis, the mean value of the three trials was considered as long as the trials differed by <10%. When the difference was >10%, new trials were carried out to obtain three valid results.

2.3. Statistical Analysis

The Shapiro–Wilk test was used to assess the normality of the variables. In all cases, the Shapiro–Wilk test *p*-value was greater than 0.05, indicating that normality can be assumed for all variables. Therefore, the variables were summarized using the mean and standard deviation. The mean value of each variable was compared between sound and amputee dogs using Student's *t*-test. The Holm correction was applied to adjust for multiple testing. Differences with a *p*-value less than 0.05 were considered statistically significant. The R Software and environment version 4.4.1 [21] was used to perform the statistical analysis.

3. Results

The mean (±SD) time from amputation to the beginning of the force and pressure platform analyses for the amputee group was 4.8 ± 1.3 months. The mean (±SD) ages of the amputee and control groups were 7 ± 1.6 and 7.4 ± 1.1 years, respectively. No statistical differences were found between the two groups ($p = 0.66$). The mean (±SD) weights of the amputee and control groups were 11.2 ± 1.8 and 11.9 ± 1.14 kg, respectively. No statistical differences were found between the two groups ($p = 0.49$).

The following table shows the mean ± SD and *p*-values of both groups (Table 1).

Regarding force values, Fvmax, Viv, Fcrmax and VIcr were significantly higher in the amputee group, while Fcamax and VIca did not significantly differ.

For the pressure data, the area of the statokinesiogram showed no differences between the amputee and sound dogs, although the orientation of the ellipse changed from horizontal to sagittal (Figures 3 and 4; Videos S2 and S3); other static data, such as PP, MP and PA, were significantly higher in the amputee group.

Table 1. Mean ± SD and *p*-values of both groups. Asterisk (*) means significant difference.

Force Values	Sound	Amputee	*p*-Value
Fvmax	99.35 ± 3.63	182.77 ± 10.59	0.0018 *
VIv	15.86 ± 1.81	28.06 ± 0.58	0.0028 *
Fcrmax	9.60 ± 1.68	25.31 ± 0.75	0.0004 *
VIcr	0.74 ± 0.31	2.49 ± 0.15	0.0028 *
Fcamax	5.21 ± 0.87	12.11 ± 2.21	0.0740
VIca	1.00 ± 0.20	1.16 ± 0.16	0.5672
Stat	0.23 ± 0.03	0.23 ± 0.05	0.9267
PP	215.8 ± 5.07	292.4 ± 10.16	0.0180 *
MP	78 ± 0.71	82.50 ± 3.26	0.0740
PA	14.50 ± 2.38	20.00 ± 1.00	0.0632

Units: Fvmax, Fcrmax, Fcamax: N (%BW); VIv, VIcr, VIca: N.s (%BW); Stat: mm^2; PP, MP: KPa; PA: cm^2.

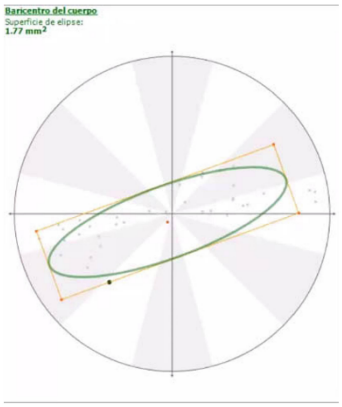

Figure 3. Statokinesiogram of a sound dog. Note the laterolateral orientation of the ellipse.

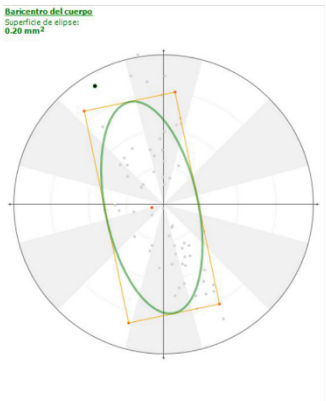

Figure 4. Statokinesiogram of an amputee dog. Note the craniocaudal orientation of the ellipse.

Additionally, beyond the numerical data, the study of the COP pathway in the animals at walk revealed that sound dogs begin contact with the ground approximately at the center of the paw and this pathway runs cranially during the support phase of the gait. However,

the amputee dog's COP came into contact with the ground more caudally, at the level of the metacarpal cushion (Figures 5 and 6; Videos S4 and S5).

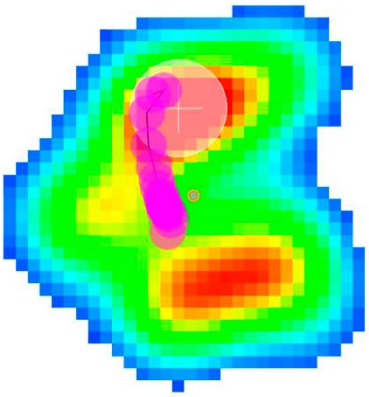

Figure 5. Paw pressure recorded during the support phase of a sound dog. The consecutive pink dots represent the COP pathway. The top of the image is cranial, bottom is caudal, right is medial and left is lateral. Note that the pathway starts at the center of the paw and runs cranially.

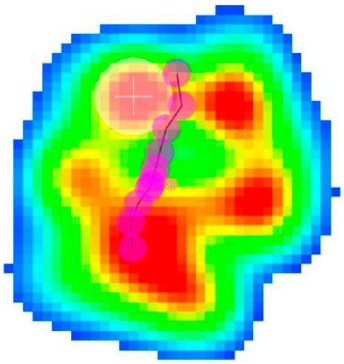

Figure 6. Paw pressure recorded during support phase of an amputee dog. The consecutive pink dots represent the COP pathway. The top of the image is cranial, bottom is caudal, right is medial and left is lateral Note that the pathway starts more caudally at the level of the metacarpal pad and runs cranially; this proves that when the limb makes contact with the ground, it is placed more cranially than sound forelimbs.

4. Discussion

The present study compared the results obtained for a list of kinetic parameters using force and pressure platforms between a group of five French bulldogs with a forelimb amputated and a group of five sound dogs of the same breed.

Prior to the biomechanical assessment, the study needed to ensure that the amputated dogs were fully adapted to the tripedal gait. Previous studies reported that most dogs are adapted within a month [3], especially if the amputation concerns the forelimbs [4,5,11]. The recovery time for normal locomotive activity may differ due to different intrinsic factors, such as age, body weight and breed [22–26]. In our case, all the dogs were totally

accustomed to the tripedal gait, given that amputation had been performed at least 4 months prior in all cases.

Dog speed and weight may alter kinetic parameters [27]; for this reason, special efforts have to be made in order to obtain reliable data to be able to make comparisons between homogeneous groups. Regarding speed, it was maintained in a narrow range to be considered "valid" as described in the methods section; on the other hand, and given that the amputee dogs were already undergoing a weight control program to avoid overloading the remaining limb, the same criteria were applied to control dogs in order to maintain them within the "ideal" weight for the breed.

The presence of a residual stump in non-complete limb amputations, such as proximal humeral osteotomies, can hinder the comparison with full-leg amputees, since in this situation the animal has the option of using it to partially maintain correct balance; this was not the case in our study because all our animals underwent full-leg amputation.

As shown in the results, almost all of the force parameters (Fvmax, Fcrmax) and their respective impulses (VIv, VIcr) showed higher values, which clearly proves that there was a net redistribution of weight to the remaining forelimb. This occurs not only in terms of force, but also in terms of the duration of the braking phase, which means that amputee dogs spend more time in this phase than sound dogs, as found in previous studies [10]. On the contrary, the Fcamax and VIca values remained the same, meaning that the propulsion force and duration did not change in the amputee group. We believe that this occurs because while the force during the braking phase has to be "assumed" by the remaining forelimb, the contribution of the hindlimbs during the propulsion phase is very important, as noted by other authors; this inverse relationship between force and phase duration has been previously published [11,28–30].

Regarding postural analysis, it has been suggested that dogs with an amputated forelimb tend to have more difficulty maintaining their balance [31,32]; however, our postural results obtained from the statokinesiograms showed that forelimb amputees maintain the same level of balance. In other words, tripedal support is as effective as quadrupedal support in terms of balance.

Previous stance studies showed that the ellipse remains with a transversal orientation in both sound and lame dogs due to dogs having a greater stability in the sagittal plane because the longitudinal axis is longer than the horizontal axis. In our study, the fact that the ellipse orientation changed to a sagittal plane was surprising because it meant that the COP pathway axis changed from transversal to primarily parallel to the dog's longitudinal axis, although the dog's balance did not change.

As occurred with changes in force, the amputee dogs also applied more pressure when their limbs came into contact with the ground, which proves that the weight redistribution at walk changes compared to dogs with a sound forelimb in cases of painful lameness [20] or, as in our case, when a forelimb has been amputated. Paw expansion is a consequence of the pressure exerted by the limb on the ground given the elastic nature of the digital and metacarpal cushions. Our results showed a clear increase in paw surface in amputee dogs, although this expansion does not seem to be proportional to the increase in pressure [33].

Finally, the limb COP pathway moved more caudally in the amputee group, which proves that the remaining forelimb is located more cranially than that in sound dogs at the beginning of the support. We believe that the increased force and pressure values, as well as alterations in limb placement during the support phase, leads to there being a greater amount stress on the remaining forelimb, especially on the structures that contribute to the body's support.

All of the increases in the force and pressure values shown here make the animals more predisposed to overuse injuries, as said in the introduction. In our opinion, preventive measures should be taken; among them, rehabilitation and physiotherapy such as hydrotherapy, flexibility training and weight control as well as environmental adaptations such as the avoidance of slippery surfaces and the use of ramps instead of stairs generally facilitate safe ambulation [13–15].

The results shown here contribute to the knowledge of dynamic and postural adaptations in dogs who have experienced a forelimb amputation. However, this study has some limitations: first, the study used a relatively low number of animals; although the fact that all of the animals used in this study are the same breed, and with the same BCS (thus, of the same morphotype), allowed for more homogeneous and reliable data and increases the strength of the conclusions, as reported in previous studies based on force platform analysis [34]. Second, weight redistribution to the hindlimbs in forelimb amputee dogs has been reported, but this fact was not considered in our study. This could be investigated in future research.

5. Conclusions

Tripedal support in dogs does not objectively imply a loss of balance in quantitative terms. However, there is an increase in the amount of force used by the remaining limbs and an altered disposition of the limbs during the support phase. These facts may potentially predispose an animal to additional injuries in the future due to the overuse of different musculoskeletal units.

Supplementary Materials: The following supporting information can be downloaded at: https://www.mdpi.com/article/10.3390/ani14131960/s1, Video S1: High speed video showing a force platform trial. Video S2: Statokinesiogram of a sound dog. Video S3: Statokinesiogram of an amputee dog. Video S4: COP pathway of a sound dog. Video S5: COP pathway of an amputee dog.

Author Contributions: Conceptualization, J.R.-A., L.M. and J.M.G.-O.; methodology J.M.V., O.R. and P.F.; investigation, P.F. and O.R.; resources, J.M.G.-O., I.P. and M.R.-P.; writing—original draft preparation P.F., O.R. and M.R.-P. writing—review and editing, J.M.V., J.R.-A. and I.P. All authors have read and agreed to the published version of the manuscript.

Funding: This research received no external funding.

Institutional Review Board Statement: Ethical review and approval were waived for this study because all the animals had owners who were informed of the study and gave written consent to participate and the animals received standard surgical procedures according to their disease.

Informed Consent Statement: Informed consent was obtained from each dog owner involved in the study.

Data Availability Statement: Data are contained within the article and Supplementary Materials.

Acknowledgments: Thanks to the dog owners for their cooperation. Amanda K. Hand for language editing.

Conflicts of Interest: The authors declare no conflicts of interest.

References

1. Black, L. Compensatory mechanisms in a dog after hind leg amputation. *J. Small Anim. Pract.* **1970**, *11*, 723–726. [CrossRef] [PubMed]
2. Fuchs, A.; Anders, A.; Nolte, I.; Schilling, N. Limb and back muscle activity adaptations to tripedal locomotion in dogs. *J. Exp. Zool. Part A Ecol. Genet. Physiol.* **2015**, *323*, 506–515. [CrossRef] [PubMed]
3. Galindo-Zamora, V.; von Babo, V.; Eberle, N.; Betz, D.; Nolte, I.; Wefstaedt, P. Kinetic, kinematic, magnetic resonance and owner evaluation of dogs before and after the amputation of a hind limb. *BMC Vet. Res.* **2016**, *12*, 20. [CrossRef] [PubMed] [PubMed Central]
4. Carberry, C.A.; Harvey, H.J. Owner satisfaction with limb amputation in dogs and cats. *J. Am. Anim. Hosp. Assoc.* **1987**, *23*, 227–232.
5. Withrow, S.J.; Hirsch, V.M. Owner response to amputation of a pet's leg. *Vet. Med. Small Anim. Clin.* **1979**, *74*, 332–334. [PubMed]
6. Kirpensteijn, J.; Van den Bos, R.; Endenburg, N. Adaptation of dogs to the amputation of a limb and their owners' satisfaction with the procedure. *Vet. Rec.* **1999**, *144*, 115–118. [CrossRef] [PubMed]
7. Ben-Amotz, R.; Dycus, D.; Levine, D.; Arruda, A.G.; Fagan, N.; Marcellin-Little, D. Stance and weight distribution after tibial plateau leveling osteotomy in fore limb and hind limb amputee dogs. *BMC Vet. Res.* **2020**, *16*, 188. [CrossRef] [PubMed] [PubMed Central]
8. Raske, M.; McClaran, J.K.; Mariano, A. Short-term wound complications and predictive variables for complication after limb amput, ation in dogs and cats. *J. Sm. Anim. Pract.* **2015**, *56*, 247–252. [CrossRef] [PubMed]
9. Goldner, B.; Fuchs, A.; Nolte, I.; Schilling, N. Kinematic adaptations to tripedal locomotion in dogs. *Vet. J.* **2015**, *204*, 192–200. [CrossRef] [PubMed]

10. Kirpensteijn, J.; van den Bos, R.; van den Brom, W.E.; Hazewinkel, H.A. Ground reaction force analysis of large breed dogs when walking after the amputation of a limb. *Vet. Rec.* **2000**, *146*, 155–159. [CrossRef] [PubMed]
11. Jarvis, S.L.; Worley, D.R.; Hogy, S.M.; Hill, A.E.; Haussler, K.K.; Reiser, R.F., 2nd. Kinematic and kinetic analysis of dogs during trotting after amputation of a thoracic limb. *Am. J. Vet. Res.* **2013**, *74*, 1155–1163. [CrossRef] [PubMed]
12. Fuchs, A.; Goldner, B.; Nolte, I.; Schilling, N. Ground reaction force adaptations to tripedal locomotion in dogs. *Vet. J.* **2014**, *201*, 307–315. [CrossRef] [PubMed]
13. Millis, D.L.; Levine, D.; Taylor, R.A. *Canine Rehabilitation and Physical Therapy*, 2nd ed.; Saunders: Philadelphia, PA, USA, 2004; pp. 201–210.
14. Vail, D.M.; Hamm, D.H.; Liptak, J.M. *Withrow and MacEwen's Small Animal Clinical Oncology*, 4th ed.; Saunders: Philadelphia, PA, USA, 2007; pp. 551–572.
15. Johnston, S.A.; Tobias, K.M. *Veterinary Surgery: Small Animal*, 2nd ed.; Elsevier: Amsterdam, The Netherlands, 2017; pp. 1210–1224.
16. Bøaszczyk, J.W.; Lowe, D.L.; Hansen, P.D. Ranges of postural stability and their changes in the elderly. *Gait Posture* **1994**, *2*, 11–17. [CrossRef]
17. Charalambous, D.; Lutonsky, C.; Keider, S.; Tichy, A.; Bockstahler, B. Vertical ground reaction forces, paw pressure distribution, and center of pressure during heelwork in working dogs competing in obedience. *Front. Vet. Sci.* **2023**, *10*, 1106170. [CrossRef] [PubMed]
18. Virag, Y.; Gumpenberger, M.; Tichy, A.; Lutonsky, C.; Peham, C.; Bockstahler, B. Center of pressure and ground reaction forces in Labrador and Golden Retrievers with and without hip dysplasia at 4, 8, and 12 months of age. *Vet. Sci.* **2022**, *9*, 1087693. [CrossRef] [PubMed]
19. Pitti, L.; Oosterlinck, M.; Díaz-Bertrana, M.L.; Carrillo, J.M.; Rubio, M.; Sopena, J.; Santana, A.; Vilar, J.M. Assessment of static posturography and pedobarography for the detection of unilateral forelimb lameness in ponies. *BMC Vet. Res.* **2018**, *14*, 151. [CrossRef] [PubMed]
20. Carrillo, J.M.; Manera, M.E.; Rubio, M.; Sopena, J.; Santana, A.; Vilar, J.M. Posturography and dynamic pedobarography in lame dogs with elbow dysplasia and cranial cruciate ligament rupture. *Vet. Res.* **2018**, *14*, 108. [CrossRef] [PubMed]
21. Available online: https://cran.r-project.org/web/packages/nlme/index.html (accessed on 14 June 2024).
22. Weigel, J.P.; Slatter, D. *Textbook of Small Animal Surgery*, 3rd ed.; Saunders: Philadelphia, PA, USA, 2003; pp. 2180–2190.
23. Dernell, W.S.; Ehrhart, N.P.; Straw, R.C. Tumors of the skeletal system. In *Withrow & MacEwen's Small Animal Clinicial Oncology*, 4th ed.; Withrow, S.J., Vail, D.M., Eds.; Saunders Elsevier: St Louis, MO, USA, 2007; pp. 540–582.
24. Brodey, R.S.; Abt, D.A. Results of surgical treatment in 65 dogs with osteosarcoma. *J. Am. Vet. Med. Assoc.* **1976**, *168*, 1032–1035.
25. Straw, R.C.; Withrow, S.J. Limb-sparing surgery versus amputation for dogs with bone tumors. *Vet. Clin. N. Am. Small Anim. Pract.* **1996**, *26*, 135–143.
26. Budsberg, S.C. Amputations. In *Small Animal Orthopedics*; Olmstead, M.L., Ed.; Mosby: St Louis, MO, USA, 1995; pp. 531–548.
27. Grabowski, A.M.; Kram, R. Effects of velocity and weight support on ground reaction forces and metabolic power during running. *J. Appl. Biomech.* **2008**, *24*, 288–297. [CrossRef] [PubMed]
28. Roush, J.K.; McLaughlin, R.M. Effects of subject stance time and velocity on ground reaction forces in clinically normal Greyhounds at the walk. *Am. J. Vet. Res.* **1994**, *55*, 1672–1676. [CrossRef] [PubMed]
29. McLaughlin, R.M.J.; Roush, J.K. Effects of subject stance time and velocity on ground reaction forces in clinically normal greyhounds at the trot. *Am. J. Vet. Res.* **1994**, *55*, 1666–1671. [CrossRef] [PubMed]
30. Budsberg, S.C.; Verstraete, M.C.; Soutas-Little, R.W. Force plate analysis of the walling gait in healthy dogs. *Am. J. Vet. Res.* **1987**, *48*, 915–918. [PubMed]
31. Cole, G.L.; Millis, D. The effect of limb amputation on standing weight distribution in the remaining three limbs in dogs. *Vet. Comp. Orthop. Traumatol.* **2017**, *30*, 59–61. [CrossRef] [PubMed]
32. Hogy, S.M.; Worley, D.R.; Jarvis, S.L.; Hill, A.E.; Reiser, R.F., 2nd; Haussler, K.K. Kinematic and kinetic analysis of dogs during trotting after amputation of a pelvic limb. *Am. J. Vet. Res.* **2013**, *74*, 1164–1171. [CrossRef] [PubMed]
33. Manera, M.E.; Carrillo, J.M.; Batista, M.; Rubio, M.; Sopena, J.; Santana, A. Static Posturography: A New Perspective in the Assessment of Lameness in a Canine Model. *PLoS ONE* **2017**, *12*, e0170692. [CrossRef]
34. Della Valle, G.; Caterino, C.; Aragosa, F.; Balestriere, C.; Piscitelli, A.; Di Palma, C.; Pasolini, M.P.; Fatone, G. Relationship between ground reaction forces and morpho- metric measures in two different canine phenotypes using regression analysis. *Vet. Sci.* **2022**, *9*, 325. [CrossRef]

4.2.2. Análisis cinemáticos:

4.2.2.1. Electrogoniometria:

Registra la actividad bioeléctrica de los músculos durante la fase de locomoción, permitiendo la evaluación de la función muscular y la detección de posibles desequilibrios musculares asociados con la cojera (López 2019; Cheng y cols., 2018; Beauchet y cols., 2007).

Figura 18. Colocación de un electrogoniómetro sobre la articulación del codo. Fuente: Hospital Clinico Veterinario de la ULPGC

4.2.2.2. Cinematografía de alta velocidad:

Se emplea la grabación de la marcha del perro con cámaras de alta velocidad para capturar el movimiento de las articulaciones y las extremidades en detalle, permitiendo un análisis biomecánico preciso de los patrones de movimiento (Manera 2017; Keegan y cols., 2000; Keegan y cols., 2002; Kramer y cols 2004, Vilar y cols., 2010).

4.2.2.3. Sensores Inerciales o unidades de medición inercial (IMU):

Son equipos electrónicos diseñados para medir la aceleración lineal y angular de un objeto en el que están integrados. Estos sensores utilizan principios de la física inercial para detectar cambios en la velocidad y orientación de un objeto en relación con un sistema de referencia (Martinez-Mendez y Huertas, 2013).

Los **sensores inerciales** típicamente incluyen acelerómetros y giroscopios. Los acelerómetros cuantifican la aceleración lineal, capturando los cambios en la velocidad de movimiento a lo largo de un eje determinado. Por otro lado, los giroscopios miden la velocidad angular o tasa de rotación en torno a un eje específico (Figueirinhas y cols., 2022).

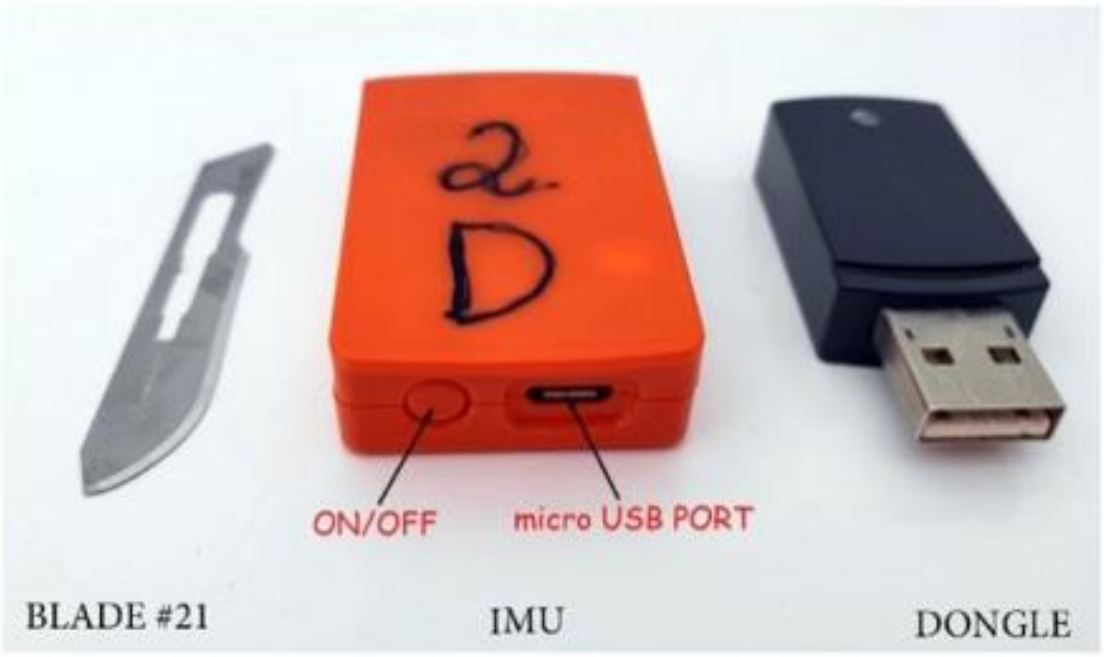

Figura 19. La apariencia externa de una IMU y la llave de conexión inalámbrica. Fuente: (Figueirinhas y cols., 2022)

Los sistemas de Unidad de Medición Inercial (IMU, por sus siglas en inglés) o sensores inerciales, han sido desarrollados comercialmente para la evaluación objetiva de la cojera en caballos. Estos dispositivos permiten la cuantificación precisa del movimiento y de las alteraciones en la locomoción equina, proporcionando datos objetivos que complementan la evaluación clínica tradicional (Hagen y cols., 2021). Estos sistemas IMU se basan en tecnología de

sensores y comprenden giroscopios, acelerómetros y magnetómetros (Keegan y cols., 2011; Starke y cols., 2012; Lopes 2021).

El IMU comercialmente disponible para caballos se ha utilizado experimentalmente en perros (Rhodin y cols., 2017). Otros sistemas IMU también se han utilizado para detectar cojeras en ovejas mediante la medición de la actividad general de estos animales (Kaler y cols., 2020).

Teóricamente, las redes neuronales artificiales intentan emular el comportamiento neuronal humano. La "estructura" interna tiene algunas similitudes (Meena y cols., 2022): las dendritas en las neuronas humanas reciben señales de otras neuronas. Estas señales se procesan en el cuerpo celular, y una señal se propaga finalmente mediante conexiones axonales a dendritas de otras neuronas. (Figura 8)

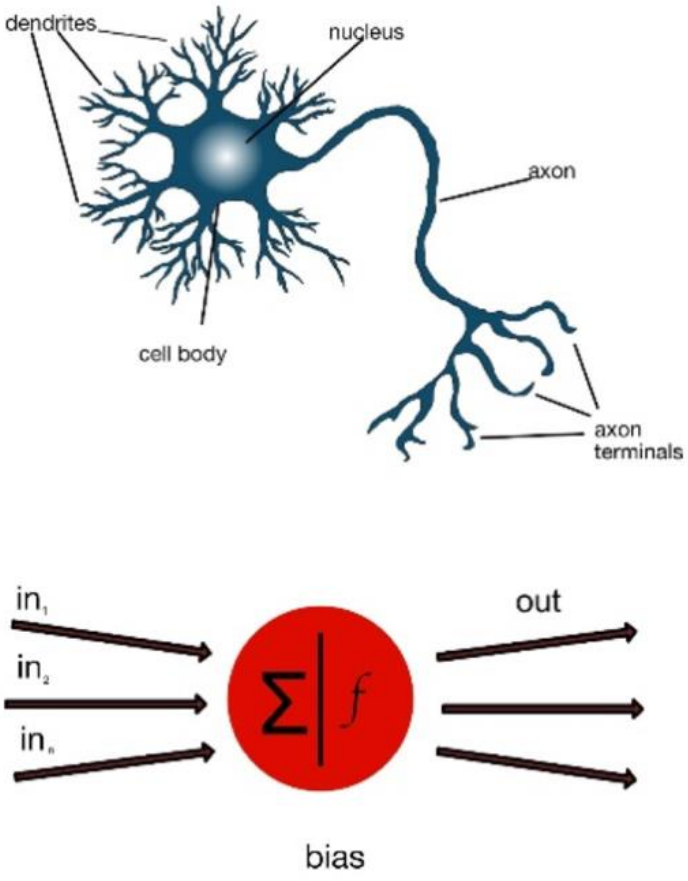

Figura 20. Estructura de una neurona (arriba) y de una neurona artificial (abajo) Fuente: (Figueirinhas y cols., 2022)

De manera similar, en una neurona artificial, los datos se reciben como entrada; luego, se aplican algoritmos matemáticos en el "cuerpo" de la neurona artificial, produciendo una salida.

Estos algoritmos se basan en la regresión lineal (Mata y cols., 2022). Por otro lado, el sesgo es una constante añadida que tiene como objetivo ajustar la salida neuronal. Esta adición intenta mejorar el resultado para imitar una situación real (Tang y cols., 2019).

En lugar de emplear una única neurona, múltiples neuronas artificiales se organizan en una red neuronal artificial (ANN, por sus siglas en inglés), estructurada en capas (Maler, 2020). Por ejemplo, la capa de entrada recibe los datos iniciales y define los parámetros para su análisis, la capa oculta se encarga del procesamiento de dichos datos, y la capa de salida entrega los resultados, clasificados en categorías específicas (Figura 19).

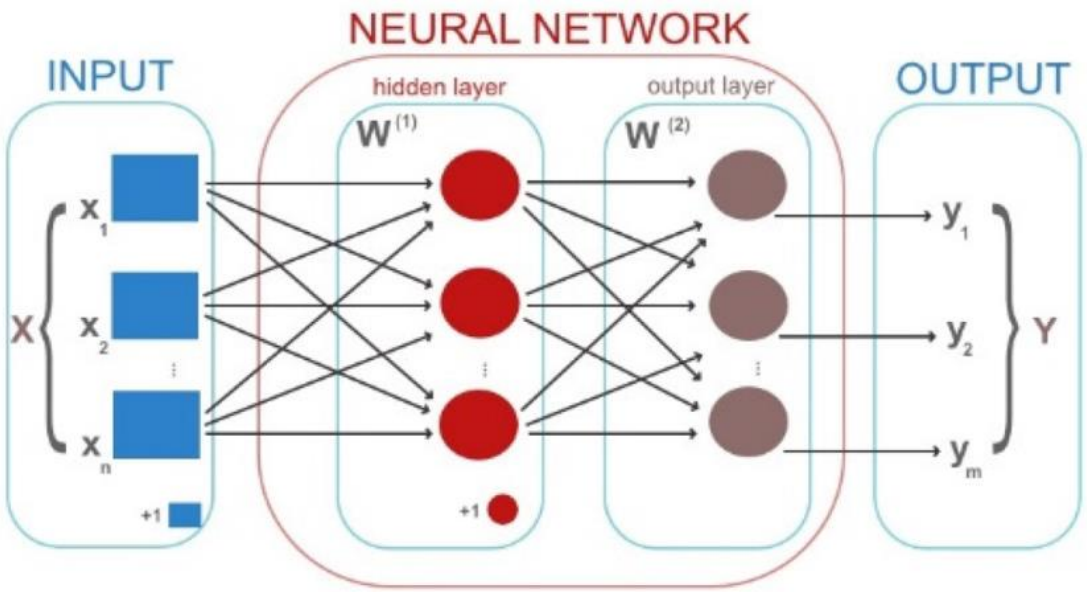

Figura 21. Estructura de una red neuronal artificial.

El empleo de la inteligencia artificial en el ámbito médico ha permitido el desarrollo de diferentes sistemas de apoyo médico para diagnósticos tempranos de tumores cutáneos y enfermedades cardiovasculares (Combalia y cols., 2019; Romiti y cols., 2020; Liu y cols., 2021).

En el campo de la veterinaria, y en el ámbito de las cojeras, existe un hardware comercial que utiliza esta tecnología para la evaluación de cojeras en caballos; sin embargo, esto no existe en perros. Por ello, se considera relevante llevar a cabo un estudio piloto enfocado en el desarrollo de una red neuronal artificial destinada a la detección de cojeras en perros.

Este enfoque busca desarrollar el potencial de las técnicas de inteligencia artificial para identificar patrones específicos de movimiento asociados con la cojera, optimizando así la precisión y objetividad en el diagnóstico clínico.

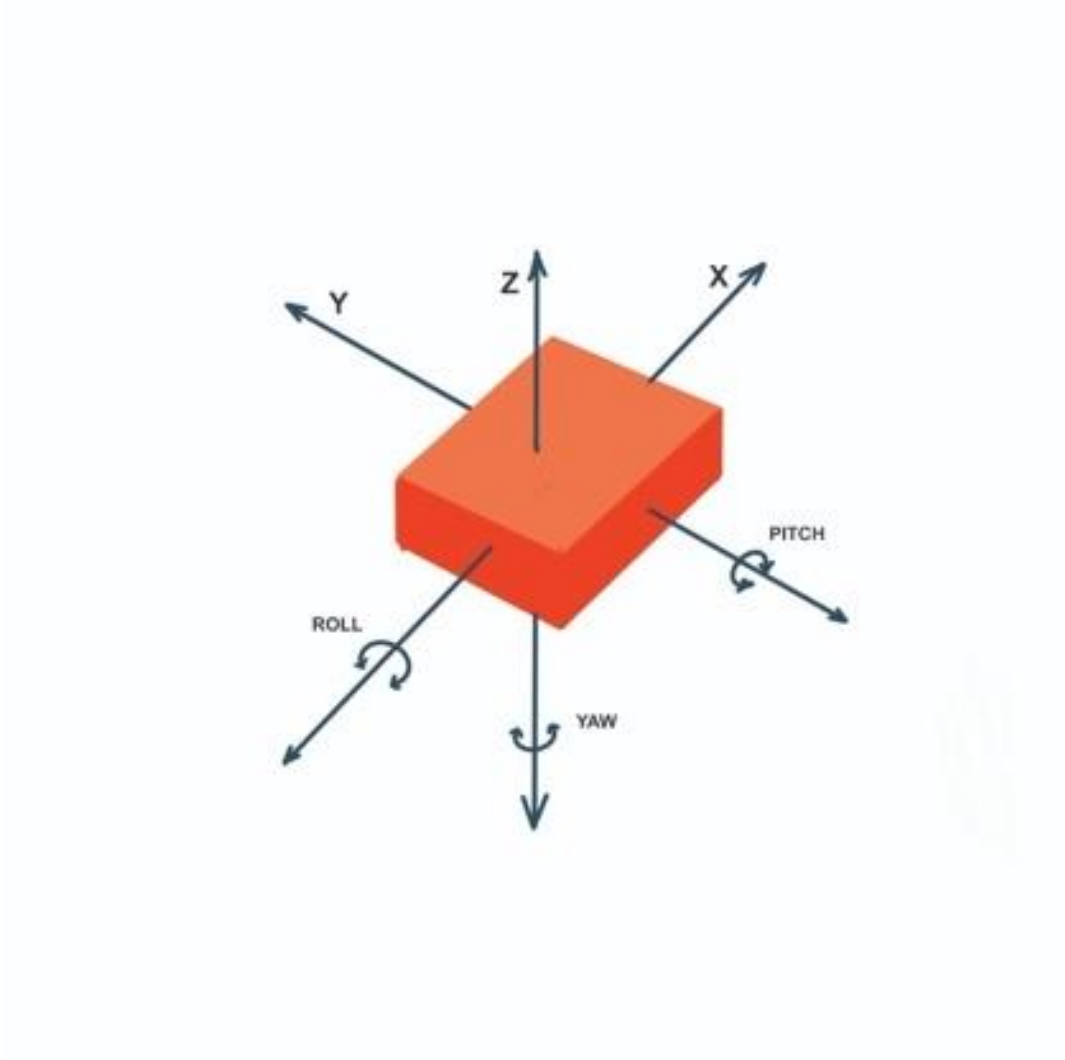

Figura 22. El giroscopio IMU proporciona datos de inclinación en los ejes X, Y y Z.
Fuente: (Figueirinhas 2022)

ARTICULO #3

Figueirinhas P, Sanchez A, Rodríguez O, Vilar JM, Rodríguez-Altónaga J, Gonzalo-Orden JM, Quesada A. Development of an Artificial Neural Network for the Detection of Supporting Hindlimb Lameness: A Pilot Study in Working Dogs. Animals (Basel). 2022 Jul 8;12(14):1755. doi: 10.3390/ani12141755. PMID: 35883302; PMCID: PMC9311578.

JCR Impact factor: 3

Cuartil: Q1

Grupo: Veterinary sciences

Posición: 13/144

animals

MDPI

Article

Development of an Artificial Neural Network for the Detection of Supporting Hindlimb Lameness: A Pilot Study in Working Dogs

Pedro Figueirinhas [1], Adrián Sanchez [2], Oliver Rodríguez [1], José Manuel Vilar [1,*], José Rodríguez-Altónaga [3], José Manuel Gonzalo-Orden [3] and Alexis Quesada [2]

[1] Departamento de Patología Animal, Universidad de Las Palmas de Gran Canaria, Trasmontaña S/N, 35416 Arucas, Spain; pedro.figueirinhas@fpct.ulpgc.es (P.F.); oliver.rodriguez@ulpgc.es (O.R.)
[2] Department of Computer Science and Institute for Cybernetics, Campus de Tafira, Universidad de Las Palmas de Gran Canaria, 35017 Las Palmas, Spain; adriangsanchez@gmail.com (A.S.); alexis.quesada@ulpgc.es (A.Q.)
[3] Departamento de Medicina y Cirugía Veterinaria, Campus de Vegazana, Universidad de León, 24071 León, Spain; jarodma@unileon.es (J.R.-A.); jmgono@unileon.es (J.M.G.-O.)
* Correspondence: jose.vilar@ulpgc.es

Simple Summary: Many of the rules considered valid in the ambit of lameness detection in domestic animals are mainly subjective or acquired after extended clinical experience. Thus, it is necessary to develop tools and/or technologies to provide objective data to discern between sound and lame animals. The main objective of this study is to develop an artificial neural network by analyzing data obtained from an inertial sensor in order to discriminate between sound and lame dogs. After different system adjustments, the neural network has been able to correctly determine whether dogs were lame in about 86% of cases. Furthermore, a web app was developed to manage and follow the different cases. An artificial neural network was designed and developed to analyze spatial data from inertial sensors and to detect motion alterations in dogs with unilateral lameness. Displayed within a user-friendly, intuitive web app, the system could be a useful tool for lameness detection for veterinary clinicians.

Abstract: Subjective lameness assessment has been a controversial subject given the lack of agreement between observers; this has prompted the development of kinetic and kinematic devices in order to obtain an objective evaluation of locomotor system in dogs. After proper training, neural networks are potentially capable of making a non-human diagnosis of canine lameness. The purpose of this study was to investigate whether artificial neural networks could be used to determine canine hindlimb lameness by computational means only. The outcome of this study could potentially assess the efficacy of certain treatments against diseases that cause lameness. With this aim, input data were obtained from an inertial sensor positioned on the rump. Data from dogs with unilateral hindlimb lameness and sound dogs were used to obtain differences between both groups at walk. The artificial neural network, after necessary adjustments, was integrated into a web management tool, and the preliminary results discriminating between lame and sound dogs are promising. The analysis of spatial data with artificial neural networks was summarized and developed into a web app that has proven to be a useful tool to discriminate between sound and lame dogs. Additionally, this environment allows veterinary clinicians to adequately follow the treatment of lame canine patients.

Keywords: artificial neural network; web app; lameness; dog; inertial sensor

Citation: Figueirinhas, P.; Sanchez, A.; Rodríguez, O.; Vilar, J.M.; Rodríguez-Altónaga, J.; Gonzalo-Orden, J.M.; Quesada, A. Development of an Artificial Neural Network for the Detection of Supporting Hindlimb Lameness: A Pilot Study in Working Dogs. *Animals* **2022**, *12*, 1755. https://doi.org/10.3390/ani12141755

Academic Editor: Yves Samoy

Received: 23 May 2022
Accepted: 5 July 2022
Published: 8 July 2022

1. Introduction

Visual evaluation of lameness varies greatly among observers, which fails to agree with objective measurements of limb function, such as kinetics and kinematics. However,

there is an increasing interest in better understanding canine lameness by using more precise and objective methods of assessment [1,2].

A recent kinematic study in dogs with experimentally induced lameness performed with a motion capture system demonstrated that symmetry measurements of vertical head and pelvic movement, which are clinical variables commonly used in the visual assessment of lameness, were enough to identify the lame limb [3].

Inertial measurement unit, or inertial sensor, (IMU) systems have been developed commercially to evaluate objective lameness in horses [4]; IMU systems are based on sensor technology and comprise gyroscopes, accelerometers, and magnetometers [5–7]. The commercially available IMU for horses has been experimentally used in dogs [8]. Other IMU systems have also been used to detect lameness in sheep by measuring the general activity of these animals [9].

The use of artificial intelligence in the medical field has enabled the development of different systems of medical support for early diagnoses of skin tumors and cardiovascular diseases [10–12]. However, there is no commercially available software for lameness detection in dogs in the same manner as in horses.

Theoretically, artificial neuronal networks try to emulate human neuronal behavior. The internal "structure" has some similarities [13]: the dendrites in human neurons receive signals from other neurons. These signals are processed in the cell body, and a signal is finally propagated by means of axonal connections to dendrites of other neurons (Figure 1).

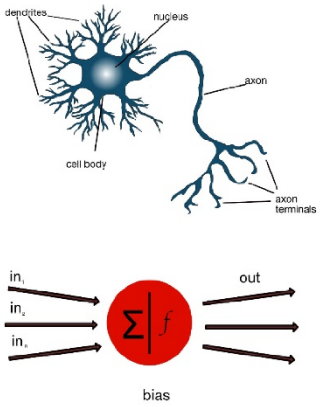

Figure 1. Structure of a neuron (**top**) and an artificial neuron (**bottom**).

Likewise, in an artificial neuron, data are received as input; then, mathematic algorithms are applied in the artificial neuron "body", producing an output. These algorithms are based on linear regression [14]. Conversely, the *bias* is an added constant that aims to adjust the neural output. This addition tries to improve the result in order to mimic a real situation [15].

Instead of utilizing a single neuron, multiple artificial neurons are grouped together in an artificial neural network (ANN), which is organized in layers [16]; for example, the *input layer* receives input data and provides the parameters for analysis, the *hidden layer* processes input data, and the *output layer* provides the output results classified in categories (Figure 2).

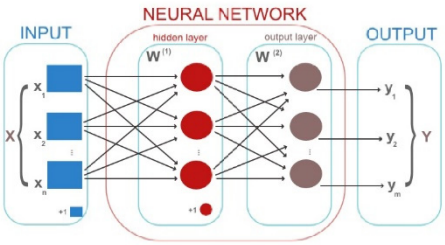

Figure 2. The structure of an ANN.

In order to correctly predict different categories with accuracy, it is necessary to "train" the network. For this purpose, it is vital to have a large amount of varied training data [17]. In this way, the network will progressively "learn" from these input data. With the *loss function*, network output data are compared with expected output.

Currently, to the authors' best knowledge, ANN technology has not been developed for lameness detection in dogs.

Based on these premises, the main purpose of this study is to develop an ANN, which with spatial data obtained from IMUs, can discern whether a dog has unilateral hindlimb lameness. Second, this study seeks to develop a web portal with the capacity to manage dog lameness data with the aim to follow up with the dog over time.

The study presented here has been designed as a "proof of concept", whose initial development has required multiple adjustments in many parameters until satisfactory performance is obtained; for this reason, the sections of materials, methods and results are merged.

2. Materials, Methods and Results

2.1. Instrumentation

For data recording, an IMU (MTw Awinda Wireless 3DOF Motion Tracker, Xsens®, Enschede, The Netherlands) was used (Figure 3).

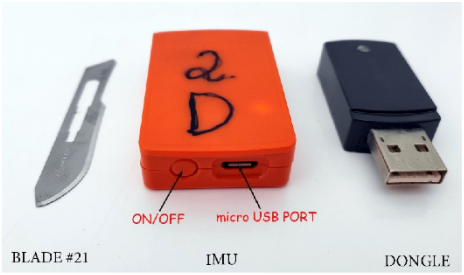

Figure 3. The external appearance of an IMU and the wireless connection dongle.

All data were collected by a dedicated software (MT Manager®, Xsens®, Enschede, The Netherlands). Data were exported with the extension. *txt*.

The IMU was positioned above the midline of the spinous processes of the sacral vertebra 2 with adhesive tape. Sensor data were digitally sampled (8 bit) at 100 Hz in real time. The device has dimensions of 4.7 × 3 × 1.3 cm and a mass of 16 g.

To observe data patterns obtained with the sensor in order to discriminate which relevant elements distinguish sound and unilaterally hindlimb lame dogs, the movement amplitude of the rump from both sides was measured (Figure 4).

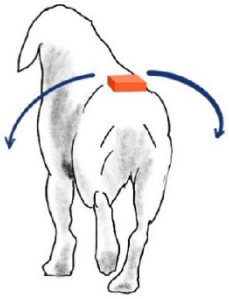

Figure 4. The IMU location. The bilateral inclination is measured with the dog at walk.

The gyroscope provides orientation data in a longitudinal direction of *pitch*, *yaw*, and *roll*. From these, the *roll* provides angular data of the lateral inclination (Figure 5).

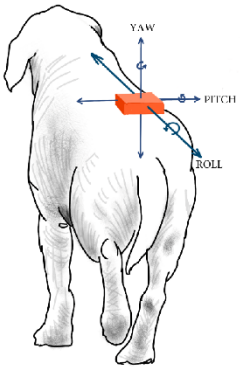

Figure 5. The IMU gyroscope provides inclination data on the X, Y, and Z axes.

2.2. Dogs

Fifteen working dogs weighing more than 15 kg were recruited for this study. Dogs weighing less than 15 kg were excluded from the study, since these animals feel the presence of the sensors more when moving, creating a "perturbed" locomotion. From the 15 working dogs, 12 dogs were used for training the ANN—7 of them were sound and 5 were lame; 3 additional dogs were used for the verification phase. Lame dog owners were clients of the Veterinary Teaching Hospital of the Universidad de Las Palmas de Gran Canaria (Spain).

2.3. Procedure

The dogs were walked straight on a leash for enough time to reach a uniform gait, next to the handler, without pulling on the leash and with the head straight; to put the dogs at the "same dynamic status"; velocity was progressively augmented to reach a maximum where the dogs were still at walk. During a walk, the alternate movements of both hindlimbs create a successive inclination on the sensor toward both sides, generating the inclination data (*roll*). Below, the inclination data for multiple consecutive steps is visualized graphically (Figure 6).

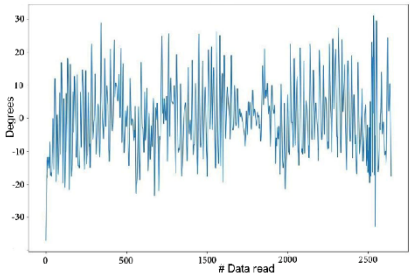

Figure 6. Lateral rump inclination data from multiple steps of a sound dog at walk.

As shown in Figure 6, the ascending and descending patterns show a certain consistency, given that the maximum and minimum inclination values are similar. However, certain isolated values appear to be out of this pattern; these anomalies can be attributed to head movements due to distractions, head shakings, etc. Data shown as boxplot graphics have a range of about 20 degrees of inclination. However, a substantial number of outliers can be observed; this fact could generate a bias when the system attempts to generalize input data. For this reason, we pre-processed the test data to eliminate "noise" or outlying values. Regarding the outlier criteria, the process carried out the use of the median of the sequence, and a cutoff was made on the percentiles, taking into account that the sampling to be used had values between 10% and 90% of the sampling. (Figure 7a,b).

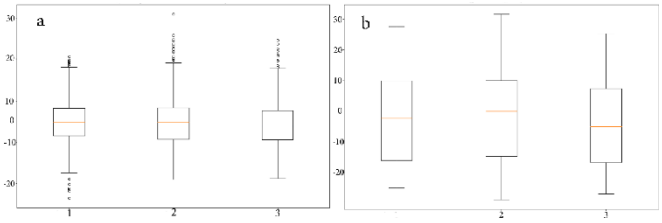

Figure 7. (**a**) Boxplot graphic before data cleaning. (**b**) Boxplot graphic after data cleaning, eliminating outlier values.

With this procedure, extraneous data not attributable to necessary motion were discarded (Figure 8).

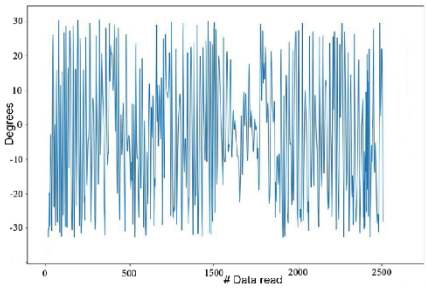

Figure 8. Graphic of the same sound dog after data cleaning; data symmetry has been increased compared with the data from Figure 6.

2.3.1. Neural Network

Design

Data obtained with the IMU were a temporal series, in which certain data depended on previous data; for this reason, a recurrent neural network (RNN) was used because this type of ANN is able to "remember" previous events [18,19]. Specifically, an RNN variant known as Long Short-Term Memory (LSTM) was chosen because it offered better performance over other RNN variants [20].

The LSTM parameters initially set were the following:

- Number of inputs: 1. The sequence of consecutive data was set to 250 as a single input.
- LSTM layers: 2.
- *Dropout*: 50%. This technique randomly "freezes" a determined number of neurons (in our case 50%) so that these neurons are ignored during the updating parameters phase. This produces neurons that are still working and are more relevant, highlighting slight changes in the training data and improving the network's ability to generalize data. As mentioned before, this technique was used exclusively during the training phase [20].
- Number of outputs: 2. Since the network output may be any numerical value, it has been normalized using a sigmoid function, giving a 0 value for sound dogs and a 1 value for lame dogs. For the final diagnosis of sound or lame, the LSTM network is complemented with a traditional ANN, known as the Fully Connected Layer (FCL).
- Number of neurons in each cell: 256. As is usual in many artificial neural networks, this parameter was obtained empirically. We chose a starting power value of 2, and through an intensive battery of tests, we chose the value that offered the best results while maintaining a reasonable computational cost.

In relation to the neural network, there is a single input at each iteration along the LSTM network, the value of which represents the degree of rump slope at each point in time. Thus, the inputs correspond to the degrees of the hindlimbs at each moment (23*, 35*, etc.) while the outputs by the network are numerical values that in our case we normalized to values between 0 and 1, thus obtaining as output a value that represents the probability that the dog has a lameness or not.

Concerning the number of layers of the LSTM network, two were used. Using a lower value (1) could cause the network not to sufficiently learn from the training data due to the low complexity of the network, and this would cause it to not be able to generalize the training data correctly. Conversely, this value was not increased for two reasons: to avoid excessive computational cost in the training phase due to the number of neurons and to avoid overtraining, which could cause the network to memorize the training data, thus impairing the generalization of the system.

Most of the training data had more than 400 data obtained from the sensors, each datum refers to the degree of inclination of the sensor at each moment of the sequence, but it was decided to limit this sequence to 250 data in order to eliminate the data from the beginning of the acquisition, since these could have certain "anomalies" due to abrupt movements of the dog at the beginning. If any sequence had less than 250, then it was filled with null values (0) until the 250 were reached. We used supervised learning where we used exactly 250 data obtained from the sensors to train the network. If more data were available, they were used to generate more training data.

The implementation of the neural network using the library *Pytorch* in *Python is showed* (Figure S1).

Training

Prior to the training phase, *cost* and *optimization* functions had been used. The *cost function* evaluates the performance of the model. It takes both predicted outputs by the model and actual outputs and calculates the extent of error in the model's prediction. Essentially, it is a measure of the network's success with the training set, where a value near 0 means that the network makes accurate predictions during training. For this purpose, the mean squared error formula was used, which is the squared sum of the

difference between the real result and the prediction generated by the neural network, i.e. $MSE = \frac{1}{n}\sum_{i=1}^{n}(y_i - \widetilde{y}_i)^2$.

Once the error has been obtained, the *weights* of the neural network should be adjusted; the *weights* determine the relevance of each network input in order to obtain better predictions. For this purpose, it is necessary to select a function that updates the weights. This is called an *optimization* function. *The gradient descent* algorithm is mostly used for these purposes [21]. In our study, we specifically used the *Adam algorithm*, which is one of the most widely used optimization algorithms due to advantages such as high efficiency and low resource consumption [22].

After this, the real and generated output were compared, and a value was given for the difference. This difference value is called *loss* and serves to adjust the *weights*. The frequency by which the weights are updated is determined by the *learning rate*, which is a *hyperparameter*. This rate was determined empirically, because setting a low learning rate makes the network learn slowly. However, a high learning rate makes the *weights* and *error function* diverge; thus, there is no learning at all. In our study, we used a standard value (0.1).

An additional hyperparameter to be settled for the neural network was the number of *epochs*, or the number of times the network receives input data in order to progressively generalize and learn from them. It was necessary to be careful setting this hyperparameter because a wrong value could lead to bad training of the neural network. In summary, *weight*, *epochs*, and *dropout* were modified in an attempt to optimize the training (Figure S2).

Thus, the first step is to set the network in training mode and allow its *weights* to be updated. After this, the training data are obtained in batches; these training data were used as input in the network to observe the generated predictions and then to check those predictions against the actual result.

During this phase, many mathematical operations are used in the network to generate output. Once this phase is finished, the *weights* of the network are updated using the *optimizer*. The aim is to adjust the weights to align with the input data; thus, the network can make better predictions in the following *epochs*.

Verification with Blind Data and Improvements

In this phase, it was necessary to validate the results with a validation data set different from the training data set, in order to assess the network's ability to generalize its behavior in the presence of unknown data; in our case, the validation set represented 20% of the available data set (3 dogs). When the system was evaluated with this set, the loss was much higher than the training phase (0.368); unfortunately, the accuracy was relatively low (0.6 or 60%) (Figure S3).

For this reason, certain improvements were necessary. For instance, the technique of the *clipping gradient* was used to avoid erroneous updates of the *weights* [23]. Furthermore, more dropout was applied (60%), and the *batch size* was readjusted to three trials. With these improvements, the accuracy of the neural network improved to 85.7%. (Figure S4).

2.3.2. Web Application

The diagnostic tool implemented by the ANN was integrated into a web management tool to manage and record all the information from the dogs in this study. This system allows veterinary professionals to collect relevant information about the dogs, including the videos of these animals with different recordings with IMUs to capture inclination data.

This web application used many programming languages and libraries in its development. Regarding the development of the server, the language "Python", along with a library called "Flask", was used. "Angular", an open code component-based framework, was used for the user interface.

Elements and User Roles

Two key elements were defined for the web application development:

– The *sessions*, which follow the dog's lameness
– The *trials*, three from each dog, with the IMU fixed to each dog's lower spine. Sensory data were synchronized with video recordings for a simultaneous visualization of the graphics and the dynamic of each dog.

Two user roles were established in the application: the *administrator*, who has full access to web functionalities and has exclusive authority to register other users in the system, and the *veterinarian*, who inputs and manages data (canine registrations in the system, data updating, view the sessions of the dogs) and can create and edit new sessions, visualize the trials to observe the angular characteristics of the analyzed dogs, and observe conclusions by the neural network.

Architecture

The web application follows a general client–server architecture, allowing the server to manipulate data in the application and offering a wide selection of "services" the client can use to obtain, modify, delete and create data in the application. The protocol "HTTP" was used for this communication (Figure 9).

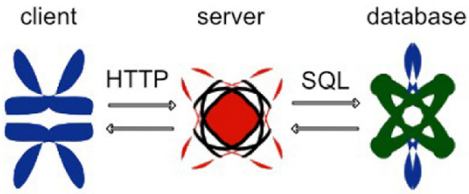

Figure 9. The communication scheme among the different app components.

Database Design

For the preservation of data, the database type SQLITE3 was used. Our database has different entities. First, there is the *dog entity* that represents the dogs created in the portal. It contains descriptive data about the dog, such as its name, date of birth, breed, weight or height, as this data may be relevant when diagnosing lameness. Second, dogs have multiple *sessions* associated with them, which shows the working sessions between a veterinarian and a dog to store multiple trials of data. The trials are in charge of storing the data obtained by the sensors, as well as their subsequent processing, to show the different inclination characteristics, to process the data in the ANN, and to offer diagnoses about the presence of lameness in the evaluated dogs.

Data Storage

The web portal was designed to allow for file uploads, video recordings, and sensory data. With this purpose, a hierarchical structure was utilized to store the different types of information (Figure 10).

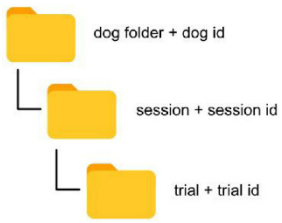

Figure 10. The file structure within the app.

Each dog has its own folder. The name of the dog's folder is composed of the prefix "dog folder" with the identifier of the dog added to ensure no two folders have the same name. For each session created, a folder is created with a name that follows the same structure, but in this case, the prefix is "session". At the next level, the trials follow the same structure as above; finally, the files relating to sensors and videos also follow a similar naming pattern.

User Interface

Different *mockups* were developed using the tool *Figma*. The development of the user interface had all the necessary elements: a good distribution of elements, a friendly color palette, and other crucial elements for the final user, the veterinarian.

The main application view shows dogs registered in the system. The interface allows for setting different filters restricting the displayed canines (Figure 11).

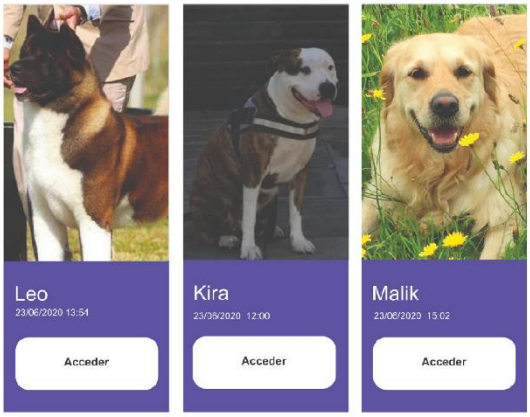

Figure 11. Access to different dogs registered in the system.

When accessing a specific dog, another view containing the essential animal registered data is displayed (Figure 12). From here, a user can access the different sessions that have been recorded for that dog (Figure 13). At the same time, for each session, the user has access to the different recorded trials, where the visualization of sensor data is synchronized with the trial video recording (Video S1) (Figure 14).

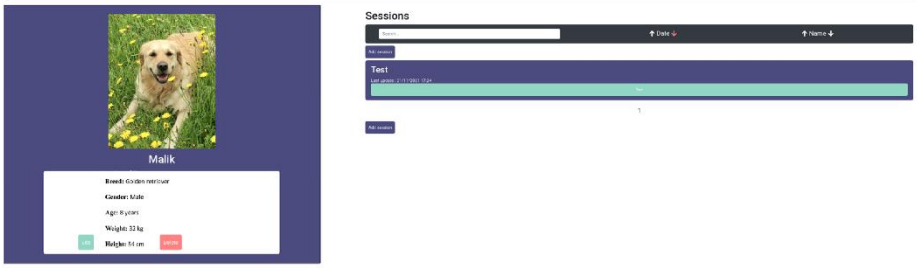

Figure 12. The essential data of a specific dog.

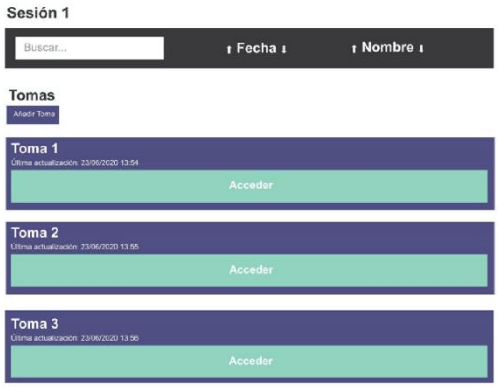

Figure 13. The access to sessions and trials of a specific dog.

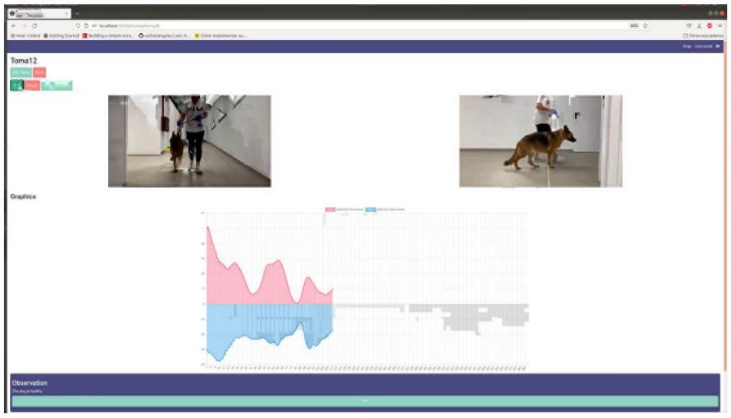

Figure 14. A screenshot of a synchronized graphic from IMU data and video recording.

Server

The development of an interface with representational state transfer (*API REST*) for the server allowed for the separation of server logic from the user interface, improving the maintenance of the application. In this way, there is a project with a series of communication functionalities within the database (creation, update, deletion, and view), and there is a separate web interface where different views can be observed.

For programming, *Python* language was used, given that it allows for the installation of several specific libraries, such as *Keras*, *Numpy* or *Pytorch*. For the web application development, the minimalist framework *Flask* was used.

Client

For the web interface development, *Angular* was used because of its quality and well-structured software, in addition to having many facilities for its development. Because the web interface is a single page application (SPA) framework, keeping all content on a single page, the page does not require reloading the browser when accessing other routes, offering greater fluidity to the user. Regarding the libraries used for the project, "Chart.js", a library

that generates multiple graphs, was used to display IMU values. For user authentication on the web page, "Angular JWT" was used. This library makes use of a token to allow for subsequent operations requested by users once they are initially authenticated by a username/password. The tokens are verified on each request made to the server to confirm that request is authorized. Finally, "SweetAlert2" was used to create pop-up windows.

3. Discussion

Our study assessed the ability of an ANN to discern if a dog is sound or lame, imitating the knowledge of an experienced veterinary clinician.

Within the context of this pilot study, we chose canines supporting hindlimb lameness because the fixation of the inertial sensor in the midline of the spinous processes of the sacral vertebra 2 was easier than on the top of the head. A recent paper was able to obtain reliable data from sensors affixed to the top of the heads of dogs with induced lameness [8]; this study used a commercially available sensor-based system to detect lameness in horses [5], in which the fixation method is undoubtedly better developed than in our experimental study. If we were able to achieve an optimal fixation of the device, we believe that our system would also be able to detect forelimb lameness, but in this case, the lameness would be evidenced by the asymmetry of the pitch angular data.

Regardless of placement, the ANN should be able to analyze data from sound dogs and differentiate them from dogs with altered locomotion due to lameness. These compensatory lameness mechanisms have been described in dogs, demonstrating that compensation occurs by changing ground reaction forces of ipsilateral and contralateral limbs in an attempt to alleviate pain [24]. These changes unload the painful limb, and they can only be achieved by dynamic postural adaptations of the head, trunk and limbs, with subsequent changes in their motion patterns [3]. Specifically, our sensors detected variations (asymmetry) of the angle of the pelvis that occur in unilateral hindlimbs lameness when a dog is at walk. For bilateral lameness detection, we think that, analogous to inertial sensor-based devices used in horses [5], at least the combined data from two or more sensors would be needed, but this still requires further investigation.

This system could also be potentially used in other four legged domestic species such as cats, since the dynamics of movement are similar. The only limitation could be that the animal will alter the movement if the device causes any discomfort.

Regarding the learning ability of the neural network and management of input data, a recent study in horses [25] obtained tridimensional data from markers recorded with cameras. The study divided the input data into one section, containing 80% of all data for training and another section with the remaining 20% excluded from the training phase. The 20% section was used only for testing to give an unbiased evaluation of the network's performance. Our study design was consistent with the previous study's proportions.

In order to obtain reliable data, the decision was made [26] to estimate input data sets > 6000 to guarantee statistical validity. The enrollment requirements for valid dogs in our study (working dog, medium to big conformation, able to walk on a leash, etc.) made this target unattainable. To avoid the need to attain this enormous amount of data, a recent study proposed identifying and deleting data that only marginally contribute to the outcome [25]. Therefore, in our case, we decided to exclude outliers that added "noise" to the data set and made the system difficult to distinguish accurately between sound and lame dogs. Other authors [27] have previously made the same corrections in similar studies involving lameness assessment.

Conversely, some authors opine that excess data are counterproductive for system performance. A network such as ours (RNN) suffers from *Vanishing Gradient Problem* [28], where a long input data set with neurons located farther away from the output data can hardly learn something new and is unable to "generalize" the patterns of the training data. For this reason, the input data to the network should be limited during the training phase [19].

For all the reasons described above, the data sets were limited to a maximum of 250 input data from the sensor. This was accomplished by initially collecting about 400 data. After deleting the outliers as described in the Materials and Methods section, there remained approximately 250 input data. If it was necessary to reach an amount of 250 data; the empty spaces were filled with 0 starting from the 0 position, as if the dog were initially still at the start of the recording of data. In this way, these additional data did not influence the learning process.

When evaluating the ANN final performance, some authors reported a correct classification lame/sound of 78.6% in horses [25]; in our study, we reached an accuracy of 85.7% in unilaterally hindlimb lame dogs, which is a similar performance.

However, our system showed different limitations and potential improvements.

First, the data collection and treatment could be automatized; second, the final diagnostic (lame/sound) should be given instantly; and third, the lameness could be quantified as in other equine models [29].

To be sure, although the performance of the proposed system is high, the authors believe that the data are somewhat limited because they were obtained from a group of dogs with a narrow conformational range. In our opinion, the decision to utilize this system as a standard tool is premature and susceptible to commercial exploitation.

4. Conclusions

The results from this study show for the first time how an ANN, analyzing inclination data from an IMU affixed on the sacral vertebra 2 of a dog, is able to differentiate among sound and unilaterally hindlimb lame dogs, detecting the asymmetries in the vertical pelvic amplitude (angle) when the animal is at walk. These results could help to further develop a fully automated system for lameness detection in the future, being able to detect frontlimb and bilateral lameness also. This will help improve objective discernment in lameness assessment in dogs.

Supplementary Materials: The following supporting information can be downloaded at: https://www.mdpi.com/article/10.3390/ani12141755/s1, Video S1: Synchronized graphic from IMU data and video recording. Figure S1: Command lines in Python language; Figure S2: The steps during the training phase, as well as the loss values, are shown; Figure S3: The system performance shows low accuracy, given that it correctly classified dogs as lame or sound in only 60% of cases; Figure S4: The accuracy of the neural network after the adjustments.

Author Contributions: Conceptualization, A.Q. and J.M.V.; methodology, A.S., P.F. and O.R.; software, A.Q. and A.S.; validation, J.R.-A. and J.M.G.-O.; formal analysis, A.Q. and J.M.V.; investigation, A.S., P.F. and O.R.; resources, J.R.-A. and J.M.G.-O.; data curation, A.S.; writing—original draft preparation, P.F.; writing—review and editing, A.Q. and J.M.V.; visualization, J.R.-A. and J.M.G.-O.; supervision, A.Q. and J.M.V.; project administration, A.Q. and J.M.V.; funding acquisition, J.R.-A. and J.M.G.-O. All authors have read and agreed to the published version of the manuscript.

Funding: The APC was funded by Laboratorio Aragó SL.

Institutional Review Board Statement: Ethical review and approval were waived for this study because all the animals were dog-owned; owners were informed about the study and gave written consent for the study. The study did not include inoculation of any substance nor pain or discomfort.

Informed Consent Statement: Informed consent was obtained from dog owners involved in the study.

Data Availability Statement: Data sets are available for researchers under reasonable request. Source code is accessible from: https://github.com/AgSanches/TFG-Backend(server); https://github.com/AgSanches/TFG-Frontend(client).

Acknowledgments: Thanks to the dog owners for their cooperation. Thanks also to Amanda K. Hand for the English edition. Joao Vasco Figueirinhas Paiva for drawing Figures 4 and 5.

Conflicts of Interest: The authors declare no conflict of interest. The funders had no role in the design of the study; in the collection, analyses, or interpretation of data; in the writing of the manuscript, or in the decision to publish the results.

References

1. Hicks, D.A.; Millis, D. Kinetic and kinematic evaluation of compensatory movements of the head, pelvis and thoracolumbar spine associated with asymmetric weight bearing of the pelvic limbs in trotting dogs. *Vet. Comp. Orthop. Traumatol.* **2014**, *27*, 453–460. [PubMed]
2. Lopez, S.; Vilar, J.M.; Rubio, M.; Sopena, J.J.; Damia, E.; Chicharro, D.; Santana, A.; Carrillo, J. Center of pressure limb path differences for the detection of lameness in dogs: A preliminary study. *BMC Vet. Res.* **2019**, *15*, 138. [CrossRef] [PubMed]
3. Gomez Alvarez, C.B.; Gustas, P.; Bergh, A.; Rhodin, M. Vertical head and pelvic movement symmetry at the trot in dogs with induced supporting limb lameness. *Vet. J.* **2017**, *229*, 13–18. [CrossRef] [PubMed]
4. Hagen, J.; Geburek, F.; Kathrinaki, V.; Naem, M.A.; Roecken, M.; Hoffmann, J. Effect of perineural anesthesia on the centre of pressure (COP) path during stance phase at trot in sound horses. *J. Equine Vet. Sci.* **2021**, *101*, 103429. [CrossRef]
5. Keegan, K.G.; Kramer, J.; Yonezawa, Y.; Maki, H.; Pai, P.F.; Dent, E.V.; Kellerman, T.E.; Wilson, D.A.; Reed, S.K. Assessment of repeatability of a wireless, inertial sensor-based lameness evaluation system for horses. *Am. J. Vet. Res.* **2011**, *72*, 1156–1163. [CrossRef]
6. Starke, S.D.; Willems, E.; May, S.A.; Pfau, T. Vertical head and trunk movement adaptations of sound horses trotting in a circle on a hard surface. *Vet. J.* **2012**, *193*, 73–80. [CrossRef]
7. Lopes, M.A.F.; Nichols, J.T.; Dearo, A.C.O.; Nelson, S.R. Effects of forelimb instrumentation on lameness detection in horses using a portable inertial sensor-based system. *J. Am. Vet. Med. Assoc.* **2021**, *259*, 892–898. [CrossRef]
8. Rhodin, M.; Bergh, A.; Gustas, P.; Gomez Alvarez, C.B. Inertial sensor-based system for lameness detection in trotting dogs with induced lameness. *Vet. J.* **2017**, *222*, 54–59. [CrossRef]
9. Kaler, J.; Mitsch, J.; Vázquez-Diosdado, J.A.; Bollard, N.; Dottorini, T.; Ellis, K.A. Automated detection of lameness in sheep using machine learning approaches: Novel insights into behavioral differences among lame and non-lame sheep. *R. Soc. Open Sci.* **2020**, *7*, 190824. [CrossRef]
10. Combalia, M.; Codella, N.; Rotemberg, V.; Carrera, C.; Dusza, S.; Gutman, D.; Helba, B.; Kittler, H.; Kurtansky, N.R.; Liopyris, K.; et al. Validation of artificial intelligence prediction models for skin cancer diagnosis using dermoscopy images: The 2019 international skin imaging collaboration grand challenge. *Lancet Digit. Health* **2022**, *4*, e330–e339. [CrossRef]
11. Romiti, S.; Vinciguerra, M.; Saade, W.; Anso Cortajarena, I.; Greco, E. Artificial intelligence (AI) and cardiovascular diseases: An unexpected alliance. *Cardiol. Res. Pract.* **2020**, *2020*, 4972346. [CrossRef] [PubMed]
12. Liu, X.; Feng, J.; Wu, Z.; Neo, Z.; Zhu, C.; Zhang, P.; Wang, Y.; Jiang, Y.; Mitsouras, D.; Li, Y. Deep neural network-based detection and segmentation of intracranial aneurysms on 3D rotational DSA. *Intero. Neuroradiol.* **2021**, *27*, 648–657. [CrossRef] [PubMed]
13. Meena, J.; Hasija, Y. Application of explainable artificial intelligence in the identification of Squamous Cell Carcinoma biomarkers. *Comput. Biol. Med.* **2022**, *146*, 105505. [CrossRef]
14. Mata, F.; Johnson, C.; Wilding, L. Cross sectional epidemiological study of the severity of buccal ulceration and sharp enamel points in ridden and unridden horses. *J. Appl. Anim. Welf. Sci.* **2022**, 1–7. [CrossRef]
15. Tang, K.; Ren, J.; Sun, F. Afann: Bias adjustment for alignment-free sequence comparison based on sequencing data using neural network regression. *Genome Biol.* **2019**, *20*, 266. [CrossRef] [PubMed]
16. Maler, L. Neural networks: How a multi-layer network learns to disentangle exogenous from self-generated signals. *Curr. Biol.* **2020**, *30*, R224–R226. [CrossRef]
17. Laudani, A.; Lozito, G.M.; Fulginei, F.R.; Salvini, A. On training efficiency and computational costs of a feed forward neural network: A review. *Comput. Intell. Neurosci.* **2015**, *2015*, 818243. [CrossRef]
18. Towardsdatascience. Available online: https://towardsdatascience.com/recognizing-speech-commands-using-recurrent-neural-networks-with-attention-c2b2ba17c837 (accessed on 14 May 2022).
19. Goulas, A.; Damicelli, F.; Hilgetag, C.C. Bio-instantiated recurrent neural networks: Integrating neurobiology-based network topology in artificial networks. *Neural Netw.* **2021**, *142*, 608–618. [CrossRef]
20. Liu, X.; Liu, C.; Huang, R.; Zhu, H.; Liu, Q.; Mitra, S.; Wang, Y. Long short-term memory recurrent neural network for pharmacokinetic-pharmacodynamic modeling. *Int. J. Clin. Pharmacol. Ther.* **2021**, *59*, 138–146. [CrossRef]
21. Gupta, H.; Jin, K.H.; Nguyen, H.Q.; McCann, M.T.; Unser, M. CNN-based projected gradient descent for consistent CT image reconstruction. *IEEE Trans. Med. Imaging* **2018**, *37*, 1440–1453. [CrossRef]
22. Kim, K.S.; Choi, Y.S. HyAdamC: A new adam-based hybrid optimization algorithm for convolution neural networks. *Sensors* **2021**, *21*, 4054. [CrossRef] [PubMed]
23. Fairbank, M.; Prokhorov, D.; Alonso, E. Clipping in neurocontrol by adaptive dynamic programming. *IEEE Trans. Neural Netw. Learn Syst.* **2014**, *25*, 1909–1920. [CrossRef] [PubMed]
24. Fischer, S.; Anders, A.; Nolte, I.; Schilling, N. Compensatory load redistribution in walking and trotting dogs with hind limb lameness. *Vet. J.* **2013**, *197*, 746–752. [CrossRef] [PubMed]
25. Schobesberger, H.; Peham, C. Computerized detection of supporting forelimb lameness in the horse using an artificial neural network. *Vet. J.* **2002**, *163*, 77–84. [CrossRef]
26. Baum, E.; Haussler, D. What size network gives valid generalization. *Neural Comput.* **1989**, *1*, 151–160. [CrossRef]
27. Cuervo, B.; Rubio, M.; Sopena, J.; Dominguez, J.M.; Vilar, J.M.; Morales, M.; Cugat, R.; Carrillo, J.M. Hip osteoarthritis in dogs: A randomized study using mesenchymal stem cells from adipose tissue and plasma rich in growth factors. *Int. J. Mol. Sci.* **2014**, *15*, 13437–13460. [CrossRef]

28. Alaeddine, H.; Jihene, M. Deep residual network in network. *Comput. Intell. Neurosci.* **2021**, *2021*, 6659083. [CrossRef]
29. McCracken, M.J.; Kramer, J.; Keegan, K.G.; Lopes, M.; Wilson, D.A.; Reed, S.K.; Lacarrubba, A.; Rasch, M. Comparison of an inertial sensor system of lameness quantification with subjective lameness evaluation. *Equine Vet. J.* **2012**, *44*, 652–656. [CrossRef]

5. CONCLUSIONES

1) En el primer estudio, después de comparar dos grupos de perros con rotura de ligamento cruzado, según la técnica y el implante utilizado (Porous TTA® o Model Xgen®), 3 meses después de la cirugía, podemos concluir que la recuperación funcional es similar para ambos procedimientos. Este estudio también muestra que la integración ósea (OI) de los implantes después de 3 meses es correcta en ambos procedimientos. También observamos que no hubo progresión de la artrosis (OA) en ambos grupos. Todas estas valoraciones fueron hechas basas en métodos subjetivos, tal como la escala Bioarth y la escala Radiológica Bioarth, demostrando así su utilidad relativa para comparar, en este caso, dos técnicas quirúrgicas similares.

2) Respecto al estudio con perros amputados, el soporte tripedal en los perros no implica objetivamente una pérdida de equilibrio en términos cuantitativos. Sin embargo, hay un aumento en la fuerza utilizada por los miembros restantes y una disposición alterada durante la fase de apoyo. Estos hechos pueden predisponer potencialmente a un animal a lesiones precoces en el futuro debido al sobreuso de diferentes unidades musculoesqueléticas.

3) Por último, los resultados de este tercer estudio muestran por primera vez cómo una red neuronal artificial (ANN), al analizar datos de inclinación de la pelvis mediante una unidad de medición inercial (IMU) fijada en la vértebra sacra de un perro, es capaz de diferenciar entre perros sanos y perros con cojera unilateral en los miembros pelvianos, detectando las asimetrías en la amplitud vertical de la pelvis cuando el animal camina.

Estos resultados podrían ayudar a desarrollar en el futuro un sistema completamente automatizado basado en esta tecnología para la detección de cojeras en perros.

6. RESUMEN

La cojera se define como una disfunción en la marcha de los animales, caracterizada por alteraciones en la capacidad de apoyo de las miembros torácicos y/o pelvianos. Este síntoma puede ser causado por diversas patologías, incluyendo dolor, debilidad muscular y trastornos articulares, y es relevante para el diagnóstico de trastornos musculoesqueléticos.

Las causas de la cojera son multifactoriales e incluyen lesiones musculares, óseas, infecciones, problemas neurológicos, objetos extraños, enfermedades sistémicas y neoplasias. En muchos casos severos, la amputación del miembro afectado se considera necesaria.

Para la evaluación de la cojera, se emplean métodos subjetivos, tales como escalas visuales y funcionales, junto con métodos objetivos que abarcan análisis cinéticos y cinemáticos. La utilización de sensores de medición inercial (IMU) ha demostrado ser eficaz en la evaluación objetiva de la cojera en medicina humana y equina; sin embargo, los estudios realizados en la especie canina son aún considerados insuficientes.

Por todo lo expuesto anteriormente, el objetivo común de esta tesis doctoral consiste en estudiar nuevos métodos de diagnóstico y evaluación de la cojera. Y por este motivo, se han diseñado tres estudios diferentes:

- Un primer estudio utilizando 30 perros con rotura de ligamento cruzado. En este estudio los animales fueron separados en dos grupos según la técnica y el implante utilizado (Porous TTA® o Model Xgen®). Con el objetivo de comprobar la utilidad de los métodos subjetivos en la valoración de cojeras, se ha utilizado la escala Bioarth para comparar el éxito de dos técnicas quirúrgicas usadas.

- Un segundo estudio utilizando 10 perros con un miembro anterior amputado, con el objetivo de profundizar de manera objetiva en el conocimiento sobre las modificaciones biomecánicas (posturales y dinámicas), en perros

amputados de las extremidades delanteras mediante el uso de plataformas de fuerza y presión.

- Un tercer estudio utilizando 15 perros, con el propósito de investigar si las redes neuronales artificiales podrían utilizarse para determinar la cojera en las extremidades traseras de los perros únicamente mediante medios computacionales.

7. SUMMARY:

Lameness is defined as a dysfunction in the gait of animals, characterized by alterations in the weight-bearing capacity of the thoracic and/or pelvic limbs. This symptom can be caused by various pathologies, including pain, muscle weakness, and joint disorders, and is relevant for the diagnosis of musculoskeletal disorders.

The causes of lameness are multifactorial and include muscular injuries, bone fractures, infections, neurological issues, foreign bodies, systemic diseases, and neoplasms. In many severe cases, amputation of the affected limb is deemed necessary.

For the evaluation of lameness, subjective methods such as visual and functional scales are employed alongside objective methods that encompass kinetic and kinematic analyses. The use of inertial measurement units (IMUs) has proven effective in the objective assessment of lameness in both human and equine medicine; however, studies conducted on canine species are still considered insufficient.

Given the aforementioned points, the common objective of this doctoral thesis is to investigate new diagnostic and evaluative methods for lameness. To this end, three distinct studies have been designed:

- The first study involves 30 dogs with cranial cruciate ligament rupture. In this study, the animals were divided into two groups based on the technique and implant used (Porous TTA® or Model Xgen®). To assess the utility of subjective methods in evaluating lameness, the Bioarth scale was utilized to compare the success of two surgical techniques employed.

- The second study includes 10 dogs with an amputated forelimb, aiming to objectively deepen our understanding of biomechanical modifications (postural

and dynamic) in dogs with forelimb amputations using force and pressure platforms.

- The third study involves 15 dogs with the purpose of investigating whether artificial neural networks could be utilized to determine lameness in the hind limbs of dogs solely through computational means.

8. BIBLIOGRAFIA

Anderson, K.L.; Zulch, H.; O'Neill, D.G.; Meeson, R.L.; Collins, L.M. Risk factors for canine osteoarthritis and its predisposing arthropathies: A systematic review. *Front. Vet. Sci.* **2020**, *7*, 220. https://doi.org/10.3389/fvets.2020.00220

Apelt, D.; Houlton, J.E.F.; McKee, W.M.; Smith, R.N. The results of surgical treatment of medial coronoid disease in 295 dogs. *Vet. Surg.* **2008**, *37*, Y46. https://doi.org/10.1111/j.1532-950X.2007.00337.x

Back, W.; Clayton, H.M.; Lanovaz, J.L. A pressure distribution study of different horse-rider interactions. *Equine Vet. J.* **2002**, *34*, 272–276. https://doi.org/10.2746/042516402776767288

Beauchet, O.; Allali, G.; Berrut, G.; Dubost, V. Is low lower-limb kinematic variability always an index of stability? *Gait Posture* **2007**, *26*, 327–328; author reply 329–330. https://doi.org/10.1016/j.gaitpost.2007.02.001

Ben-Amotz, R.; Dycus, D.; Levine, D.; Arruda, A.G.; Fagan, N.; Marcellin-Little, D. Stance and weight distribution after tibial plateau leveling osteotomy in fore limb and hind limb amputee dogs. *BMC Vet. Res.* **2020**, *16*, 188. https://doi.org/10.1186/s12917-020-02402-7

Berg, J.A.; Sævik, B.K. Minimally invasive percutaneous elastic plate osteosynthesis as a treatment option for tibial diaphyseal fracture in skeletally immature dogs. *Open Vet. J.* **2023**, *13*, 1744–1751. https://doi.org/10.5455/OVJ.2023.v13.i12.23

Black, L. Compensatory mechanisms in a dog after hind leg amputation. *J. Small Anim. Pract.* **1970**, *11*, 723–726. https://doi.org/10.1111/j.1748-5827.1970.tb05576.x

Bland, S.D. Canine osteoarthritis and treatments: a review. *Vet. Sci. Dev.* **2015**, *5*(2). https://doi.org/10.xxxx (falta DOI, si lo tienes, agrégalo aquí).

Bøaszczyk, J.W.; Lowe, D.L.; Hansen, P.D. Ranges of postural stability and their changes in the elderly. *Gait Posture* **1994**, *2*, 11–17.

Boynosky, N.A.; Stokking, L. Atherosclerosis associated with vasculopathic lesions in a golden retriever with hypercholesterolemia. *Can. Vet. J.* **2014**, *55*, 484–488.

Brown, D.C.; Boston, R.C.; Coyne, J.C.; Farrar, J.T. Development and psychometric testing of an instrument designed to measure chronic pain in dogs with osteoarthritis. *Am. J. Vet. Res.* **2007**, *68*, 631–637. https://doi.org/10.2460/ajvr.68.6.631

Carberry, C.A.; Harvey, H.J. Owner satisfaction with limb amputation in dogs and cats. *J. Am. Anim. Hosp. Assoc.* **1987**, *23*, 227–232.

Charalambous, D.; Lutonsky, C.; Keider, S.; Tichy, A.; Bockstahler, B. Vertical ground reaction forces, paw pressure distribution, and center of pressure during heelwork in working dogs competing in obedience. *Front. Vet. Sci.* **2023**, *10*, 1106170. https://doi.org/10.3389/fvets.2023.1106170

Cheng, Y.S.; Reisdorf, R.; Vrieze, A.; Moran, S.L.; Amadio, P.C.; An, K.N.; Zhao, C. Kinetic analysis of canine gait on the effect of failure tendon repair and tendon graft. *J. Biomech.* **2018**, *66*, 63–69. https://doi.org/10.1016/j.jbiomech.2017.10.041

Cid, J.M. *Temas de Historia de la Veterinaria*; Universidad de Murcia: Murcia, Spain, 2000.

Cimino Brown, D.; Boston, R.C.; Coyne, J.C.; Farrar, J.T. Development and psychometric testing of an instrument designed to measure chronic pain in dogs with osteoarthritis. *Am. J. Vet. Res.* **2007**, *68*, 631–637. https://doi.org/10.2460/ajvr.68.6.631

Clayton, H.M.; Hobbs, S.J. The effect of limb stiffness and joint viscosity on the mechanical efficiency of the trot. *Equine Vet. J.* **2017**, *49*, 762–767. https://doi.org/10.1111/evj.12724

Combalia, M.; Codella, N.; Rotemberg, V.; Carrera, C.; Dusza, S.; Gutman, D.; Helba, B.; Kittler, H.; Kurtansky, N.R.; Liopyris, K.; y cols. Validation of artificial intelligence prediction models for skin cancer diagnosis using dermoscopy images: The 2019 international skin imaging collaboration grand challenge. *Lancet Digit. Health* **2022**, *4*, e330–e339.

Cuervo, B.; Rubio, M.; Sopena, J.; Dominguez, J.M.; Vilar, J.; Morales, M.; Cugat, A.; Carrillo, J.M. Hip osteoarthritis in dogs: A randomized study using mesenchymal stem cells from adipose tissue and plasma rich in growth factors. *Int. J. Mol. Sci.* **2014**, *15*, 13437–13460. https://doi.org/10.3390/ijms150813437

De Feo, G.; Lubas, G.; Citi, S.; Puccinelli, C.; Papini, R.A. Bone lesions in a young dog and a NEEM (*Azadirachta indica*) spray as the only preventive measure against leishmaniasis: A case report. *Zoonotic Dis.* **2022**, *2*, 95–110.

Denny, H.R.; Gibbs, C.; Waterman, A.E.; O'Neill, T. Combined tibial plateau levelling osteotomy and cranial closing wedge osteotomy of the tibia for the repair of cranial cruciate ligament rupture in 126 dogs. *Vet. Rec.* **2020**, *186*, 389. https://doi.org/10.1136/vr.105671

Duval, J.M.; Budsberg, S.C.; Flo, G.L.; Sammarco, J.L. Breed, sex, and body weight as risk factors for rupture of the cranial cruciate ligament in young dogs. *J. Am. Vet. Med. Assoc.* **1999**, *215*, 811–814.

Engstig, M.; Vesterinen, S.; Morelius, M.; Junnila, J.; Hyytiäinen, H.K. Effect of femoral head and neck osteotomy on canines' functional pelvic position and locomotion. *Animals* **2022**, *12*, 1631. https://doi.org/10.3390/ani12131631

Erne, J.B.; Walker, M.C.; Strik, N.; Alleman, A.R. Systemic infection with *Geomyces* organisms in a dog with lytic bone lesions. *J. Am. Vet. Med. Assoc.* **2007**, *230*, 537–540.

Evans, R.; Horstman, C.; Conzemius, M. Accuracy and optimization of force platform gait analysis in Labradors with cranial cruciate disease evaluated at a walking gait. *Vet. Surg.* **2005**, *34*, 445–449.

Figueirinhas, P.; Sanchez, A.; Rodríguez, O.; Vilar, J.M.; Rodríguez-Altónaga, J.; Gonzalo-Orden, J.M.; Quesada, A. Development of an Artificial Neural Network for the Detection of Supporting Hindlimb Lameness: A Pilot Study in Working Dogs. *Animals* **2022**, *12*, 1755. https://doi.org/10.3390/ani12141755

Finka, D.C.; Luna, O.R.; Mills, D.E. A critical review of objective and subjective methods for detecting pain in dogs and cats. *Vet. J.* **2019**, *250*, 40–50. https://doi.org/10.1016/j.tvjl.2019.04.001

Fuchs, A.; Anders, A.; Nolte, I.; Schilling, N. Limb and back muscle activity adaptations to tripedal locomotion in dogs. *J. Exp. Zool. A Ecol. Genet. Physiol.* **2015**, *323*, 506–515. https://doi.org/10.1002/jez.1936

Fuchs, A.; Goldner, B.; Nolte, I.; Schilling, N. Ground reaction force adaptations to tripedal locomotion in dogs. *Vet. J.* **2014**, *201*, 307–315. https://doi.org/10.1016/j.tvjl.2014.05.012

Galindo-Zamora, V.; von Babo, V.; Eberle, N.; Betz, D.; Nolte, I.; Wefstaedt, P. Kinetic, kinematic, magnetic resonance and owner evaluation of dogs before and after the amputation of a hind limb. *BMC Vet. Res.* **2016**, *12*, 20. https://doi.org/10.1186/s12917-016-0644-5

Goldner, B.; Fuchs, A.; Nolte, I.; Schilling, N. Kinematic adaptations to tripedal locomotion in dogs. *Vet. J.* **2015**, *204*, 192–200. https://doi.org/10.1016/j.tvjl.2015.03.003

Gomez Alvarez, C.B.; Gustas, P.; Bergh, A.; Rhodin, M. Vertical head and pelvic movement symmetry at the trot in dogs with induced supporting limb lameness. *Vet. J.* **2017**, *229*, 13–18. https://doi.org/10.1016/j.tvjl.2017.10.002

Gundersen, K.; Millis, D.; Zhu, X. Development and testing of a stifle function score in dogs. *Front. Vet. Sci.* **2022**, *9*, 895567. https://doi.org/10.3389/fvets.2022.895567

Hagen, J.; Geburek, F.; Kathrinaki, V.; Naem, M.A.; Roecken, M.; Hoffmann, J. Effect of perineural anesthesia on the centre of pressure (COP) path during stance phase at trot in sound horses. *J. Equine Vet. Sci.* **2021**, *101*, 103429. https://doi.org/10.1016/j.jevs.2021.103429

Heikkilä, H.M.; Hielm-Björkman, A.K.; Morelius, M.; Larsen, S.; Honkavaara, J.; Innes, J.F.; Laitinen-Vapoavouri, O.M. Intra-articular botulinum toxin A for the treatment of osteoarthritic joint pain in dogs: A randomized, double-blinded, placebo-controlled clinical trial. *Vet. J.* **2014**, *200*, 162–169. https://doi.org/10.1016/j.tvjl.2014.01.018

Hicks, D.A.; Millis, D. Kinetic and kinematic evaluation of compensatory movements of the head, pelvis and thoracolumbar spine associated with asymmetric weight bearing of the pelvic limbs in trotting dogs. *Vet. Comp. Orthop. Traumatol.* **2014**, *27*, 453–460. https://doi.org/10.3415/VCOT-13-07-0119

Hielm-Björkman, A.K.; Kuusela, E.; Liman, A.; Markkola, A.; Saarto, E.; Huttunen, P.; et al. Evaluation of methods for assessment of pain associated with chronic osteoarthritis in dogs. *J. Am. Vet. Med. Assoc.* **2003**, *222*, 1552–1558. https://doi.org/10.2460/javma.2003.222.1552

Hielm-Björkman, A.K.; Kapatkin, A.S.; Rita, H.J. Reliability and validity of a visual analogue scale used by owners to measure chronic pain attributable to osteoarthritis in their dogs. *Am. J. Vet. Res.* **2011**, *72*, 601–607. https://doi.org/10.2460/ajvr.72.5.601

Hielm-Björkman, A.K.; Roine, J.; Elo, K.; Lappalainen, A.; Junnila, J.; Laitinen-Vapaavuori, O. An un-commissioned randomized, placebo-controlled double-blind study to test the effect of deep sea fish oil as a pain reliever for dogs suffering from canine OA. *BMC Vet. Res.* **2012**, *8*, 157. https://doi.org/10.1186/1746-6148-8-157

Hittmair, K.M.; Groessl, V.; Mayrhofer, E. Radiographic and ultrasonographic diagnosis of stenosing tenosynovitis of the abductor pollicis

longus muscle in dogs. *Vet. Radiol. Ultrasound* **2012**, *53*, 135–141. https://doi.org/10.1111/j.1740-8261.2011.01943.x

Horstam, C.L.; Conzemius, M.G.; Evans, R.; Gordon, W.J. Assessing the efficacy of perioperative oral carprofen after cranial cruciate surgery using noninvasive, objective pressure platform gait analysis. *Vet. Surg.* **2004**, *33*, 286–292. https://doi.org/10.1111/j.1532-950X.2004.04044.x

Hudson, J.T.; Slater, M.R.; Taylor, L.; Scott, H.M.; Kerwin, S.C. Assessment of long-term outcomes of gonadectomy of dogs: a retrospective study. *J. Am. Vet. Med. Assoc.* **2010**, *214*, 182–187. https://doi.org/10.2460/javma.214.5.182

Hudson, J.T.; Slater, M.R.; Taylor, L.; Scott, H.M.; Kerwin, S.C. Assessing repeatability and validity of a visual analogue scale questionnaire for use in assessing pain and lameness in dogs. *Am. J. Vet. Res.* **2004**, *65*, 1634–1643. https://doi.org/10.2460/ajvr.65.12.1634

Innes, J.F.; Barr, A.R.S. Clinical natural history of the postsurgical cruciate deficient canine stifle joint: year 1. *J. Small Anim. Pract.* **1998**, *39*, 325–332. https://doi.org/10.1111/j.1748-5827.1998.tb05160.x

Innes, J.F.; Barr, A.R.S. Can owners assess outcome following treatment of canine cruciate ligament deficiency? *J. Small Anim. Pract.* **1998**, *39*, 373–378. https://doi.org/10.1111/j.1748-5827.1998.tb05222.x

Jarvis, S.L.; Worley, D.R.; Hogy, S.M.; Hill, A.E.; Haussler, K.K.; Reiser, R.F. 2nd. Kinematic and kinetic analysis of dogs during trotting after amputation of a thoracic limb. *Am. J. Vet. Res.* **2013**, *74*, 1155–1163. https://doi.org/10.2460/ajvr.74.9.1155

Jones, S.D.; Koolmees, P.A. A Concise History of Veterinary Medicine. New Approaches to the History of Science and Medicine; Cambridge University Press: Cambridge, UK, **2022**.

Kaler, J.; Mitsch, J.; Vázquez-Diosdado, J.A.; Bollard, N.; Dottorini, T.; Ellis, K.A. Automated detection of lameness in sheep using machine learning

approaches: Novel insights into behavioral differences among lame and non-lame sheep. *R. Soc. Open Sci.* **2020**, *7*, 190824. https://doi.org/10.1098/rsos.190824

Kalff, S.; Butterworth, S.J.; Miller, A.; Keeley, B.; Baines, S.; McKee, W.M. Lateral patellar luxation in dogs: a retrospective study of 65 dogs. *Vet. Comp. Orthop. Traumatol.* **2014**, *27*, 130–134. https://doi.org/10.3415/VCOT-13-05-0064

Keegan, K.G.; Wilson, D.A.; Smith, B.K.; Wilson, D.J. Changes in kinematic variables observed during pressure-induced forelimb lameness in adult horses trotting on a treadmill. *Am. J. Vet. Res.* **2000**, *61*, 612–619. https://doi.org/10.2460/ajvr.61.6.612

Keegan, K.G.; Yonezawa, Y.; Pai, P.F.; Wilson, D.A. Accelerometer-based system for the detection of lameness in horses. *Biomed. Sci. Instrum.* **2002**, *38*, 107–112.

Keegan, K.G.; Kramer, J.; Yonezawa, Y.; Maki, H.; Pai, P.F.; Dent, E.V.; Kellerman, T.E.; Wilson, D.A.; Reed, S.K. Assessment of repeatability of a wireless, inertial sensor-based lameness evaluation system for horses. *Am. J. Vet. Res.* **2011**, *72*, 1156–1163. https://doi.org/10.2460/ajvr.72.8.1156

Kerwin, S.C.; Taylor, A.R. Neurologic Causes of Thoracic Limb Lameness. *Vet. Clin. North Am. Small Anim. Pract.* **2021**, *51*, 357–364. https://doi.org/10.1016/j.cvsm.2020.12.003

Kirpensteijn, J.; Van den Bos, R.; Endenburg, N. Adaptation of dogs to the amputation of a limb and their owners' satisfaction with the procedure. *Vet. Rec.* **1999**, *144*, 115–118. https://doi.org/10.1136/vr.144.4.115

Kirpensteijn, J.; van den Bos, R.; van den Brom, W.E.; Hazewinkel, H.A. Ground reaction force analysis of large breed dogs when walking after the amputation of a limb. *Vet. Rec.* **2000**, *146*, 155–159. https://doi.org/10.1136/vr.146.6.155

Klausner, J.S.; Peck, J.N.; Hennessey, P.W.; DeBowes, R.M. Arthroscopic debridement for treatment of medial compartment disease of the canine elbow. *J. Am. Vet. Med. Assoc.* **1999**, *215*, 1052–1056. PMID: 10535645

Klein, M.K.; McCarthy, R.J. Osteosarcoma in Dogs and Cats: A Review of the Literature. *Vet. Clin. North Am. Small Anim. Pract.* **2020**, *50*, 755–770. https://doi.org/10.1016/j.cvsm.2020.03.002

Klußmann, S.; Meyer-Lindenberg, A.; Brühschwein, A. Arthrographic description of the canine carpal joint cavities and its recesses. *Anat. Histol. Embryol.* **2024**, *53*, e13026. https://doi.org/10.1111/ahe.13026

Kramer, J.; Keegan, K.G.; Kelmer, G.; Wilson, D.A. Objective determination of pelvic movement during hind limb lameness by use of a signal decomposition method and pelvic height differences. *Am. J. Vet. Res.* **2004**, *65*, 741–747. https://doi.org/10.2460/ajvr.65.6.741

Kunkel, K.A.; Rochat, M.C. A review of lameness attributable to the shoulder in the dog: part two. *J. Am. Anim. Hosp. Assoc.* **2008**, *44*, 163–170. https://doi.org/10.5326/0440163

López, S. Uso del plasma rico en plaquetas en osteoartritis y fracturas en la especie canina: aspectos funcionales y de seguridad (Tesis Doctoral). *Universidad de Las Palmas de Gran Canaria*, **2019**.

LaPrade, M.D.; Melugin, H.P.; Hale, R.F.; Leland, D.P.; Bernard, C.D.; Sierra, R.J.; Trousdale, R.T.; Levy, B.A.; Krych, A.J. Incidence of Hip Dysplasia Diagnosis in Young Patients With Hip Pain: A Geographic Population Cohort Analysis. *Orthop. J. Sports Med.* **2021**, *9*, 2325967121989087. https://doi.org/10.1177/2325967121989087

Lascelles, B.D.; Roe, S.C.; Smith, E.; Reynolds, L.; Markham, J.; Marcellin-Little, D. Evaluation of a pressure walkway system for measurement of vertical limb forces in clinically normal dogs. *Am. J. Vet. Res.* **2006**, *67*, 277–282. https://doi.org/10.2460/ajvr.67.2.277

Lau, S.F.; Hazewinkel, H.A.W.; Voorhout, G. Etiologies of medial coronoid disease. In *Proceedings of the 33rd Annual Meeting of the International Elbow Working Group*, Singapore, 24 September **2018**; pp. 8–10.

Limpens, C.; Smits, V.T.M.; Fieten, H.; Mandigers, P.J.J. The effect of MRI-based screening and selection on the prevalence of syringomyelia in the Dutch and Danish Cavalier King Charles Spaniels. *Front. Vet. Sci.* **2024**, *11*, 1326621. https://doi.org/10.3389/fvets.2024.1326621

Liptak, J.M.; Dernell, W.S. Bone Tumors. In *Veterinary Surgery: Small Animal*, 5th Edition; Elsevier: **2021.**

Liu, X.; Feng, J.; Wu, Z.; Neo, Z.; Zhu, C.; Zhang, P.; Wang, Y.; Jiang, Y.; Mitsouras, D.; Li, Y. Deep neural network-based detection and segmentation of intracranial aneurysms on 3D rotational DSA. *Interv. Neuroradiol.* **2021**, *27*, 648–657. https://doi.org/10.1177/15910199211029097

Lopes, M.; Fernandes, A.M.; Kjöllerström, H.J.; Santos, R. Influence of breed and training on stride kinematics, ground reaction forces, and metabolic cost of transport in show jumping horses. *PLoS ONE* **2020**, *15*, e0235171. https://doi.org/10.1371/journal.pone.0235171

Lopes, M.A.F.; Nichols, J.T.; Dearo, A.C.O.; Nelson, S.R. Effects of forelimb instrumentation on lameness detection in horses using a portable inertial sensor-based system. *J. Am. Vet. Med. Assoc.* **2021**, *259*, 892–898. https://doi.org/10.2460/javma.259.7.892

Lopez, S.; Vilar, J.M.; Rubio, M.; Sopena, J.J.; Damia, E.; Chicharro, D.; Santana, A.; Carrillo, J. Center of pressure limb path differences for the detection of lameness in dogs: A preliminary study. *BMC Vet. Res.* **2019**, *15*, 138. https://doi.org/10.1186/s12917-019-1923-4

MacFarlane, P.A.; Kwon, Y.M.; Higginson, J.S. A comprehensive kinematic and kinetic analysis of the vertical jump and its application to talent identification in equestrian athletes. *J. Biomech.* **2018**, *74*, 125–132. https://doi.org/10.1016/j.jbiomech.2018.04.023

Madsen, J.S.; Svalastoga, E. Early diagnosis of hip dysplasia—A stress radiographic study. *Vet. Comp. Orthop. Traumatol.* **1995**, *8*, 114–117.

Malek, S.; Sample, S.J.; Schwartz, Z.; Nemke, B.; Jacobson, P.B.; Cozzi, E.M.; Schaefer, S.L.; Bleedorn, J.A.; Holzman, G.; Muir, P. Effect of analgesic therapy on clinical outcome measures in a randomized controlled trial using client-owned dogs with hip osteoarthritis. *BMC Vet. Res.* **2012**, *8*, 185. https://doi.org/10.1186/1746-6148-8-185

Maler, L. Neural networks: How a multi-layer network learns to disentangle exogenous from self-generated signals. *Curr. Biol.* **2020**, *30*, R224–R226. https://doi.org/10.1016/j.cub.2020.02.057

Malouin, F.; Bedard, P. Evaluation of head motility and posture in cats with horizontal torticollis. *Exp. Neurol.* **1983**, *81*, 559–570. https://doi.org/10.1016/0014-4886(83)90131-4

Manera, M.E.; Carrillo, J.M.; Batista, M.; Rubio, M.; Sopena, J.; Santana, A.; Vilar, J.M. Static Posturography: A New Perspective in the Assessment of Lameness in a Canine Model. *PLoS ONE* **2017**, *12*, e0170692. https://doi.org/10.1371/journal.pone.0170692

Martinez-Méndez, R.; Huertas, M.R. Uso de sensores inerciales en la medición y evaluación de movimiento humano para aplicaciones en la salud. Universidad Autónoma del Estado de México, Facultad de Ingeniería **2021**. https://www.researchgate.net/publication/263198667

Mata, F.; Johnson, C.; Wilding, L. Cross-sectional epidemiological study of the severity of buccal ulceration and sharp enamel points in ridden and unridden horses. *J. Appl. Anim. Welf. Sci.* **2022**, *1*, 1–7. https://doi.org/10.1080/10888705.2022.2005592

McCarthy, R.N.; O'Connor, J.J. Ground Reaction Forces in Veterinary Medicine: Implications for Canine Rehabilitation. *Vet. J.* **2021**, *267*, 105578. https://doi.org/10.1016/j.tvjl.2021.105578

McDonnell, J.J.; Platt, S.R.; Clayton, L.A. Neurologic conditions causing lameness in companion animals. *Vet. Clin. North Am. Small Anim. Pract.* **2001**, *31*, 17–38. https://doi.org/10.1016/S0195-5616(01)50006-2

McGavin, M.D.; Zachary, J.F. *Pathologic Basis of Veterinary Disease*; Elsevier Saunders: **2012;** pp. 207–208.

Meena, J.; Hasija, Y. Application of explainable artificial intelligence in the identification of Squamous Cell Carcinoma biomarkers. *Comput. Biol. Med.* **2022**, *146*, 105505. https://doi.org/10.1016/j.compbiomed.2022.105505

Millis, D.L. *Canine Rehabilitation and Physical Therapy*, 2nd ed.; Saunders: Philadelphia, PA, USA, **2004**; pp. 211–227.

Mölsä, S.H.; Hielm-Bjorkman, A.K.; Laitinen-Vapaavuori, O.M. Force platform in clinically healthy Rottweilers: comparison with Labrador. *Vet. Surg.* **2010**, *39*, 701–707. https://doi.org/10.1111/j.1532-950X.2010.00758.x

Morris, J.S.; Denny, H.R. Current Concepts in the Management of Osteosarcoma in Dogs. *J. Am. Vet. Med. Assoc.* **2022**, *260*, 563–570. https://doi.org/10.2460/javma.260.5.563

Oosterlinck, M.; Bosmans, T.; Gasthuys, F.; Polis, I.; Van Ryssen, B.; Dewulf, J.; Pille, F. Accuracy of pressure plate kinetic asymmetry indices and their correlation with visual gait assessment scores in lame and nonlame dogs. *Am. J. Vet. Res.* **2011**, *72*, 820–825. https://doi.org/10.2460/ajvr.72.6.820

Oosterlinck, M.; Pille, F.; Huppes, T.; Gasthuys, F.; Back, W. Comparison of pressure plate and force plate gait kinetics in sound Warmbloods at walk and trot. *Vet. J.* **2010**, *186*, 347–351. https://doi.org/10.1016/j.tvjl.2009.08.024

Otero, P.E.; Fuensalida, S.E.; Tarragona, L.; Díaz, A.; Sanchez, M.F.; Micieli, F.; Waxman, S.; Zaccagnini, A.C.; Donati, P.A.; Portela, D.A. Ultrasound-guided caudal quadratus lumborum block combined with the greater ischiatic notch plane block as motor-protective analgesia for the pelvic

limb in dogs. *Vet. Anaesth. Analg.* **2024**, *51*, 97–106. https://doi.org/10.1016/j.vaa.2023.11.001.

Patterson, D.F.; McCarthy, R.J. Advances in the Diagnosis and Treatment of Canine Osteosarcoma. *Vet. Med. Sci.* **2023**, *9*, 1–10.

Pereira, A.G.; Aquino, A.M. Application of force platforms in the evaluation of gait in dogs: a literature review. *Vet. Med. Sci.* **2019**, *5*, 473–480.

Perry, K.L.; Déjardin, L.M. Canine medial patellar luxation. *J. Small Anim. Pract.* **2021**, *62*, 315–335.

Ramírez-Flores, G.I.; Del Angel-Caraza, J.; Quijano-Hernández, I.A.; Hulse, D.A.; Beale, B.S.; Victoria-Mora, J.M. Correlation between osteoarthritic changes in the stifle joint in dogs and the results of orthopedic, radiographic, ultrasonographic and arthroscopic examinations. *Vet. Res. Commun.* **2017**, *41*, 129–137.

Raske, M.; McClaran, J.K.; Mariano, A. Short-term wound complications and predictive variables for complication after limb amputation in dogs and cats. *J. Small Anim. Pract.* **2015**, *56*, 247–252.

Rhodin, M.; Bergh, A.; Gustas, P.; Gomez Alvarez, C.B. Inertial sensor-based system for lameness detection in trotting dogs with induced lameness. *Vet. J.* **2017**, *222*, 54–59.

Rodriguez, J. La displasia de cadera en el dogo canario: Determinación del índice de distracción. Tesis Doctoral, Universidad de Las Palmas de Gran Canaria, 2003.

Romiti, S.; Vinciguerra, M.; Saade, W.; Anso Cortajarena, I.; Greco, E. Artificial intelligence (AI) and cardiovascular diseases: An unexpected alliance. *Cardiol. Res. Pract.* **2020**, *2020*, 4972346.

Roush, J.K. In vivo biomechanical evaluation of orthopedic disease using force plate technology. *Vet. Surg.* **2010**, *39*, 585–593.

Ruoff, C.M.; Kerwin, S.C.; Taylor, A.R. Diagnostic Imaging of Discospondylitis. *Vet. Clin. North Am. Small Anim. Pract.* **2018**, *48*, 85–94.

Rychel, J.K. Diagnosis and treatment of osteoarthritis. *Top. Companion Anim. Med.* **2010**, *25*, 20–25.

Sánchez-Carmona, A.; Velasco, A.; Chico, A.; Agut Giménez, A.; Closa, J.M.; Rial, J. Desarrollo de una escala de valoración radiológica del grado de osteoartrosis para las articulaciones de la rodilla y el codo en el perro - Escala "BIOARTH". *Rev. Of. AVEPA* **2006**, *26*, 269–277.

Schachar, J.; Bocage, A.; Nelson, N.C.; Early, P.J.; Mariani, C.L.; Olby, N.J.; Muñana, K.R. Clinical and imaging findings in dogs with nerve root signature associated with cervical intervertebral disc herniation. *J. Vet. Intern. Med.* **2024**, *38*, 1111–1119. https://doi.org/10.1111/jvim.16982

Schwarz, P.D.; Marcellin-Little, D.J.; Lascelles, B.D. Comparison of vertical forces in normal Greyhounds between force platform and pressure walkway measurement systems. *Vet. Comp. Orthop. Traumatol.* **2012**, *25*, 11–16.

Smith, G.K.; Gregor, T.P.; Rhodes, W.H.; Biery, D.N. Evaluation of risk factors for degenerative joint disease associated with hip dysplasia in German Shepherd Dogs, Golden Retrievers, Labrador Retrievers, and Rottweilers. *J. Am. Vet. Med. Assoc.* **2001**, *219*, 1719–1724.

Smith, G.K.; Mayhew, P.D.; Kapatkin, A.S.; McKelvie, P.J.; Shofer, F.S.; Gregor, T.P. Evaluation of risk factors for degenerative joint disease associated with hip dysplasia in German Shepherd Dogs, Golden Retrievers, Labrador Retrievers, and Rottweilers. *J. Am. Vet. Med. Assoc.* **2001**, *219*, 1719–1724. https://doi.org/10.2460/javma.2001.219.1719

Smith, G.K. Canine hip dysplasia: Understanding and treating a common cause of lameness. *Vet. Clin. Small Anim. Pract.* **2015**, *45*, 1323–1335.

Starke, S.D.; Willems, E.; May, S.A.; Pfau, T. Vertical head and trunk movement adaptations of sound horses trotting in a circle on a hard surface. *Vet. J.* **2012**, *193*, 73–80. https://doi.org/10.1016/j.tvjl.2011.09.020

Tang, K.; Ren, J.; Sun, F. Afann: Bias adjustment for alignment-free sequence comparison based on sequencing data using neural network regression. *Genome Biol.* **2019**, *20*, 266. https://doi.org/10.1186/s13059-019-1880-x

Taylor, B.M.; Tipton, C.M.; Adrian, M.; Karpovich, P.V. Action of certain joints in the legs of the horse recorded electrogoniometrically. *Am. J. Vet. Res.* **1966**, *27*, 85–89.

Thrall, D.E. Hip and pelvis. In *Textbook of Veterinary Diagnostic Radiology*, 5th ed.; Elsevier Health Sciences: St. Louis, MO, USA, **2007**, pp. 385–420.

Thrall, D.E. *Textbook of Veterinary Diagnostic Radiology*, 7th ed.; Elsevier Health Sciences: St. Louis, MO, USA, **2018**.

Tobias, K.M.; Johnston, S.A. *Veterinary Surgery: Small Animal*, 1st ed.; Saunders: St. Louis, MO, USA, **2011**, p. 2332.

Tomlin, J.L.; Pead, M.J.; Langley-Hobbs, S.J.; Muir, P. Radial carpal bone fracture in dogs. *J. Am. Anim. Hosp. Assoc.* **2001**, *37*, 173–178.

Van Weeren, P.R.; Pfau, T.; Rhodin, M. Associations between ground reaction force measurements and forelimb kinematics and kinetics in sound horses trotting on a treadmill. *Equine Vet. J.* **2017**, *49*, 493–500. https://doi.org/10.1111/evj.12668

Vidoni, B.; Aghapour, M.; Kneissl, S.; Vezzoni, A.; Gumpenberger, M.; Hechinger, H.; Tichy, A.; Bockstahler, B. Inter-Observer Agreement in Radiographic Diagnosis of Coxofemoral Joint Disease in a Closed Cohort of Four-Month-Old Rottweilers. *Animals* **2022**, *12*, 1269. https://doi.org/10.3390/ani12091269

Vilar, J.M.; Miró, F.; Santana, A.; Spinella, G. Biokinematics under competitive racing conditions in young Standardbred trotter horses: A preliminary report. *J. Equine Vet. Sci.* **2010a**, *30*, 432–435. https://doi.org/10.1016/j.jevs.2010.07.002

Vilar, J.M.; Ramirez, G.; Spinella, G.; Martinez, A. Kinematic characteristics of myositis ossificans of the semimembranosus muscle in a dog. *Can. Vet. J.* **2010b**, *51*, 289–292.

Vilar, J.M.; Cuervo, B.; Rubio, M.; Sopena, J.; Domínguez, J.M.; Santana, A.; Carrillo, J.M. Effect of intraarticular inoculation of mesenchymal stem cells in dogs with hip osteoarthritis by means of objective force platform gait analysis: Concordance with numeric subjective scoring scales. *Vet. Res.* **2016**, *12*, 223. https://doi.org/10.1186/s13567-016-0372-3

Vilar, J.M.; Morales, M.; Santana, A.; Spinella, G.; Rubio, M.; Cuervo, B.; Cugat, R.; Carrillo, J.M. Controlled, blinded force platform analysis of the effect of intraarticular injection of autologous adipose-derived mesenchymal stem cells associated to PRGF-Endoret in osteoarthritic dogs. *BMC Vet. Res.* **2013**, *9*, 131. https://doi.org/10.1186/1746-6148-9-131

Vincent-Johnson, N.A. American canine hepatozoonosis. *Vet. Clin. North Am. Small Anim. Pract.* **2003**, *33*, 905–920.

Virag, Y.; Gumpenberger, M.; Tichy, A.; Lutonsky, C.; Peham, C.; Bockstahler, B. Center of pressure and ground reaction forces in Labrador and Golden Retrievers with and without hip dysplasia at 4, 8, and 12 months of age. *Vet. Sci.* **2022**, *9*, art. no. 1087693. https://doi.org/10.3389/fvets.2022.1087693

Wallace, L.J. Total hip replacement. *Vet. Clin. North Am. Small Anim. Pract.* **2005**, *35*, 1231–1253.

Wallborn, F.; Söffler, C.; Winkels, P.; Hess, M.; Engelhardt, P. Leishmania infantum-induced bone lesions in a dog. *Tierarztl Prax Ausg K Kleintiere Heimtiere* **2016**, *44*, 278–282.

Walton, M.B.; Cowderoy, E.; Lasclles, D.; Innes, J.F. Evaluation of construct and criterion validity for the “Liverpool osteoarthritis in dogs” (LOAD) clinical metrology instrument and comparison to two other instruments. *PLoS ONE* **2013**, *8*, e58125. https://doi.org/10.1371/journal.pone.0058125

Walton, M.B.; Cowderoy, E.C.; Wustefeld-Janssens, B.; Lascelles, B.D.; Innes, J.F. Mavacoxib and meloxicam for canine osteoarthritis: A randomized clinical comparator trial. *Vet. Rec.* **2014**, *175*, 280. https://doi.org/10.1136/vr.101819

Wehrenpfennig, P.; Schmierer, P. Ectrodactyly with Polydactyly in a Dog—Case Description and Description of Surgical Therapy with Resection and Fusion Podoplasty. *Animals* **2024**, *14*, 1647. https://doi.org/10.3390/ani14111647

Wijdicks, C.A.; Griffith, C.J.; Johansen, S.; Engebretsen, L.; LaPrade, R.F. Injuries to the medial collateral ligament and associated medial structures of the knee. *J. Bone Joint Surg. Am.* **2010**, *92*, 1266–1280. https://doi.org/10.2106/JBJS.I.01344

Wilson, A.M.; McGuigan, M.P.; Su, A.; van Den Bogert, A.J.; Roy, R.R. Nonlinear viscoelasticity in equine tendon: An in vitro study of stress relaxation and creep. *J. Biomech.* **2001**, *34*, 1573–1578. https://doi.org/10.1016/S0021-9290(01)00135-6

Withrow, S.J.; Hirsch, V.M. Owner response to amputation of a pet’s leg. *Vet. Med. Small Anim. Clin.* **1979**, *74*, 332–334.

Zhalniarovich, Y.; Mieszkowska, M.; Przyborowska-Zhalniarovich, P.; Głodek, J.; Sobolewski, A.; Waluś, G.; Adamiak, Z. A novel tibial tuberosity advancement technique with cranial implant fixation (TTA CF): A pilot study in sheep. *Vet. Res.* **2018**, *14*, 231.https://doi.org/10.1186/s13567-018-0605-5

Zomer, H.D.; Cooke, P.S. Advances in drug treatments for companion animal obesity. *Biology* **2024**, *13*, 335. https://doi.org/10.3390/biology13050335